CYTOSYSTEMATICS, SEX CHROMOSOME TRANSLOCATIONS AND SPECIATION IN AFRICAN MOLE-RATS (BATHYERGIDAE: RODENTIA)

By

Jane Lynda Deuve

Dissertation presented for the Degree of

Doctor of Philosophy – Zoology

at

Stellenbosch University

Botany and Zoology Department
Faculty of Science
Supervisor: Prof. T.J. Robinson
Co-supervisor: Dr J. Britton-Davidian
Date: 12th February 2008

Declaration

I, the undersigned, hereby declare that the work contained in this thesis is my own original work and that I have not previously in its entirety or in part, submitted it at any university for a degree.

Jane Lynda Deuve Date: 12th February 2008

Abstract

The Bathyergidae are subterranean rodents endemic to Africa south of the Sahara. They are characterised by divergent diploid numbers that range from 2n=40 in *Fukomys mechowi* to 2n=78 in *F. damarensis*. In spite of this variation there is limited understanding of the events that shaped the extant karyotypes and in an attempt to address this, and to shed light on the mode and tempo of chromosomal evolution in the African mole-rats, a detailed analysis of both the autosomal and sex chromosome components of the genome was undertaken. In addition to G- and C-banding, *Heterocephalus glaber* (2n=60) flow-sorted painting probes were used to conduct cross-species chromosome painting among bathyergids. This allowed the detection of a balanced sex chromosome-autosome translocation in *F. mechowi* that involved a complex series of rearrangements requiring fractionation of four *H. glaber* autosomes and the subsequent translocation of segments to sex chromosomes and to the autosomal partners. The fixation of this rare rearrangement has probably been favoured by the presence of an intercalary heterochromatic block (IHB) that was detected at the boundary with the translocated autosomal segment. Male meiosis in *Cryptomys*, the *Fukomys* sister clade, was investigated by immunostaining of the SCP1 and SCP3 proteins involved in the formation of the synaptonemal complex. This allowed confirmation of a Y-autosome translocation that is shared by *C. hottentotus* subspecies. We discuss reduced recombination between Y and X_2 that seems to be heterochromatin dependent in the *C hottentotus* lineage, and the implications this holds for the evolution of a meiotic sex chromosome chain such as has been observed in platypus. By extending cross-species chromosome painting to *Bathyergus janetta*, *F. damarensis*, *F. darlingi* and *Heliophobius argenteocinereus*, homologous chromosomal regions across a total of 11 species/subspecies and an outgroup were examined using cladistic and bioinformatics approaches. The results show that *Bathyergus*, *Georychus* and *Cryptomys* are karyotypically highly conserved in comparison to *Heterocephalus*, *Heliophobius* and *Fukomys*. *Fukomys* in particular is characterised by a large number of rearrangements that contrast sharply with the conservative *Cryptomys*. The occurrence and fixation of rearrangements in these species has probably been facilitated by vicariance in combination with life history traits that are particular to these mammals.

Opsomming

Die Bathyergidae is ondergrondse knaagdiere wat endemies tot Afrika is suid van die Sahara. Hulle word gekarakteriseer deur ‘n verskeidenheid van dipolïed getalle wat variëer van 2n=40 in *Fukomys mechowi* tot 2n=78 in *F. damarensis*. Ten spyte van die variasie, is kennis beperk ten opsigte van gebeurtenisse wat kon lei tot die huidige kariotipes. Om hierdie gebrek aan te spreek en lig te werp op die manier en tempo van chromosoom evolusie in Afrika molrotte is hierdie studie onderneem waarin beide outosomale en geslagschromosomale komponente van die genoom in detail geanaliseer word. Addisioneel tot G- en C-band tegnieke is *Heterocephalus glaber* (2n=60) vloei-gesorteerde merkers gebruik om ‘chromosoom vergelykings op molekulêre vlak tussen die bathyergids uit te voer. Dit het toegelaat om vas te stel dat ‘n gebalanseerde geslagschromosoom-outosoom translokasie in *F. mechowi,* wat ‘n komplekse reeks herrangskikkings behels, die opbreek van vier *H. glaber* autosome tot gevolg gehad het en die gevolglike verplasing van segmente na die geslagschromosome en hul outosomale maats kon vasgestel word. Die totstandkoming van die raar herrangskikking is moontlik bevoordeel deur die teenwoordigheid van ‘n interkalerende heterochromatien blok (IHB), wat gevind is by die grens met die getranslokeerde outosomale segment. Manlike meiose in *Cryptomys*, die *Fukomys* sustergroep, is ook gebestudeer deur immunokleuring van die SCP1 en SCP3 proteïene betrokke by die vorming van die sinaptonemale kompleks. Dit het die Y-chromosoom verplasing wat *C. hottentotus* subspecies in gemeen het, bevestig. Ons bespreek verminderde rekombinasie tussen Y en X_2, wat wil voorkom om heterochromatien afhanklik te wees in die *C hottentotus* lyn, en die implikasie wat dit inhou vir die evolusie van ‘n meiotiese geslagschromosoom ketting soos gevind by platypus. Kruis-spesies chromosoom kleuring is uitgebrei na *Bathyergus janetta*, *F. damarensis*, *F. darlingi* en *Heliophobius argenteocinereus*, en homoloë chromosomale streke is oor ‘n totaal van 11 spesies/subspesies en ‘n buitegroep gebestudeer deur gebruik te maak van kladistiese en bioinformatiewe benaderings. Die resultate het getoon dat *Bathyergus*, *Georychus* en *Cryptomys* kariotipies hoogs gekonserveerd is in vergelyking met *Heterocephalus*, *Heliophobius* en *Fukomys*. *Fukomys* word veral gekarakterisieer deur ‘n hoë aantal herrangskikkings wat in skrille kontras staan met die konserwatiewe *Cryptomys*. Die voorkoms en fiksasie van herrangskikkings in hierdie spesies word moontlik

geondersteun deur vikariansie in kombinasie met die lewensgeskiedenis-eienskappe wat eie is aan hierdie soogdiere

Acknowledgments

Being determined as well as stubborn (and slightly masochistic) have been important attributes to achieve my doctorate, but most importantly I had a unique coaching that I would like to acknowledge.

I found an outstanding environment in the department of Botany and Zoology that I want to thank for having hosted me during these three years and half of studies. I also want to thank the department for having awarded me an International Student Bursary for the three consecutive years of my study.

I thank my supervisor Terry Robinson who introduced me to the (dark) world of cytogenetics. I would like to express my gratitude for his guidance and his patience in the write-up of my thesis. In addition I am very obliged to Terry for sponsored my participation at the Zoological Society of Southern Africa's (ZSSA) meetings in 2005 and 2007, as well as the 2nd Congress of the International Cytogenetics and Genome Society (ICGS) that was held in Kent (UK) in July 2006 where I had the opportunity to present my results as a spoken paper. I am also thankful to Terry for having financed my PhD and for providing an opportunity for me to complete my doctorate in the Evolutionary Genomics Group (EGG).

I also warmly thank my co-supervisor Janice Britton-Davidian who has been much more available than what I thought was possible when 9000km separated us, and whose insightful comments were more helpful than she may think.

This project would not have been possible without the ideal collaboration with Prof Nigel Bennett who provided us with several specimens from a wide range of African localities.

I heartily thank my husband Francesco for having endured the "co-lateral effects" of the PhD experience, and for his precious moral support.

I met in Stellenbosch companions who also enrolled in PhD in 2004 and with whom we shared beautiful days (and nights!) cruising the Cape region and the local bars, and with whom we also shared the difficult times of this engagement. So I affectionately thank my fellow young Drs Gwenaelle Pound, Clement Gilbert and Arnaud Villaros. Thank you Gwen for being such a true friend, Clem for having been always available for my work-related interrogations (especially around a beer) and Arnaud for your consoling Boeuf Bourguignon.

I have a very grateful thought toward my mentors-friends-colleagues Gauthier Dobigny, Paul Waters, Aurora Ruiz-Herrera and Anne Ropiquet who offered their knowledge, their time, their patience, their inspiration and their enthusiasm.

All the hours spent in the lab or on the microscope were made very pleasant thanks to all my lab mates from the EGG Bettin Jansen Van Vuuren, Victor Rambau, Woody Cotterill, Aadrian Engelbrecht, Hanneline Smit, Conrad Matthee, Sandy Willow-Munroe, Prince Kaleme, Thomas Lado, Sampath Lokugulapati, Rauri Bowi, Savel Daniels, Sophie Van Der Heyden, Jane Sakwa, Krystal Tolley, Keshni Gopal, Lizel Mortimer, Potiphar Kalima and Nico Solomon

The life beside the one in the department has been very stimulating and I also want to thank all the friends I met in South Africa who made the whole experience just a beautiful one! I thank Amandine (who enrolled for a PhD, the crazy one!), Ibo, Nox, Savel, Aman' (the Tall), Aman' (the Short), Tom, Valerie-Tweze, LeeSa, Chris, Schalk, la famille Moyen, Maya, Melanie, Selam, Kora, Simeon, Marna (thank you for the traduction!) and Sandile and his family.

I can not leave South Africa without remembering last time I left my friends in France to come to Stellenbosch to start my doctorate. Beside the geographic distance my metropolitan friends always showed a great interest in what I was doing and were of great support. So thank you to Nora, Milette, Myriam, Manue, Mylene, Momode, Lili, Framboise, Delf, Jo, Juli, Nico, Farid and Mr Sous.

I am infinitely thankful to my family who has always encouraged me to never give up nor drop a dream. Thanks Chrissie for your interest in my work, Merci Mimitte, Keke, Helene, Jerome, Max and Julien for your support. Choukrane to all my family in Algeria, and especially to my grand-mother for being spiritually always connected to me.

Finally, I want to thank my two X's donors, merci Maman for always showing me that you had faith in me and merci J-P for contaminating me your scientific spirit.

Table of contents

List of Tables

List of Figures

CHAPTER 1

INTRODUCTION

1.1 DISTRIBUTION AND ECOLOGY

The term Bathyergidae is derived from the Greek *bathys* (deep) and *ergo* (work). Bathyergids are obligatory subterranean rodents endemic to Africa (Figure 1 and Figure 2). Although usually regarded as comprising five genera, very recently this has been revised to six (Kock *et al.* 2006). These are: *Heterocephalus* comprising a single species the naked mole-rat, *H. glaber*, which is restricted to the arid regions of East Africa. The monotypic *Heliophobius* with a single species, *H. argenteocinereus*, known as the silvery mole-rat which is distributed through the south-east of the Democratic Republic of Congo (DRC), southern Kenya and Tanzania, with its range extending to central Mozambique. *Georychus* is similarly monotypic with *G. capensis,* the Cape mole-rat, occurring as an endemic species in South Africa where it survives as disjunct populations with no record of occurrence between these isolated areas. *Bathyergus* contains two species: *B. suillus*, the Cape dune mole-rat, and *B. janetta*, the Namaqua dune mole-rat, both of which are associated with sand dunes of south and southwestern Africa. The remaining genera *Cryptomys* and *Fukomys* are discussed in detail below.

There are several lines of evidence that suggest that *Cryptomys* should be split into two clades (Figure 2), *Cryptomys sensu stricto* and *Fukomys* (Honeycutt *et al.* 1987, Nevo *et al.* 1987, Honeycutt *et al.* 1991, Allard and Honeycutt 1992, Janecek *et al.* 1992, Faulkes *et al.* 1997, Walton *et al.* 2000, Faulkes *et al.* 2004, Ingram *et al.* 2004, Kock *et al.* 2006). *Cryptomys sensu stricto* includes four subspecies within

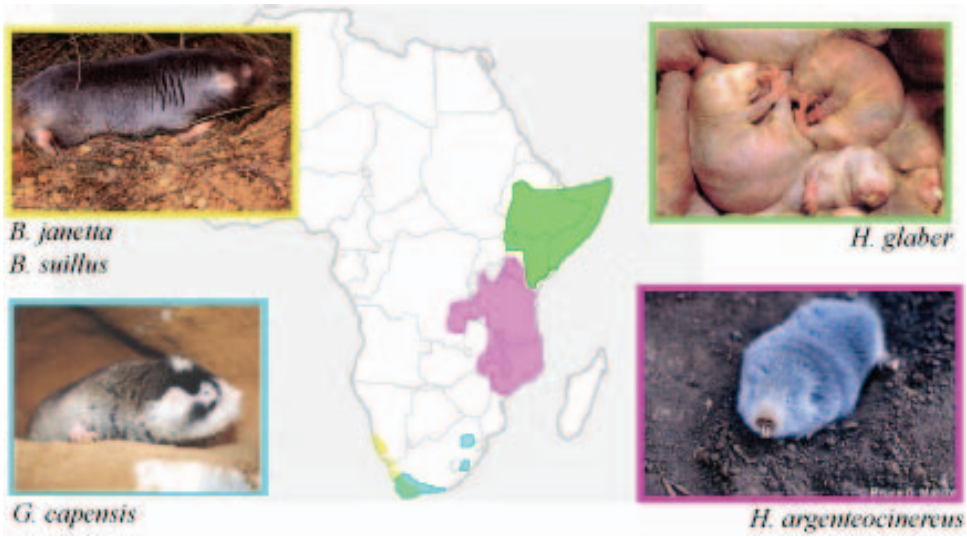

Figure 1: Distribution map of *Heterocephalus* (green), *Heliophobius* (pink), *Bathyergus* (yellow) and *Georychus* (turquoise).

C. hottentotus (Bennett and Faulkes 2000) although arguments to increase this to five (Ingram *et al.* 2004) or six (Faulkes *et al.* 2004) have been mooted. Here we follow Bennett and Faulkes (2000) and accept the following subspecies: *C. h. hottentotus* (common mole-rat), *C. h. natalensis* (Natal mole-rat), *C. h. pretoriae* (Highveld mole-rat) and *C. h. nimrodi* (Matabeleland mole-rat). They are all South African lineages with the exception of *C. h. nimrodi* which is found in southern Zimbabwe. The sixth and most recent genus is *Fukomys* which comprises 12 species, these are: *F. foxi*, *F. zechi*, *F. ochraceocinereus* with distributions in Nigeria, Ghana and Sudanian savannah; *F. bocagei*, *F. damarensis*, *F. mechowi*, *F. darlingi*, *F. amatus*, *F. kafuensis*, *F. anselli*, *F. micklemi* and *F. whytei*, all of which occur within the Zambezi region defined as comprising Zambia, Angola, Namibia, Botswana, Zimbabwe as well as the DRC. In addition to these formal descriptions many of the cytological races detected within *Fukomys* are thought to possibly represent distinct biological species (Van Daele *et al.* 2004, Van Daele *et al.* 2007b).

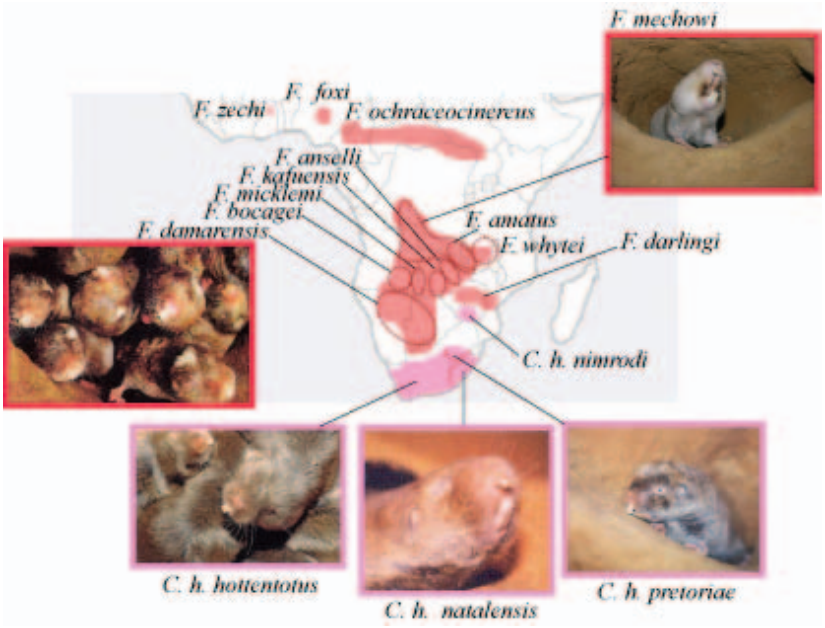

Figure 2: Distribution map of *Fukomys* (red) showing the approximate geographic limits for the twelve recognised species of this genus and similar data for the four *Cryptomys* species (pink).

African mole-rats spend the great majority of their lives underground occurring rarely above the surface (Jarvis and Bennett 1991). As an adaptation to this subterranean life they have fusiform bodies, short legs and their external pinnae are small. The eyes are reduced and they see poorly, if at all (Eloff 1958, Skinner and Chimimba 2005). Most have loose skin permitting them to reverse directions easily in a very narrow space. Excavation is done mostly with the teeth and their limbs are used to move earth freed using the incisors (the exception to this is *Bathyergus* which uses only its limbs). Their lips are tightly closed behind their protruding incisors preventing earth from entering the mouth. Their tails are short and these are used as a tactile organ when the animals are reversing. The pelage also serves a sensory function and many bathyergids have long, sensitive hairs scattered over their bodies. These are the only hairs present on the naked mole-rat, *H. glaber*, but most bathyergids have a thick, soft pelage (De Graaff 1981, Nowak 1999, Bennett and Faulkes 2000). As summarized in Table 1 the various species occur in a wide range of

physical and climatically divergent habitats and vegetation types. Mole-rats exhibit a pronounced size-polymorphism with species ranging from ~30g (*H. glaber*) to ~2kg (*B. suillus*) (Bennett and Faulkes 2000 and references therein); they similarly show a wide range of social organization (Jarvis and Bennett 1990) making them excellent models for studying various aspects of sociobiology.

Table 1: Summary of the most important ecological and behavioural characteristics encountered in bathyergids (from Jarvis and Bennett 1990, Bennett and Faulkes 2000, Scharff *et al.* 2001, Bennett and Jarvis 2004, Skinner and Chimimba 2005 and N.C. Bennett personal communication). Dashes indicate an absence of data.

Species name	Group size	Social system	Mean body mass (g)	Mean gestation (day)	Diet	Soil	Mean annual rainfall (mm/yr)	Mean burrow length (m)
Heterocephalus glaber	80-295	Eusocial	33	72	geophytes	mainly hard soil	360	3027
Heliophobius argenteocinereus	1	Solitary	160	87	roots & geophytes	often very compact	910	47
Bathyergus janetta	1	Solitary	330(♀)-450(♂)		aerial & geophytes	dune sands	80	189
B. suillus	1	Solitary	630(♀)-930(♂)	52	aerial & geophytes	dune sands	550	256
Georychus capensis	1	Solitary	180	46	aerial & geophytes	soft to more solid	560	48
Cryptomys hottentotus hottentotus	2-14	Social	57(♀)-77(♂)	63	geophytes	compact soils	540	464
C. h. natalensis	2-3	Social	88(♀)-106(♂)	68	geophytes & grass rhizomes	compact soils	400-600	181
C. h. pretoriae	up to 12	Social	125(♀)-184(♂)	64	geophytes	soft & moist soils	700	-
Fukomys mechowi	4-20	Social	272	104	geophytes & earthworms	lateritic & sandy soils	1120	200
F. amatus	up to 10	Social	67	100	-	-	890	-
F. damarensis	12-41	Eusocial	104	85	geophytes	soft Kalahari sands	390	1000
F. darlingi	5-9	Social	65	59	tubers & rootstocks	compact sandy clay soils	770	-

Family and social structure ranges from strictly solitary in *Bathyergus*, *Georychus* and *Heliophobius* to cooperative breeding in most of *Cryptomys* and

Fukomys species; the exception to this is *F. damarensis* which, together with *H. glaber*, is eusocial (Jarvis and Bennett 1990). *Fukomys damarensis* and *H. glaber* are the only two mammalian species known to be eusocial (Jarvis 1981, Jarvis and Bennett 1993) showing all three criteria traditionally required for acceptance of eusociality (Wilson 1971): (i) reproductive division of labour, (ii) overlap of generations, and (iii) cooperative care of the young. *Heterocephalus glaber* burrows are sometimes occupied by as many as 300 colony dwellers (Brett 1991), with one reproductively active female – the largest individual of the colony. When she attains her queen status, in addition to an increase in mass, her vertebrae lengthen (Jarvis and Bennett 1991, O'Riain *et al.* 1996). The *H. glaber* queen reproduces with as many as three males (Jarvis *et al.* 1994). In social groups which are much smaller in number (up to 20 members), reproduction is similarly restricted to a single breeding female and a small number of males (Jarvis and Bennett 1993, Jarvis *et al.* 1994). The driving force leading to such extreme altruism in African mole-rats has attracted a great deal of discussion in the literature and in addition to Hamilton's model of kin selection (Hamilton 1964), a popular alternative that has been proposed emphasizes ecological conditions as a significant factor in the development of altruism (Jarvis 1978, Bennett 1988, Lovegrove and Wissel 1988, Lovegrove 1991, Jarvis *et al.* 1994, Faulkes *et al.* 1997). In terms of the latter there is substantial evidence to suggest that the degree of sociality is linked to two major ecological factors, the annual precipitation in a specific region and its predictability, as well as the abundance and distribution of the food resource, specifically underground storage organs and roots. The "aridity-food-distribution hypothesis" proposed by Jarvis (1978), and later supported by Bennett (1988) and Lovegrove and Wissel (1988) was used to explain the degree of sociality exhibited by particular mole-rat species. However, Western Asian spalacids

(underground rodents living in an arid environment where food is scarce) are strictly solitary (Nevo 1991), so other factors are probably responsible for the rise of sociality in bathyergids.

1.2 PHYLOGENETIC REVIEW

Mole-rats belong to Rodentia, an order which contains almost half of the extant species of mammals (2052 of the approximately 5400 currently recognized species, Carleton and Musser 2005). Rodents are ecologically and morphologically very diverse but they share one characteristic - their dentition is highly specialised for gnawing. All rodents have a single pair of upper and lower incisors followed by a gap (diastema), and then by one or more molar or premolar. The incisors are rootless and grow continuously. The most recent classification (Carleton and Musser 2005) divides Rodentia into five suborders: Myomorpha, Anomaluromorpha, Castorimorpha, Sciuromorpha and Ctenohystrica (that groups the Ctenodactylomorphi and Hystricognathi infraorders) all of which are strongly supported by molecular data (Huchon *et al.* 2007, Figure 3).

African mole-rats form a monophyletic clade within Hystricognathi (see Figure below). Their monophyly is supported by morphological synapomorphies that include: (i) highly flared angle of the lower jaw, (ii) structures of the hyoid, laryngeal, and pharyngeal region, (iii) reduced infraorbital foramen compare to other Hystricognathi (De Graaff 1981). Nevo *et al.* (1987) provided the first non-morphologically based phylogeny for the group. They used variation in 20 biochemical loci to construct a presence or absence matrix for *G. capensis, B. suillus*, *B. janetta, F. damarensis, C. h. hottentotus* and *C. h. natalensis*, and these data were used to derive a parsimony tree. Their cladogram, without the use of an outgroup, proposed *Bathyergus* as the most divergent taxon (but *Heliophobius* and

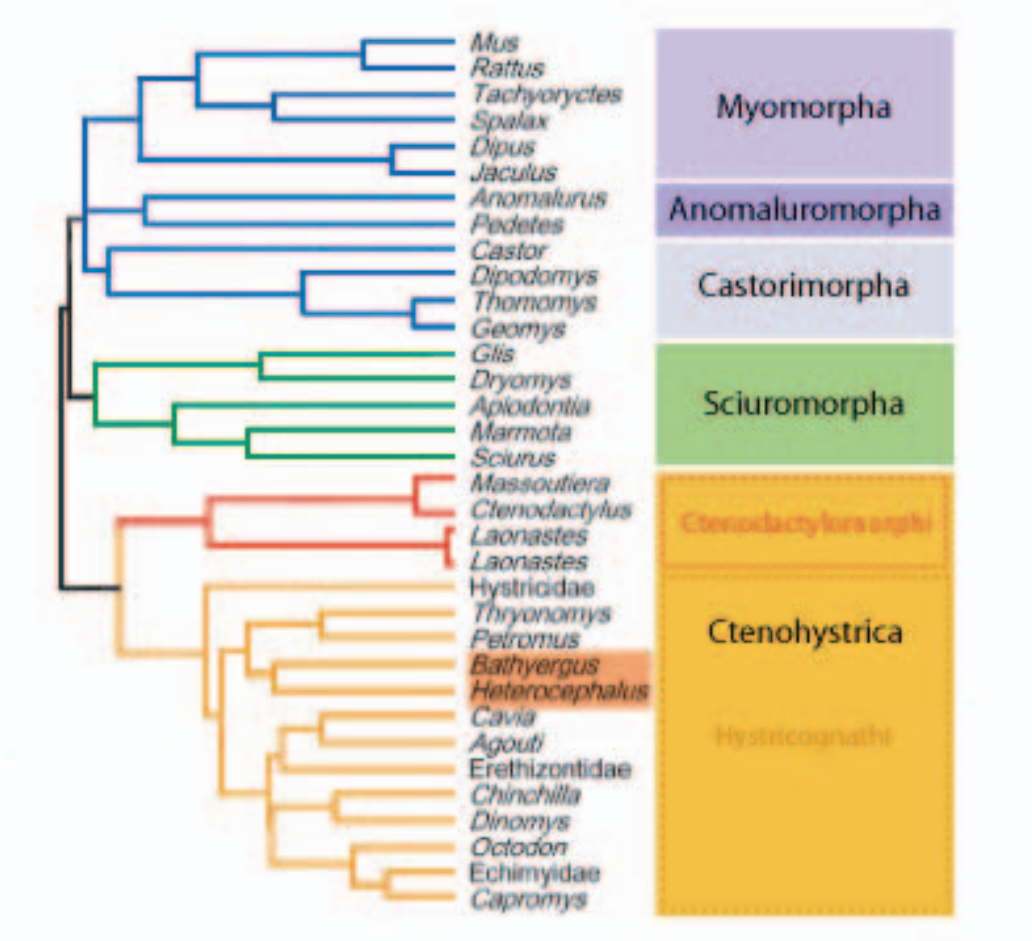

Figure 3: Maximum likelihood rodent phylogeny reconstructed from the combined dataset comprising four nuclear genes (the alpha 2B adrenergic receptor ADRA2B, the growth hormone receptor GHR, the interphotoreceptor retinoid binding protein IRBP and the von Willebrand Factor vWF) and two mitochondrial genes, cytochrome b (cyt b) and the small ribosomal subunit (12S rRNA). The tree is adapted from Huchon *et al.* (2007) and includes the suborders and infraorders recognised by Carleton and Musser (2005). The two bathyergid genera investigated in Huchon *et al.* (2007) study, *Bathyergus* and *Heterocephalus,* are highlighted in orange.

Heterocephalus were not taken into account). Subsequently Honeycutt *et al.* (1987) analysed mtDNA restriction fragment length variation that included representative of all genera, specifically *G. capensis*, *B. suillus*, *B. janetta*, *C. h. hottentotus*, *C. h. natalensis*, *F. damarensis*, *H. argenteocinereus* and *H. glaber*. Fifteen restriction endonucleases yielded 126 restriction fragments that were used in a cladistic analysis. The tree, which was rooted at the midpoint, defined two phylogenetic clades: one containing *Cryptomys sensu lato* (i.e. including the *Fukomys* representatives) and

Heterocephalus as sister taxa, and the other comprising *Georychus*, *Heliophobius* and a basal *Bathyergus*. As sociality in the mole-rats was found in two genera, *Heterocephalus* and *Cryptomys sensu lato*, it was tempting to hypothesize that these two taxa may have been derived from an eusocial common ancestor (Honeycutt *et al.* 1987). Subsequently Allard and Honeycutt (1992) sequenced a 812 base-pair region of the 12S rRNA gene and a phylogenetic analysis was performed with *Petromus typicus* and *Thryonomys swinderianus* as outgroup species. The tree obtained was not consistent with that referred to above and the presence of eusocial/social behaviour was no longer seen as a synapomorphy uniting *Heterocephalus* and *Cryptomys sensu lato*. *Heliophobius* and *Heterocephalus* are the first to diverge, the remaining taxa forming a trichotomy. One consistent result within *Cryptomys sensu lato* was that *C. h. hottentotus* and *C. h. natalensis* were more closely related to each other than either was to *F. damarensis* which, at that time, was still part of *Cryptomys sensu lato*.

Several years later Faulkes *et al.* (1997) extended the molecular information to include cyt b gene sequences (557 informative sites). The consensus tree resulting from parsimony analysis placed *Heterocephalus* as the basal genus, the second most divergent lineage was *Heliophobius*, and the evolutionary relationship among three other genera was unresolved. Two clades were distinct within *Cryptomys sensu lato*. One grouped the *C. hottentotus* subspecies from South Africa and southern Zimbabwe (*C. h. natalensis, C. h. nimrodi, C. h. pretoriae* and *C. h. hottentotus*), the other species from Zaire, Angola, Namibia, Zambia, Botswana and northern Zimbabwe (*F. mechowi, F. bocagei, F. damarensis, F. darlingi* and *F. amatus*). The two clades were also characterised by a high nucleotide divergence. The cyt b (1140bp sequence) genetic distances between any representatives of the southern and northern clade varied between 20.6 - 24.24%. This is as great as the specific differences between *F.*

damarensis and *B. suillus* (21.13%), and those between *F. damarensis* and *G. capensis* (22.77%) (Faulkes *et al.* 2004). More recently Walton *et al.* (2000) and Ingram *et al.* (2004) added nuclear sequences to the data matrix and the combined maximum parsimony analysis (12S rRNA+intron 1 of the nuclear transthyretin, TTR) recovered the same tree retrieved from the analysis of the cyt b gene sequences alone. The division of *Cryptomys sensu lato* into two genera led Kock *et al.* (2006) to propose a new genus, *Fukomys*, for the more northern clade. These studies (Walton *et al.* 2000, Faulkes *et al.* 2004, Ingram *et al.* 2004) did not investigate the relationships within *Fukomys* and this important aspect formed the recent focus of a molecular phylogeny based on sequences of the complete cyt b gene (Van Daele *et al.* 2007b).

The Van Daele *et al.* (2007b) study included all *Fukomys* species with the exception of *F. foxi*, *F. zechi* and *F. ochraceocinereus*. The analyses resolved six major clades, Bocagei, Mechowi, Whytei, Darlingi, Damarensis and Micklemi; some of these grouped more than one species together (see Figure 4). The relationships among subspecies within *C. hottentotus* have been investigated by Faulkes *et al.* (2004) using cyt b and 12S rRNA. Their findings place *C. h. hottentotus* basal, followed by *C. h. nimrodi* and then by the subspecies *C. h. pretoriae* and *C. h. natalensis*. A summary of these results are presented schematically in Figure 4.

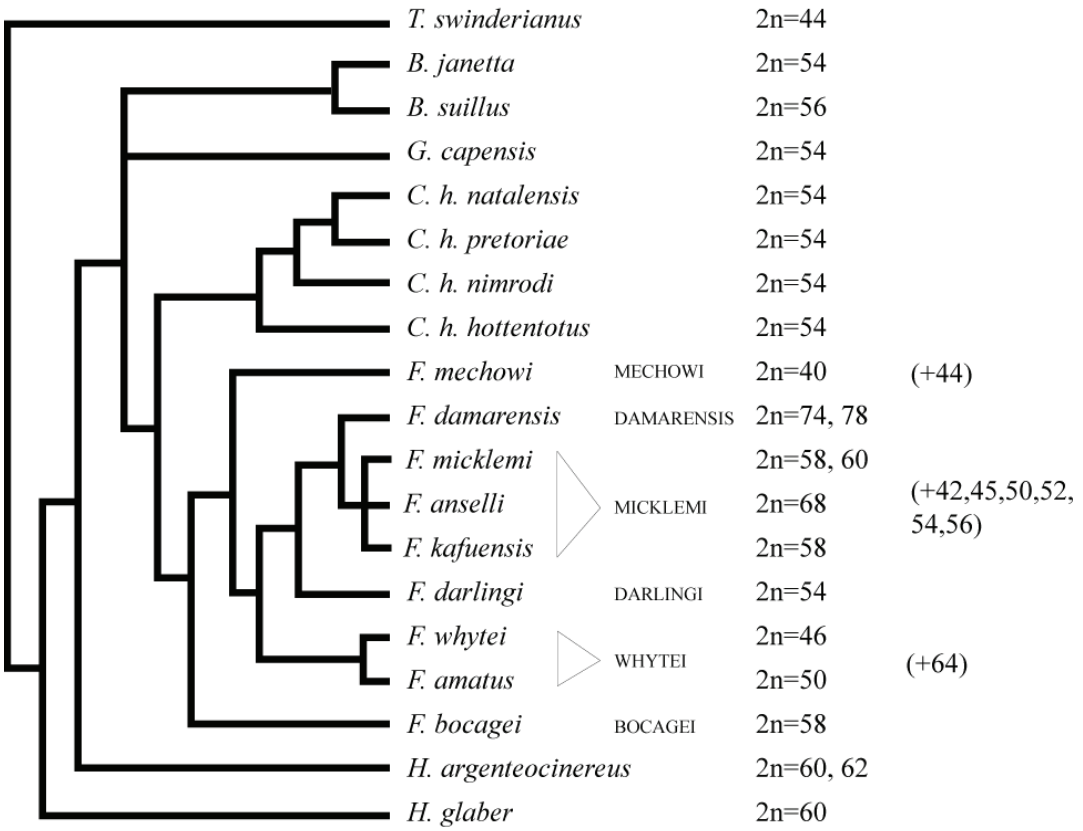

Figure 4: Simplified molecular tree of the Bathyergidae evolutionary relationships summarising data from Faulkes *et al.* (2004), Ingram *et al.* (2004) and Van Daele *et al.* (2007b). All currently recognised genera form well-supported monophyletic clades. *Heterocephalus* is basal followed by *Heliophobius* and by an unresolved trichotomy formed by *Bathyergus*, *Georychus* and *Cryptomys sensu lato* that includes *Fukomys* and *Cryptomys sensu stricto*. Source citations for the diploid numbers (2n), which are mapped to the right of the tree, are listed in Appendix 1. Values in parentheses correspond to diploid numbers recorded for cytological races of *Fukomys* (see page 16 for details).

1.3 BIOGEOGRAPHIC HISTORY

As with many African rodents the Bathyergidae is not well represented in the geological record. The earliest fossils linked to the Bathyergidae are those of three genera found in the early Miocene beds of East Africa and Namibia (Lavocat 1973, 1978). Of these *Bathyergoides neotertiarus* is the largest and although related to the family, it is also clearly distinct from it. On the other hand, *Proheliophobius leakeyi* recorded from Uganda is allocated with confidence to the bathyergids, it closely resembles extant genera *Heterocephalus* and *Heliophobius* (Lavocat 1978, Faulkes *et*

al. 2004). The coincidental appearance of *Heterocephalus* fossils together with extinct bathyergid ancestors supports an early divergence of *Heterocephalus*. *Paracryptomys* is known from part of a skull from the early Miocene beds of the Namib. All three genera had moderately large infraorbital foramina suggesting that the small infraorbital foramen characteristic of the extant family members is a secondary characteristic associated with a subterranean lifestyle (Lavocat 1973 reviewed in Jarvis and Bennett 1990).

The Ugandan Miocene deposits have been dated at a minimum age of 17.8 MY (Bishop *et al.* 1969), however, calibration points that can be used to estimate divergence times are limited; four studies providing dating can be found in the literature. Allard and Honeycutt (1992) estimate the origin of the family at approximately 38 MYA based on the rate of 12S rRNA nucleotide substitutions per site, per year, using a variety of mammalian evolutionary rates as calibration points, and assuming a molecular clock. Faulkes *et al.* (2004) used a similar approach with their cyt b dataset but with a different calibration point (40-48 MY for the age of the family taken from Huchon and Douzery (2001). The results are presented in Table 2. Ingram *et al.* (2004) on the other hand used fossil evidence that dated the divergence of *Heliophobius* at 20-19 MY (Lavocat 1973) and a non-parametric rate smoothing method (Sanderson 2003) that allows for a unique substitution rate for each branch of the tree, rather than the single rate enforced under a molecular clock. Using this approach they estimated ages of the various lineages based on a combined dataset of 12S rRNA and TTR sequences; their findings are compared to those of the other studies in Table 2.

Table 2: Estimated ages of bathyergid lineages in MY provided by independent studies for which the calibration dates are indicated in bold.

Divergence	Dates provided by Allard and Honeycutt (1992)	Dates provided by Faulkes *et al.* (2004)	Dates provided by Ingram *et al.* (2004)	Dates provided by Van Daele *et al.* (2007b)
Heterocephalus	38	**40-48**	35	
Heliophobius		32-40	**20**	
Bathyergus,Georychus, Cryptomys sensu lato		20-26	16-17	
Fukomys from *Cryptomys*		12-17	10-12	**10-11**
Bocagei clade from all other clades below				4-5.7
Mechowi clade from all other clades below				3.5-5
Whytei clade from all other clades below				2.3-3.3
Darlingi clade from all other clades below				1.8-2.7
Damarensis clade from Micklemi clade				1.4-2.1

The three investigations referred to above suggest an early Eocene East African origin for the family, predating the volcanism and rifting activities that have occurred in East Africa (Van Couvering and Van Couvering 1976, Elbinger 1989). Constrained in the north by Ethiopian highlands (Baker *et al.* 1971), radiation occurred in central-southern Africa probably facilitated by an arid corridor (Van Couvering and Van Couvering 1976, Honeycutt *et al.* 1991). The East African rift system includes two branches, the Kenya rift and the Western rift, as well as the great African lakes and associated volcanoes. The Kenya rift began to form approximately 23 MYA while volcanism shaped the Western rift at ~12 MYA in the north, and at approximately 7 MYA in the south (Van Couvering and Van Couvering 1976, Elbinger 1989). The current distribution of *Heliophobius* on both sides of the Kenyan Rift suggests that its divergence was probably independent of the Rift formation, a view that is in line with the estimates suggested by Faulkes *et al.* (2004, Figure 5a-b).

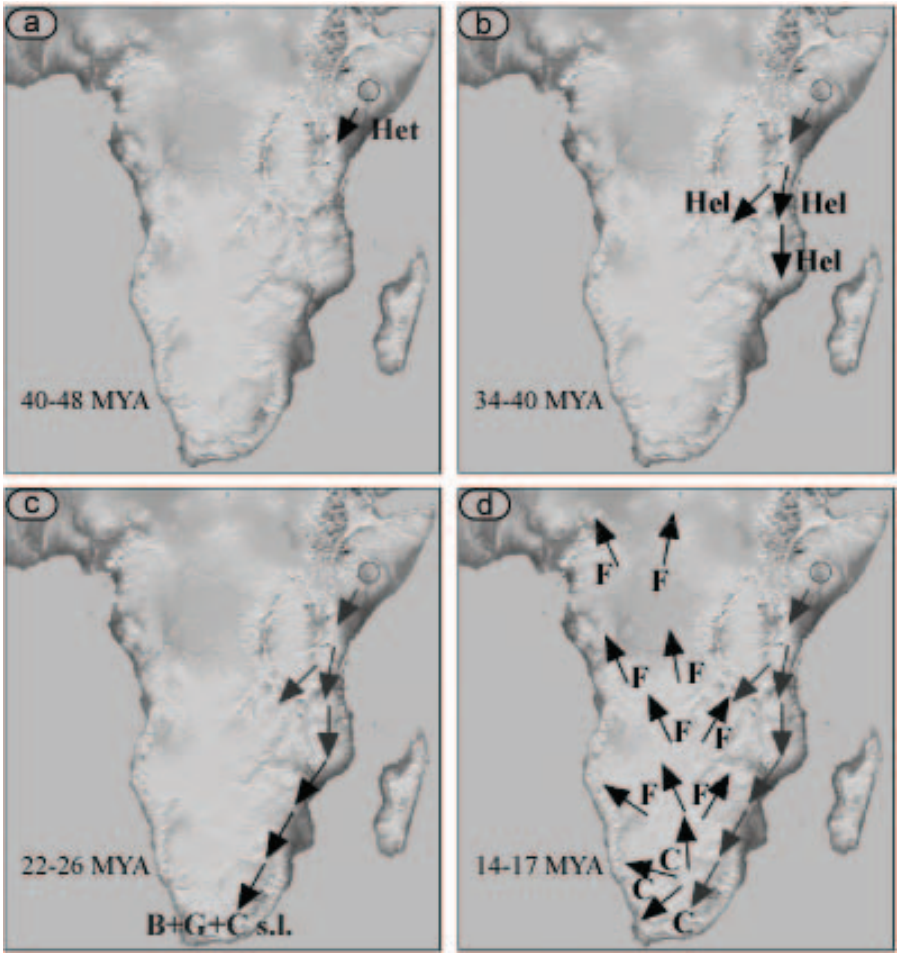

Figure 5: Phylogeographical trends for the bathyergids genera. (**a**): initial divergence of *Heterocephalus* (Het) lineage from the common ancestor of the family in East Africa; (**b**): divergence of *Heliophobius* (Hel) and movement from East Africa into Southern Africa. (**c**): divergence of the last common ancestor to *Bathyergus* (B), *Georychus* (G) and *Cryptomys sensu lato* (C s.l.). (**d**): *Cryptomys sensu lato* diverges into two clades, *Cryptomys sensu stricto* (C) radiating predominantly in South Africa and *Fukomys* (F) spreading north. Redrawn and modified from Faulkes *et al.* (2004).

The divergence estimates for *Bathyergus*, *Georychus* and *Cryptomys sensu lato* at either 20-26 MYA (Faulkes *et al.* 2004) or 16-17 MYA (Ingram *et al.* 2004) are consistent with a period of volcanism in the Kenya rift, an event that might have favoured a radiation in southern Africa rather than in the north and west (Figure 5c). *Cryptomys sensu lato* diverged into its two subclades during the early and middle Miocene (12-17 MYA or 10-12 MYA) at a critical period of rifting activity in both the Kenya and the young Western rifts (Figure 5d). It has been mentioned (Ingram *et*

al. 2004) that the separation of these two genera roughly follows the paleo-Zambezi river which crossed Botswana to join the Orange and Limpopo river systems (Thomas and Shaw 1988). However, the dramatic changes in river drainage in this region of Africa was certainly promoted by tectonics and it seems that the Ovamboland-Kalahari-Zimbabwe crustal flexure (Cotterill 2003) restricts *Fukomys* to the north and *Cryptomys* to the south (see Figure 6).

The southern *Cryptomys* clade speciated almost exclusively within South Africa while the northern *Fukomys* clade underwent an extensive radiation particularly in the vicinity of the vast catchments of the Zambezi river. An initial spread of *Fukomys* has left extant and disjunct populations in Ghana (*F. zechi*), Nigeria (*F. foxi*) and Nigeria/Sudan/Uganda (*F. ochraceocinereus*), all of which are basal in the *Fukomys* phylogeny (Ingram *et al.* 2004). These species have been isolated by the formation of the tropical rainforest in the Congo basin. Further volcanism in the East Africa rift during Miocene seems to have almost completely isolated *Heterocephalus* and *Heliophobius* populations to the east, and restricted *Fukomys* and *Cryptomys* to the west of the Rift. Exceptions such as *F. whytei* populations in western Tanzania and *Heliophobius* populations in Malawi are known, but the latter might actually have diverged before the rift restricted movement (Faulkes *et al.* 2004, Van Daele *et al.* 2007a).

Van Daele *et al.* (2007b) used the estimated divergence of *Cryptomys* and *Fukomys* (10-11 MYA) provided by Ingram *et al.* (2004) as a calibration point to calculate divergence times within the Zambian *Fukomys*. According to Van Daele *et al.* (2004, 2007a, 2007b) following the divergence of the clade that colonised the north of the tropical rainforest and a clade which colonised the Zambezian savanna belt, the latter's distribution (and radiation) has been mainly determined by the

configuration of the region's river system. Divergences have been calculated for the six major *Fukomys* clades (see Figure 4 above). The divergence of Bocagei, Mechowi, Whytei and Darlingi occurred during Pliocene, whereas the Damarensis and Micklemi diversification are Pleistocene events (see Table 2). According to Van Daele *et al* (2004, 2007a, 2007b) the general distribution of the extant *Fukomys* clades would have been determined in the Holocene as a result of the merging and fragmentation of river courses driven by crustal flexion associated with climatic shifts. Figure 6 shows the correlation between the general distribution of the extant *Fukomys* clades and the Holocene river system configuration.

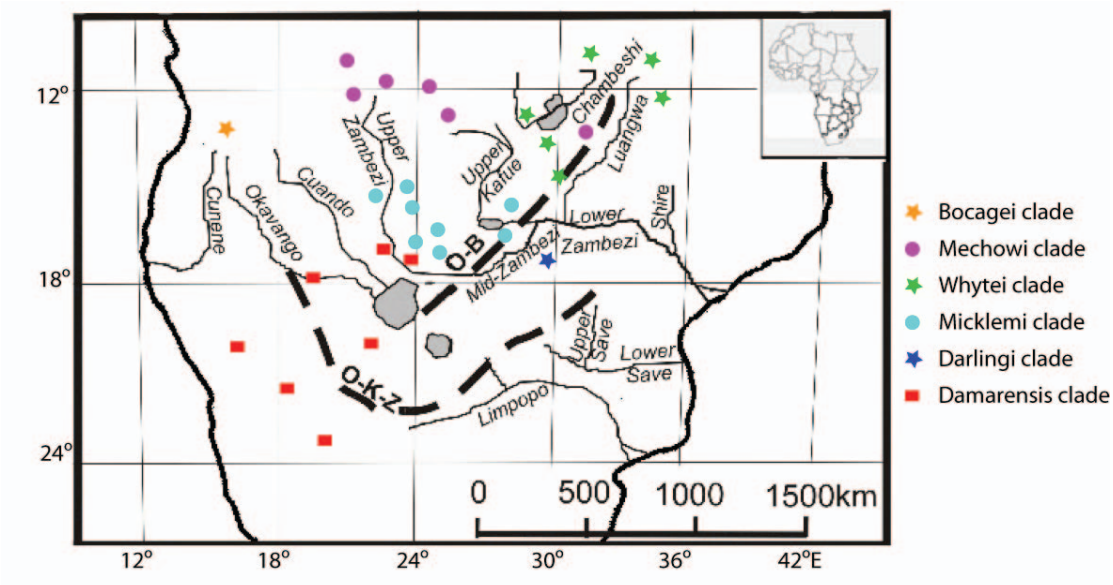

Figure 6: Distribution of the six *Fukomys* clades overlaid on a Holocene map of the Zambezi region showing the principal drainage systems. Dashed lines show the axis of the two major crustal flexures of the region. O-B: Okavango-Bangweulu and O-K-Z: Ovamboland-Kalahari-Zimbabwe. Redrawn from Cotterill 2003, Van Daele *et al.* 2007a.

The influence of geomorphological factors on speciation has been investigated for many mammals including the baboon, giraffe, wildebeest, lechwe antelope and pukus (Cotterill 2003). They all exhibit anomalies in distribution that are associated with particular landforms such as the Zambezi river (for giraffes and wildebeests) and

escarpments (for pukus). In fact Burda (2001) suggests that vicariance associated with the heterogeneous geomorphology of the region constitutes a plausible model for dichopatric and perhaps peripatric speciation of *Fukomys* mole-rats.

1.4 CHROMOSOMAL DIVERSITY IN BATHYERGIDAE

Chromosomal diversity within bathyergids has been a topic of interest for the past 30 years and this is reflected in the relatively rich cytogenetic literature on these species (summarised in Appendix 1). *Heterocephalus glaber*, the first lineage to have diverged, is reported to have 2n=60 (George 1979, Capanna and Merani 1980), followed by *H. argenteocinereus* for which George (1979) reported a 2n=60 karyotype (from the east side of the Rift) that is thought to be identical to *H. glaber*. In contrast Scharff *et al.* (2001) described a Zambian specimen of the same species having 2n=62 (based on three animals without any published karyotype).

Heliophobius populations from both sides of the rift have a high sequence divergence (Ingram *et al.* 2004; 12S rRNA corrected pairwise difference = 7.3-13.3%) and the existence of two distinct diploid numbers, possibly representing two different species, needs further sampling for confirmation. Similarly, *G. capensis* might comprise more than one species based on sequence divergence (Honeycutt *et al.* 1987, Nevo *et al.* 1987) but to date specimens collected from two of its three geographically disjunct distribution areas (Figure 1) have an invariant 2n=54 (Matthey 1956, Nevo *et al.* 1986). *Bathyergus janetta* is also reported to have a 2n=54 and *B. suillus* 2n=56 (Nevo *et al.* 1986) with the latter possessing three autosomal acrocentric pairs, whereas *B. janetta* displays only autosomal metacentrics (Nevo *et al.* 1986). The diploid number 2n=54 is similarly characteristic of *Cryptomys sensu stricto* (Nevo *et al.* 1986, Faulkes *et al.* 2004) although the *C. h. natalensis* and *C. h. hottentotus* karyotypes vary in their autosomal fundamental numbers (aFN= 100 and 102

respectively, Nevo *et al.* 1986), possibly reflecting heterochromatic arm variation among them.

Finally *Fukomys*, in sharp contrast to its sister clade *Cryptomys sensu stricto*, shows the highest karyotypic diversity in the family; it is also the most speciose genus. The diploid numbers vary from 2n=40 in *F. mechowi* (Macholan *et al.* 1993) to 2n=74 and 78 in *F. damarensis* (Nevo *et al.* 1986). Between these two extremes, however, there is a wide diversity in chromosome numbers: 2n=46 (*F. whytei*), 2n=50 (*F. amatus*), 2n=54 (*F. darlingi*), 2n=58 (*F. kafuensis* and *F. bocagei*), 2n=58, 60 (*F. micklemi*), 2n=66, 70 (*F. foxi*), 2n=68 (*F. anselli*). Additionally Van Daele *et al.* (2004) provided evidence of new karyotypes with diploid numbers that reflect either intraspecific chromosomal variation, or the presence of new, undescribed species all of which have Zambian localities: 2n=42 (Dongo), 2n=44 (Salujinga), 2n=45 (Lochinvar), 2n=50 (Kalomo, Faulkes *et al.* 1997), 2n=52 (Chinyingi), 2n=54 (Monze), 2n=56 (Watopa and Livingstone), 2n=64 (Kasama, Kawalika *et al.* 2001). These cytotypes were included in the Van Daele *et al.* (2007b) molecular phylogeny. The diploid numbers are shown to the right of the respective clades (see Figure 4). As mentioned previously, whether this diversity represents intraspecific variation or distinct biological species is presently not known. These "new" diploid numbers are based on sample sizes that vary from one (for the localities Chinyingi, Lochinvar, Salujinga and Watopa) to five (Livingstone). Moreover the karyotypes presented by Van Daele *et al.* (2004) are Giemsa stained precluding comparisons that could provide insights on the types of chromosomal rearrangements distinguishing them. Interestingly the authors note that the Micklemi clade contains highly diverse cytotypes (Figure 4) among which the level of sequence variation is low (between 1.7% and 3.7% for the mean cyt b uncorrected pairwise distance), whereas the Whytei

clade, which has a more conservative pattern of chromosomal diversification, has a much higher level of sequence divergence (from 3.1% to 9.1%). Because Whytei is an older lineage (Table 2) it has been suggested that the low karyotypic diversity results from the elimination of unfit diploid combinations (Van Daele *et al.* 2007b). On the other hand, Micklemi represents a younger radiation and with sufficient time unfit karyotypes may similarly disappear. This prompts the question whether a larger Darlingi sample (only one *F. darlingi* specimen was included in their study) would reveal a karyotypic diversity intermediate between Whytei and Micklemi given that the Darlingi clade is thought to have diverged after Whytei, but before Micklemi. Alternatively Darlingi is truly monotypic due to its less fractured environment than that of the Zambezi region which would result in increased vicariance. Irrespective of these considerations, however, the Van Daele *et al.* (2007b) and Kawalika *et al.* (2001) studies clearly show that a series of simple fusions or fissions would not accommodate karyotypic diversity observed in these mole-rats.

1.5 CYTOGENETIC APPROACH

Genomic comparisons offer insights into past changes that have characterised the evolutionary history of extant lineages. Comparative cytogenetics initially relied on the gross morphological analysis permitted by Giemsa staining of metaphase cells. This provided information on diploid number (2n), fundamental number (FN), the morphology of chromosomes (biarmed or acrocentric) and the centromere position. The discovery of staining methods such as GTG-banding (Seabright 1971) allowed for identification of homologues within and among species karyotypes. However these methods are limited in instances where the karyotypes comprise highly rearranged chromosomes. With chromosome painting procedures (fluorescence *in situ* hybridization or FISH), individual chromosomes from a given species can be

physically isolated using fluorescence-activated cell-sorting and the DNA extracted and labelled with a particular fluorescence dye (Ferguson-Smith *et al.* 1998). The amplified chromosome painting probes can be hybridized to metaphase chromosome of a target species allowing for a significant improvement in the resolution of genomic comparisons. The choice of the taxa used in the sorting process is important and is generally based on chromosome number. The higher the number the more fragmented the genome; painting using these "fragments" results in increased resolution. Cross-species chromosome painting (Zoo-FISH) allows the characterisation of conserved whole chromosomes, conserved chromosome blocks (with a minimal definition of 5Mbp – Scherthan *et al.* 1994) and conserved syntenic associations (adjacent conserved segments having homologies to two or more different chromosomes from the donor species).

Changes observed among genomes reflect past chromosomal rearrangements (Figure 7) which are considered as Rare Genomic Changes (RGC, Rokas and Holland 2000) since they are infrequent, and therefore less homoplasic. Their use in inferring phylogenetic relationships led to the development of a new subdiscipline that is referred to as phylogenomics (O'Brien and Stanyon 1999).

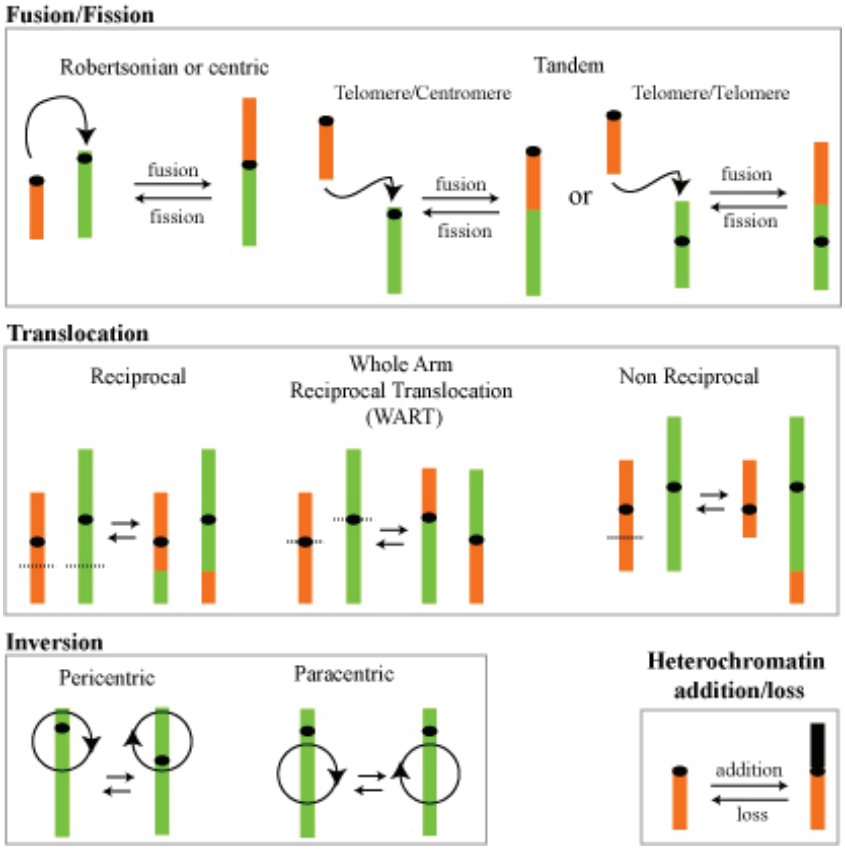

Figure 7: Schematic representation of the main structural changes that could potentially underpin cladogenic events. Centromeres are indicated by black ellipses.

There are differences in recording the types of characters to be used to construct chromosomal phylogenies. Dobigny *et al.* (2004a) recommend the use of chromosome rearrangements as the characters and their presence or absence as the character state, whereas Robinson and Seiffert (2004) advocate the use of breakpoints, i.e. the junctions between syntenies identified in chromosome painting studies. These would be expected to be strongly conserved. In their approach the breakpoint is the character and its presence or absence the character state. Independent of the method used, however, ancestral states are defined through comparison with an appropriate outgroup and synapomorphies can be identified for phylogenetic reconstruction. Chromosomal phylogenies have been successfully conducted using breakpoints as characters (e.g. Neusser *et al.* 2001, Muller *et al.*

2003, Li *et al.* 2004, De Oliveira *et al.* 2005), or chromosomal rearrangements (e.g. Nie *et al.* 2002, Volobouev *et al.* 2002, Matsubara *et al.* 2004, Dobigny *et al.* 2005, Perelman *et al.* 2005).

In addition to the "cytogenetic approaches" outlined above, bioinformatic models have been developed to cater for the analysis of data resulting from genome sequencings projects. One of these entails the calculation of genomic distance which is defined as the minimum number of inversions, translocations, fusions, and fissions required to convert one genome to another. Genomic distance was first studied by Hannenhalli and Pevzner (1995) who developed an algorithm to compute a rearrangement scenario between human and mouse. This single pairwise comparison was subsequently expanded to accommodate the analysis of multiple genomes simultaneously. This led to Bourque and Pevzner (2002) developing the Multiple Genome Rearrangements (MGR) model which searches for rearrangements that reduce the total genomic distance between the genomes that are being compared using a reiterative approach until they converge to common ancestry. In other words, the algorithm "looks for rearrangements that reduce the total distance to the other genomes, and iteratively *reverse history*" (Bourque 2006). MGR has been used to trace the evolutionary process of genome reorganization based on DNA sequences from human, mouse, rat and chicken (Bourque *et al.* 2005) and in the reconstruction of the putative ancestral murid karyotype. This led to suggestions (Bourque *et al.* 2006) that the mathematical approach and cytogenetic analysis should be seen as complementary to each other (see Froenicke *et al.* 2006 and Robinson *et al.* 2006 for further debate on this issue). MGR has been applied to a larger dataset comprising human, mouse, rat, cat, cattle, dog, pig and horse (Murphy *et al.* 2005) allowing for a detailed analysis of the dynamics of mammalian chromosome evolution. The

advantages of this approach is that it allows the detection of smaller genomic segments, the orientation of conserved segments in ancestors, and the handling of fast evolving lineages. By replacing genes with chromosomal syntenies detected by chromosome painting, the MGR algorithm can provide an estimation of the genomic distance between karyotypes and inferences on evolutionary relationships.

1.6 PREAMBLE

Neither the mitochondrial DNA based RFLP (Restriction Fragment Length Polymorphism) phylogeny (Honeycutt *et al.* 1987), nor studies using nuclear and/or mitochondrial sequences (Allard and Honeycutt 1992, Walton *et al.* 2000, Ingram *et al.* 2004) have managed to clarify relationships between *Bathyergus, Georychus* and *Cryptomys sensu lato*. However, resolving the bathyergid evolutionary tree is of importance given the species' wide distribution in Africa and hence their potential to inform the biogeography of the region. Furthermore, the high diversity of karyotypes makes *Fukomys* a useful cytogenetic model to investigate chromosomal speciation as well as the phylogenetic utility, nature, and tempo of chromosomal change. The contrasting karyotypically highly diverse *Fukomys* and karyotypically conservative *Cryptomys* raise fascinating questions concerning the factors driving chromosomal diversification in Bathyergidae.

Among the great diversity of rearrangements underpinning the chromosomal rearrangements in Rodentia, a subset has been identified that deal with sex-autosome translocations (Viegas-Pequignot *et al.* 1982, Ratomponirina *et al.* 1986, Dobigny *et al.* 2002, Veyrunes *et al.* 2004, 2007 and references therein). Sex autosome translocations are considered highly deleterious (King 1993, Ashley 2002, Dobigny *et al.* 2004b) due, among others, to: (i) Differences in replication timing requirements between sex chromosomes and autosomes. (ii) The risk of interference with X

chromosome inactivation (XCI, the silencing of one X in females) due to the presence of autosomal material in the sex vesicle. (iii) The risk of XCI spreading to the autosomal compartment. Therefore sex chromosome-autosome rearrangements are seen as strong cladogenic events, and the survey of their occurrence forms an important complementary approach to the study of bathyergid cytogenetics and its interpretations in an evolutionary framework.

1.7 OBJECTIVES

The aims of this investigation were twofold. First, I attempted to explore the mode and tempo of chromosomal evolution in the Bathyergidae. This entailed a detailed analysis of both the autosomal and sex chromosome components and their inspection by conventional banding, cross-species chromosome painting and immunostaining. Secondly, given the utility of chromosomal characters for determining evolutionary relationships and their relative under utilization in phylogeny reconstruction, the phylogenetic content of the comparative cytogenetic data obtained in this investigation was interrogated using cladistic approaches as well as recent computational analyses that have conventionally been used for the analysis of large genome sequence assemblies.

1.8 ORGANIZATION OF THE DISSERTATION

Most of the information contained in this dissertation has been published and forms in large part the substance of Chapters 2-4. This has, to some extent, impacted on the format and organization of the work. The citations to these sections are:

Chapter 2: Deuve JL, Bennett NC, O'Brien PCM, Ferguson-Smith MA, Faulkes CG, Britton-Davidian J, Robinson TJ (2006) Complex evolution of X and Y

autosomal translocations in the giant mole-rat, *Cryptomys mechowi* (Bathyergidae). *Chromosome Res* **14**: 681-691.

Chapter 3: Deuve JL, Bennett NC, Ruiz-Herrera A, Waters PD, Britton-Davidian J, Robinson TJ (2008) Dissection of a Y-autosome translocation in *Cryptomys hottentotus* (Rodentia, Bathyergidae) and implications for the evolution of a meiotic sex chromosome chain. *Chromosoma* (DOI 1007/s00412-007-0140-6).

Chapter 4: Deuve JL, Bennett NC, Britton-Davidian J, Robinson TJ (2008) Chromosomal phylogeny and evolution of the African mole-rats (Bathyergidae). *Chromosome Res* (In Press).

CHAPTER 2

COMPLEX EVOLUTION OF BALANCED X AND Y AUTOSOMAL TRANSLOCATIONS IN *FUKOMYS MECHOWI*

2.1 INTRODUCTION

One of the most striking of the species in the genus *Fukomys* is the Giant mole-rat, *F. mechowi,* which is distributed from northern Zambia through southern DRC to central Angola (Bennett and Faulkes 2000). The only cytogenetic data on this species are limited to a description of the G- and C-banding patterns and the number of NORs (nucleolar organizing regions) (Macholan *et al.* 1993). The Giant mole-rat has a diploid chromosome complement of 2n=40 and a fundamental number (FN) of 80. The X chromosomes were reported to be heteromorphic (one X chromosome being metacentric, the other submetacentric – see Figure 5 in the Macholan *et al.* 1993 publication). Of particular interest was the size attributed to both the X and Y chromosomes. The X was reported to comprise 11.5% of the haploid set (the average size for eutherian mammals is ~5%, Graves 1995) and the submetacentric Y, 9.5% of the haploid set (average eutherian size is ~2.5%, Graves 1995). The uncommonly large size of the sex chromosomes prompted Macholan *et al.* (1993) to suggest that this reflected either heterochromatic expansion (in the case of the X heterochromatin extends from the centromere distally for approximately two thirds of Xq, while in the case of the Y the entire Yq is C-band positive), or sex autosome translocation, or a combination of both processes. No evidence was, however, provided to substantiate any of these suggestions.

The availability of chromosome specific painting probes and improved methods of fluorescence *in situ* hybridization (FISH) provides a ready means for unambiguously determining both the presence of a sex chromosome-autosome translocation, as well as the identification of the translocation partners. Although cross-species painting using commercial painting probes (*i.e.* mouse, rat, human) would address these questions, the large genetic differences between the donor species from which the paints are derived and the target can often prove problematic. To circumvent this, and as part of a larger chromosomal phylogenetic study on the bathyergids, we have used painting probes derived from the naked mole-rat *Heterocephalus glaber*, a species whose genome (2n=60) is highly fragmented compared to that of *F. mechowi* (2n=40). The rationale being that the large *F. mechowi* chromosomes are likely to be hybridized by several small *H. glaber* chromosomes thus allowing a more detailed analysis of the rearrangements that have shaped the *F. mechowi* karyotype and, particularly pertinent to this investigation, its sex chromosome complement. Here molecular cytogenetic evidence is presented to corroborate the unusual presence of balanced sex-autosome translocations (*i.e.* homologues fused respectively to both the X and Y chromosomes) in this species. In addition, it is shown that the X-autosomal boundary is delimited by the presence of an intercalary heterochromatic block (IHB) which, as has been hypothesised for several other mammals (reviewed in Dobigny *et al.* 2004b), is thought to prevent the spread of X inactivation to the translocated autosome thus providing a means of escaping the potentially deleterious effects associated with this type of chromosomal rearrangement.

2.2 MATERIAL AND METHODS

2.2.1 Conventional Cytogenetics

2.2.1.1 Cell culture and harvest

Chromosome harvest is possible only during cells division. This can be done using bone marrow, short-term lymphocyte culture, and the method of choice followed in this investigation, long-term fibroblast culture. To this end cell lines were established from each specimen included in this study (Table 3). Where available this included both sexes. Live animals were collected under permit from the Department of Nature Conservation, Western and Northern Cape Province, the Ezemvelo Department of Nature Conservation, KwaZulu Natal and the Gauteng Department of Environment and Tourisms to N. C. Bennett, except for the *H. glaber* material which was provided by M.J. O'Riain from a laboratory colony maintained at the University of Cape Town, South Africa. In this section of the work we present results for *H. glaber* and *F. mechowi*.

Table 3: List of the species included in the study showing their original collection localities (RSA= Republic of South Africa, ZIM= Zimbabwe, TANZ= Tanzania) and corresponding grid references, the sexes of the individuals, their diploid number and the total number of specimens for each species/subspecies. Dash indicates an absence of information.

Species name	Locality	Grid Ref.	Sex	2n	Numbers of individuals
Bathyergus janetta	Garies RSA	30º33'S 17º58'E	♀	54	1
			♂	54	1
B. suillus	Cape Town Airport RSA	33º55'S 18º25'E	♀	54	1
			♂	54	2
Georychus capensis	Wakkerstroom RSA	27º21'S 30º7'E	♀	54	1
			♂	54	1
	Darling RSA	33º22'S 18º22E	♀	54	1
			♂	54	1
	University of Cape Town RSA	33º55'S 18º25'E	♀	54	1
			♂	54	1

Table 3 continued

Fukomys mechowi	Chingola ZAMBIA	12º31'S 27º51'E	♀	40	3
			♂	40	1
	Ndola ZAMBIA	12º58'S 28º37'E	♀	40	1
			♂	40	2
F. damarensis	Hotazel RSA	27º11'S 22º58'E	♀	80	4
			♂	80	6
	Dordabis NAMIBIA	22º56'S 17º36'E	♀	80	4
			♂	80	3
F. darlingi	Goromonzi ZIM	17º51'S 31º22'E	♀	54	4
			♂	54	4
Cryptomys hottentotus natalensis	Glengarry RSA	30º23' S 29º40' E	♀	54	2
			♂	53	3
	Howick RSA	29º25' S 30º13' E	♂	53	1
C. h. hottentotus	Steinkopf RSA	29º16' S 17º43' E	♀	54	1
	Sani-Pass RSA	29º38' S 29º26' E	♀	54	1
			♂	53	2
	Bain's kloof RSA	33º37' S 19º0' E	♀	54	1
			♂	53	1
C. h. pretoriae	Pretoria RSA	25º42' S 28º13' E	♀	54	1
			♂	53	3
Heliophobius argenteocinereus	Morogoro TANZ	5º10'S 38º23'S	♀	62	2
			♂	62	1
Heterocephalus glaber	University of Cape Town colony derived from ETHIOPIA	-	♂	60	1
Thryonomys swinderianus	Umfolozi flats Natal RSA	28º30'S 32º10'E	♀	44	1
			♂	44	2

Specimens were received alive and immediately after sacrifice (using Halothane, Safe Line Pharmaceuticals**,** University of Stellenbosch Ethics Clearance Certificate # 2006B01006) biopsies were established from intercostal muscles, ribs and tails. Testis were collected for meiotic studies. Tissues used to start primary cell cultures (muscle, rib and tail) were sampled under sterile conditions, cleaned in 70% ethanol (EtOH) and placed in culture medium (Dulbecco's Modified Eagle Medium, DMEM, with 4.5g/l Glucose & L-Glutamine from BioWhittaker supplemented with 10-15% (v/v) foetal calf serum, FCS from GIBCO). Biopsies were incubated overnight with 5% CO_2 at 37ºC or 31ºC, a choice that was guided by the body temperature of the species concerned (see Table 4 below). If free of contamination the following day, the tissue was minced using a sterile scalpel blade and placed in 25cm^2

tissue culture flasks (NUNC) with 2-3ml culture medium and placed back in the incubator.

Table 4: Core body temperatures for some bathyergids species (from N.C. Bennett, personal communication) used as guides for cell culture.

Species name	Body temperature
Bathyergus janetta	34.8ºC
B. suillus	35ºC
Georychus capensis	36.4ºC
Fukomys mechowi	33.7ºC
F. damarensis	35ºC
F. darlingi	33ºC
Cryptomys hottentotus natalens	33.8ºC
C. h. hottentotus	34ºC
C. h. pretoriae	35.8ºC
Heterocephalus glaber	32ºC
Heliophobius argenteocinereus	35ºC

The cell growth could be enhanced by adding Amniomax (Gibco) (Culture Medium/Amniomax in 3/1 v/v). When cells reached confluence the explants were cryo-preserved (FCS/DiMethylSulphOxide or DMSO from SIGMA in 90/10 v/v) in liquid nitrogen. Cell cultures were similarly stored when established.

Mitotic cells were blocked at metaphase by adding 10-30µl colcemid (10µg/mL; Gibco) to the culture medium for 1-3h. Chromosomes were harvested following trypsin treatment and the cells incubated in a prewarmed hypotonic solution (0.075M KCl) at 37ºC for 20 min; fixation was by 3:1 methanol: acetic acid and cell suspensions were kept at -20ºC for future use. Microscope slides were prepared by dropping 10µl of the fixed cell suspension onto cleaned slides (Marienfeld) that were briefly flamed. The droplet of cell suspension was allowed to spread and then overlaid with a second drop of fixative to improve the quality of the chromosome preparations.

2.2.1.2 Giemsa-banding (GTG-banding)

GTG-banding (Seabright, 1971) by trypsin digestion stains AT rich DNA and this technique was used to identify specific chromosomes (and rearrangements) in order to construct species/subspecies karyotypes and to perform comparisons across karyotypes. Slides for G-banding were baked overnight at 65ºC, dipped in trypsin (0.05% in PBS pH=7) for 30 sec-2 min; the enzymatic action was stopped by rinsing the slides in 0.035M phosphate solution (KH_2PO_4, pH= 7.0) with 2% FCS. A 5% Giemsa solution (in KH_2PO_4, pH= 7.0) was used to stain the digested chromosomes for 6 min, and the slides were then briefly rinsed in water and air dried.

2.2.1.3 Constitutive heterochromatin banding (CBG-banding)

C–banding followed Sumner (1972). Freshly prepared slides were used. A pretreatment comprising 30 min in 0.2M HCl at room temperature was followed after which the slides were air dried. Slides were placed in saturated $Ba(OH)_2$ (B&M Scientific) at 50ºC for 10 sec-2 min and immediately and thoroughly rinsed in distilled water and 0.2M HCl to remove the residual $Ba(OH)_2$. Meiotic chromosomes were more sensitive to this treatment than mitotic preparations and the $Ba(OH)_2$ concentration was consequently halved to 2.5%. Rinsed slides were placed in 2xSSC at 50ºC for 25 min and then stained for 6 min in a 5% Giemsa solution (in KH_2PO_4, pH= 7.0). Images are captured with a CCD camera coupled to an Olympus BX60 microscope. Chromosomes can be sequentially G- and C- banded by recording coordinates of the images captured after the first treatment and retrieving them after C-banding protocol on the same slides.

2.2.2 Chromosome Painting

2.2.2.1 Flow-sorting and generation of chromosome-specific painting probes

Chromosome-specific painting probes were made from bivariate flow-sorted chromosomes (Yang *et al.* 1995, Ferguson-Smith *et al.* 1998) of *H. glaber* (2n=60) by the Cambridge Resource Centre for Comparative Genomics from tissue provided by Drs C.G. Faulkes and T. Hartman, Queen Mary, University of London. Briefly, chromosomes are stained with chromomycin that stains GC rich DNA and Hoescht that stains AT rich DNA. The chromosomes were sorted usind a dual laser cell sorter and isolated according to size and AT:GC ratio. Chromosome-specific probes were made from these isolated chromosomes by degenerate oligonucleotide primed PCR (DOP-PCR) using 6MW primers (Telenius *et al.* 1992). The same primers were used to label the chromosome paints with biotin-dUTP or digoxigenin-dUTP (Roche).

2.2.2.2 Generation of LINE-1 probes

Two LINE-1 degenerate primers (L1R 5'-ATTCTRTTCCATTGGTCTA-3'; and L1F 5'-CCATGCTCATSGATTGG-3') were designed from regions conserved between mouse, rat, rabbit and human L1 (Dobigny *et al.* 2002). These primers amplify a 290bp fragment within the open reading frame (ORF) II of L1. A FISH probe was synthesized from genomic DNA extracted from *F. mechowi* female tissue and fluorescently labelled with biotin using the following cycling parameters: 30 cycles of 94ºC, 30s; 52.5ºC, 50s; 72ºC, 30s, following a 2 min denaturation at 94ºC.

2.2.2.3 Fluorescence in situ hybridization

In situ hybridization of *H. glaber* painting probes to mole-rat chromosomes followed Yang *et al.* (1997a) reviewed in Rens *et al.* (2006) whereas the protocol used

to hybridize LINE-1 probes was adapted from Waters *et al.* (2004). Hybridization using chromosome paints was performed using 4µl of labelled material with 10µl of hybridization buffer (50% deionized formamide, 10% dextran sulphate, 2xSSC, 0.5M phosphate buffer pH=7.3 and 1xDenhardt's solution). The probes were denaturated at 70ºC for 10 min and pre-annealed for 15-30 min at 37ºC. The freshly prepared slides underwent a pre-treatment before hybridization could proceed. They were placed for 5 min at RT in a 3:1 acetic acid: methanol solution (cleaning step) and then passed through a series of 70, 80, 90, 100% ethanol washes each lasting 1 min at RT (dehydrating step); hereafter the slides were air dried. The next step is optional but is necessary when the chromosomes are sheathed in cytoplasm. Treatment of the slides in pepsin (0.1%, Sigma P-7000, dissolved in 10mM HCl) at 37ºC degrades the cytoplasm and facilitates probe access to the chromatin. Two washes in 2xSSC for 5 min at RT followed (to stop the action of the enzyme) after which slides are passed through a series of 70, 80, 90, 100% ethanol washes before slides are aged 1h at 65ºC. The denaturation of the mitotic chromosomes was done by incubation in 70% formamide/30% 2xSSC solution at 65ºC for 1-2 min; this was arrested by dipping the slides in ice-cold 70% ethanol. Finally, following a series of washes in 70, 80, 90, 100% ethanol, pre-annealed paints were applied to the slides. These were covered with 22x22 mm^2 cover-slips sealed with rubber cement and then incubated for 48-72 hours at 37ºC in a humid chamber.

After hybridization the slides were washed in two 5 min incubations in 50% formamide/50% 2xSSC (v/v) at 40-42ºC followed by two 5 min incubations in 2x SSC at 40-42ºC and 5 min in 4x SSC/0.05% Tween 20 (4XT) at the same temperature. Biotinylated probes were detected with streptavidin conjugated with the fluorochrome Cy3 (Amersham Biosciences). Digoxigenin probes were detected using

an antibody coupled with FITC fluorochrome (Roche). Preparations were counterstained with 4',6-diamidino-2-phenylindole (DAPI, Roche). After detection slides were mounted in Vectashield mounting medium and the DAPI, Cy3 and FITC images were captured with a CCD camera coupled to an Olympus BX60 fluorescence microscope and analysed using the Genus imaging System (Applied Imaging version 2.75).

2.2.2.4 Flow-sorting characterization

The assignment of the flow-sorted peaks was done by hybridization of each fluorescently labelled flow-sort to DAPI banded *H. glaber* metaphase chromosome spreads. Where more than one chromosome was isolated in a specific peak we used double colour hybridizations to resolve any ambiguity.

2.3 RESULTS

2.3.1 G-banded chromosomes and flow karyotype of *H. glaber*

The G-banded karyotype of *H. glaber* (Figure 8) was used as a reference to assign the flow-sorted painting probes. It consists of 19 biarmed and 10 acrocentric autosomal pairs. The X is a large submetacentric chromosome and the Y is the second smallest acrocentric chromosome in the complement.

Figure 8: G-banded karyotype of a male *H. glaber*, 2n=60. The horizontal scale bar corresponds to 50μm.

The *H. glaber* karyotype (2n=60, XY) resolved into 26 peaks (Figure 9). Chromosome paints were generated from each of the 26 chromosomal pools and assigned by FISH to DAPI stained *H. glaber* chromosomes. All 26 painting probes successfully hybridized; 20 to a single chromosome (nos. 1-4, 8, 10-14, 16-18, 21, 23, 25, 28, 29, X and Y) six each painted more than one chromosome (nos. 5+6, 9+22, 15+18, 19+25, 26+27 and 6+7+20). Because chromosome 18 and 25 were isolated in pure form it was possible to characterize chromosome 15 using the probe 15+18; similarly chromosome 19 could be detected using the probe 19+25. Moreover, since probes 5+6 and 6+7+20 share chromosome 6 this chromosome could be identified using two-colour FISH. Peaks containing 26+27 and 19+25 could not be further resolved. Although the peak containing 6+7+20 was useful for identifying

chromosome 6 (see above) we were unable to resolve chromosome 7 and 20. Consequently the only painting probe lacking is *H. glaber* chromosome 24.

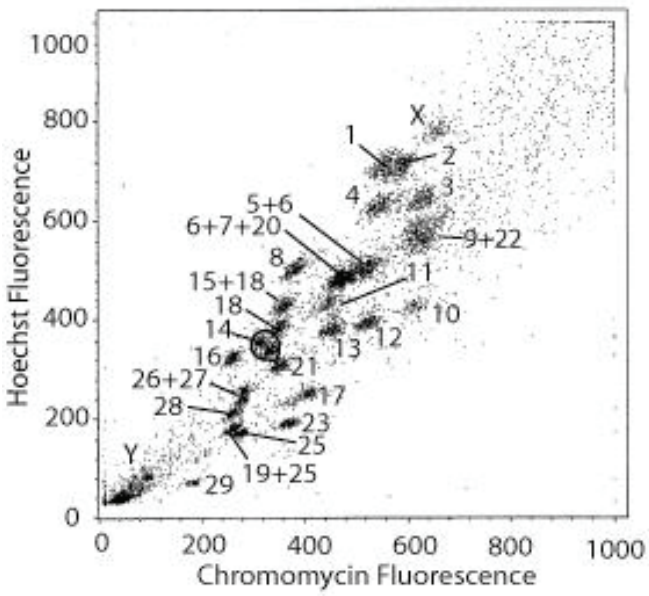

Figure 9: Flow karyotype of *H. glaber* showing the assignment of flow-peaks to specific chromosomes as ordered in Figure 8.

2.3.2 Hybridization of *H. glaber* painting probes onto chromosomes of *F. mechowi*

The arrangement of the G-banded chromosomes of *F. mechowi* follows Macholan *et al.* (1993). The approximate regions of homology with *H. glaber* are shown in Figure 10. The *H. glaber* paints revealed 45 homologous regions in the *F. mechowi* genome. The results show that six *H. glaber* chromosomes (HGL 6, 18, 28, 16, 29 and the X) are retained *in toto* in the *F. mechowi* genome although fused to other autosomal segments (see Figure 10 – respectively FME 2, 4, 5, 7, 13, and the X). Two *H. glaber* chromosomes (HGL 15 and 25) are each retained as a single chromosome (*i.e.* unfused) in *F. mechowi* (FME 12 and 17). Thirteen *H. glaber*

chromosomes (HGL 1-3, 5, 8, 10-14, 17, 21 and 23) produce two or more signals on *F. mechowi* chromosomes 1-3, 5-11, 14, 16, 18 and X (Figure 10). No conclusions can be made in respect of the syntenies involving HGL 7, 9, 20, 22, 26 and 27 since these chromosomes were not purely isolated in our painting probes (see above). The painting probes HGL 4 and Y did not produce any discernible signal in the *F. mechowi* genome. In the case of the Y this is probably because of the largely heterochromatic nature of this chromosome and the 40-48 MY divergence time (Faulkes *et al.* 2004) between these lineages. The distal two thirds of FME 13 and the entire FME 19 were not hybridized using any of the HGL painting probes.

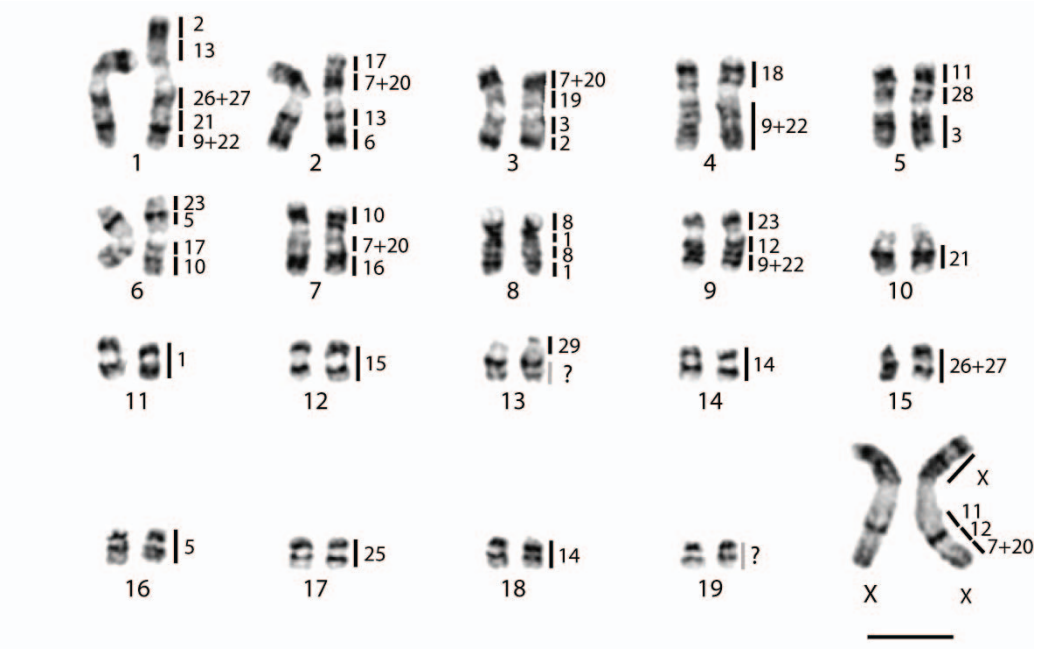

Figure 10: G-banded karyotype of *F. mechowi* (2n=40) with the approximate regions of homology to *H. glaber* as determined by cross-species FISH shown to the right of each chromosomal pair. Question marks show regions that have not been hybridized by any of the *H. glaber* paints. The horizontal scale bar corresponds to 100µm.

2.3.3 Molecular cytogenetic dissection of *F. mechowi* sex chromosomes

The *F. mechowi* X and Y chromosomes can be identified by the large blocks of heterochromatin they carry which is clearly visible following C-banding (Figure 11).

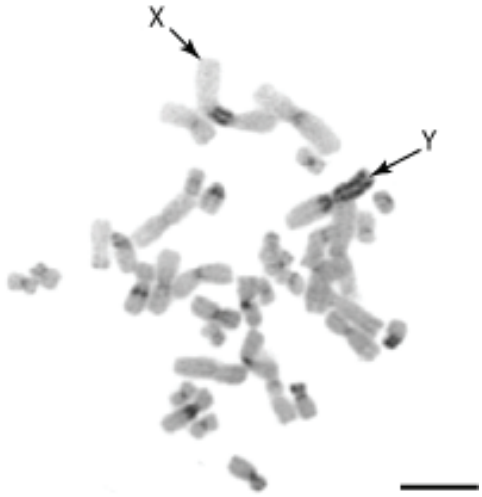

Figure 11: C-banded metaphase of a male *F. mechowi*. The sex chromosomes are identified by arrows. The horizontal scale bar corresponds to 100μm.

The results of *H. glaber* painting probes HGL X, HGL 11, HGL 12 and HGL 7+20 on *F. mechowi* chromosomes are presented for both female (Figure 12a, c and e) and male (Figure 12b, d and f). HGL 11 produced one signal on an autosomal pair (*F. mechowi* 5 see Figure 10), and one on each of the sex chromosomes (both the X and the Y) close to the heterochromatic/euchromatic junction on these chromosomes (Figure 12a and b). The *H. glaber* chromosome 12 painting probe similarly produced two sets of signals in *F. mechowi*; one on *F. mechowi* pair 9 (Figure 10) and one each on the distal two thirds of Xq and Yp respectively (Figure 12c and d). Cross-species painting using the probe HGL 7+20 resulted in hybridization signals on *F. mechowi* autosomes 2, 3 and 7 (Figure 10), and on the X and Y chromosomes distal to HGL 12 (Figure 12e and f). Therefore, the sequence of hybridization on both the X and the Y

chromosomes from the centromere to Xqter and Ypter respectively is HGL 11-12-7+20 (Figure 12g – the Y is inverted to facilitate the comparison).

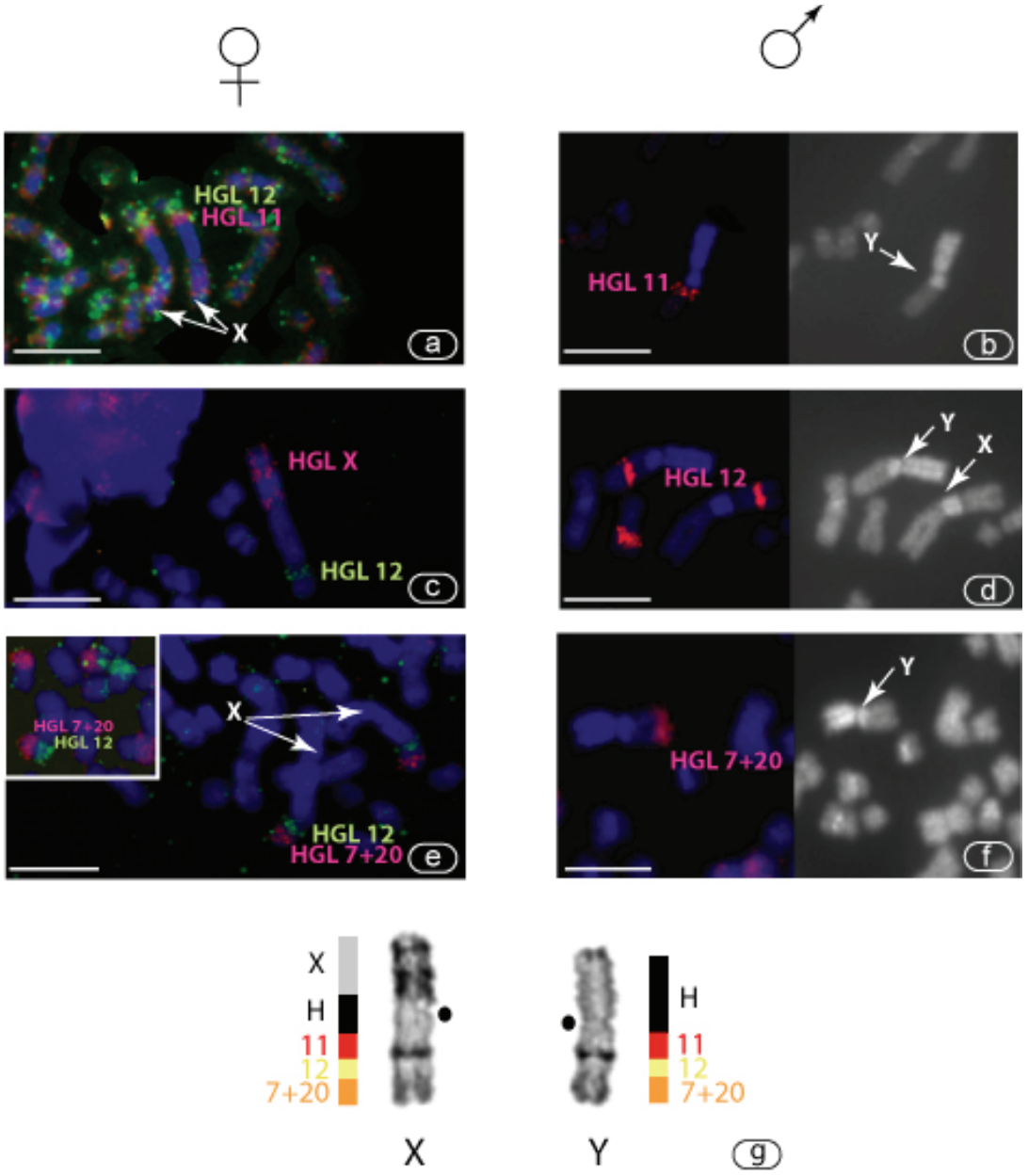

Figure 12: (**a**) to (**f**) FISH hybridization of *H. glaber* painting probes (HGL) on *F. mechowi* metaphase chromosomes. In the case of the male we have included the DAPI image (grey) which clearly shows the large heterochromatic blocks on the sex chromosomes (IHBs). (**a**), (**c**) and (**e**) show FISH results on a female and (**b**), (**d**) and (**f**) on a male. Hybridization patterns obtained using painting probes: (**a**) HGL 11 and HGL 12 (**b**) HGL 11, (**c**) HGL X and HGL 12, (**d**) HGL 12, (**e**) HGL 12 and HGL 7+20 (inset shows hybridization of HGL 12 and HGL 7+20 on *B. janetta*) and (**f**) HGL 7+20. (**g**) Schematic representation of the FISH results above and their relative positions on the *F. mechowi* X and Y chromosomes. Heterochromatic regions are marked with an H. Black dots correspond to centromere positions. The Y chromosome is inverted to facilitate the sex chromosome comparisons. Arrows indicate the sex chromosomes. The horizontal scale bar corresponds to 100µm.

2.3.4 Hybridization of LINE-1 probes on *F. mechowi* metaphases

The hybridization pattern of LINE-1 elements on *F. mechowi* female metaphase chromosomes is of equal intensity on the sex and autosomal chromosomes (Figure 13). Slight banding patterns are visible on well differentiated chromosomes. The heterochromatic regions are free of hybridization which is particularly evident on the two X chromosomes which show an absence of signal along the entire IHB.

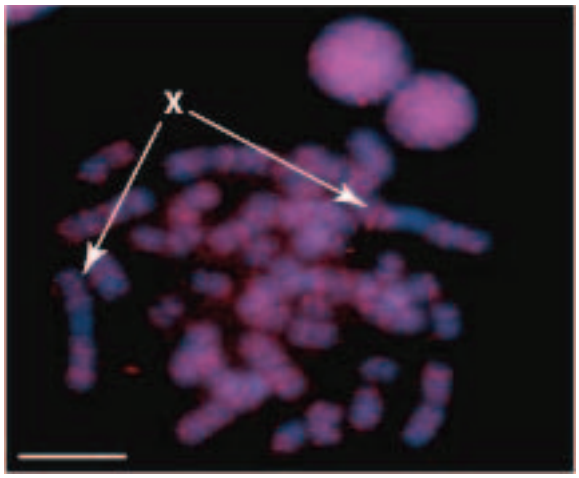

Figure 13: FISH pattern obtained with LINE-1 probe. The horizontal scale bar corresponds to 100μm.

2.4 DISCUSSION

In order to compensate for unequal X gene dosage between the mammalian sexes (two Xs in females and one X in males), X chromosome inactivation (XCI) has evolved to transcriptionally silence one of the Xs in female somatic cells (Ohno *et al.* 1959, Lyon 1961, Russell and Bangham 1961). As a consequence, the inactive X replicates later than the active X (Priest *et al.* 1967, Takagi 1974). In cases where an X chromosome is translocated to an autosome, the possibility that X inactivation could spread to the adjacent autosomal compartment and thus interfere with its

replication timing is thought to negatively effect the establishment of this type of rearrangement in the evolutionary process (Ashley 2002). Nonetheless, in spite of these considerations, X-autosome translocations are not that uncommon in mammals (e.g. rodents - Viegas-Pequignot *et al.* 1982, Ratomponirina *et al.* 1986, Dobigny *et al.* 2002, Veyrunes *et al.* 2004; shrews -Pack *et al.* 1993; cetartiodactyls - Vassart *et al.* 1995, Yang *et al.* 1997b; carnivores -Fredga 1972; bats -Tucker 1986). The Giant mole rat, *F. mechowi,* represents a new addition to these taxa.

We have identified that at least three rearrangements involving *H. glaber* chromosomes 7, 20, 12, 11 and X are required to reconstruct the *F. mechowi* sex chromosomes using the *H. glaber* chromosomes as template. The *H. glaber* chromosomes involved produced in total eight hybridizations signals in the *F. mechowi* genome of which five are present on autosomes in associations with other adjacent syntenies, and three are present on the sex chromosomes. These are in sequence from the centromere distally to Xqter and Ypter, HGL11-HGL12-HGL7+20 (Figure 12g). The analysis of closely related taxa permits us to illustrate the likely sequence of events that shaped the morphology of the *F. mechowi* sex chromosomes (Figure 14). First, the adjacent synteny HGL12-HGL7+20 forms a single autosome in *B. janetta* (see inset Figure 12e) that can also be identified by G-banding comparison in the monotypic *G. capensis*. Since *Bathyergus*, *Georychus* and *Cryptomys sensu lato* (that comprises *Cryptomys sensu stricto* and *Fukomys*) are part of an unresolved trichotomy (Ingram *et al.* 2004 and Figure 4), it is possible to infer that this synteny was present in the last common ancestor to these three genera preceding translocation to the sex chromosomes. Secondly, since it is unlikely that additions to the X and the Y chromosomes are independent events, it is assumed that additions were initially

restricted to one of the two sex chromosomes and then recombined to the other (Graves and Foster 1994).

To elucidate the events that led to the unusual sex chromosome configurations in *F. mechowi* two equally parsimonious explanations are proposed. These are illustrated in Figure 14.

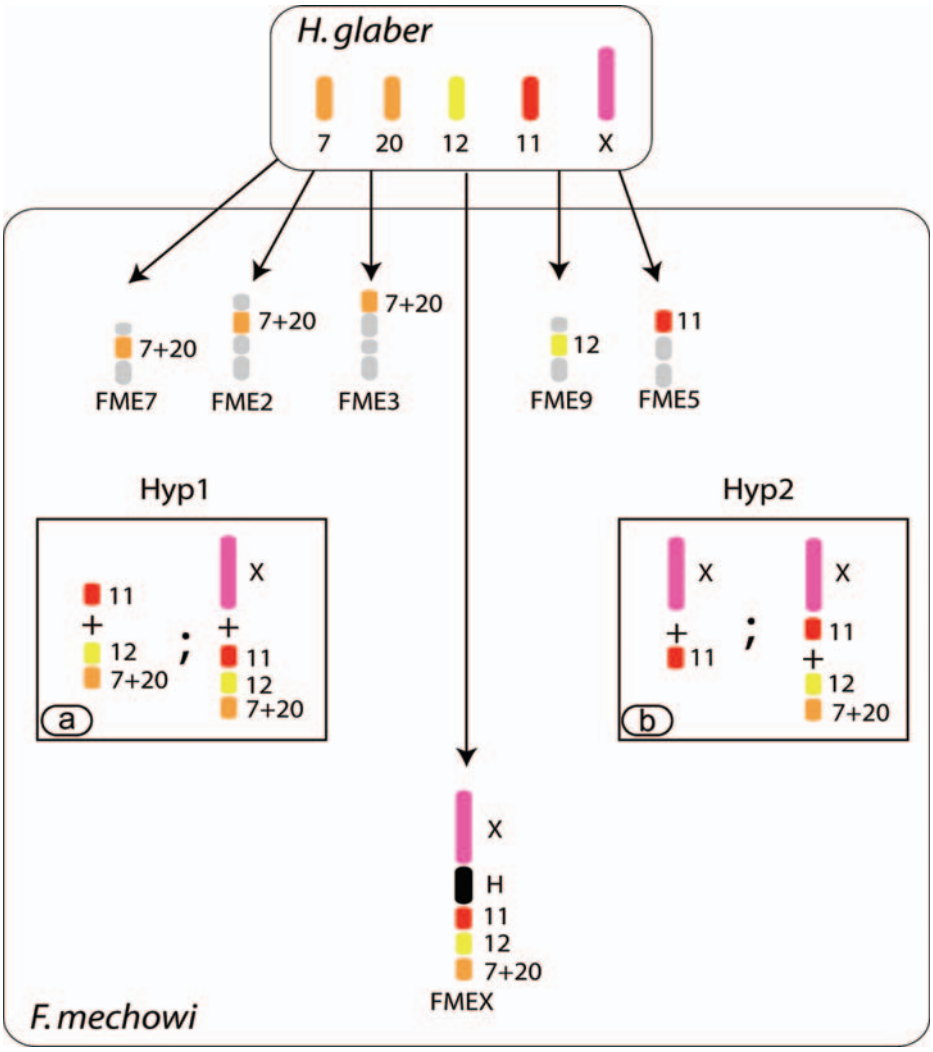

Figure 14: Representation of *H. glaber* chromosomes 7, 20, 12, 11 and X, linked by arrows to the six *F. mechowi* chromosomes in which the corresponding sites of hybridization were detected. Because *H. glaber* 7 and 20 were sorted in the same chromosome peak they are represented by the same colour. The grey blocks on the *F. mechowi* chromosomes represent the other HGL syntenies. The two equally parsimonious explanations for the derivation of the *F. mechowi* X-autosome translocation are shown in insets (**a**) and (**b**). The '+' represents a fusion or a translocation. Only one chromosome is represented per pair. Heterochromatic blocks are marked with an H.

The first hypothesis (Figure 14a) entails an initial event (fusion or translocation) that occurred between an HGL 11 segment and the adjacent synteny HGL12-HGL7+20; this syntenic combination was subsequently translocated to the X. In the second hypothesis (Figure 14b), HGL 11 was translocated to the X followed by its subsequent translocation to HGL12-HGL7+20. Definitive evidence in support of one or other of these competing hypotheses should follow the investigation of species closely related to *F. mechowi*, in particular the Damaraland mole-rat, *F. damarensis* and Mashona mole-rat, *F. darlingi*.

The almost ubiquitous presence of a block of heterochromatin delimiting the translocated segments in species with a sex-autosome translocation (if no heterochromatin is present, it has been suggested that another type of repetitive sequence such as rDNA might be present, Veyrunes *et al.* 2004) has led several authors (reviewed in Dobigny *et al.* 2004b) to suggest that the IHB might be positively selected for, thus allowing viable X-autosome chromosome translocations to become fixed in the evolutionary process. The detection of an IHB in the *F. mechowi* X is consistent with its possible role in allowing for differences in replication timing and in preventing XCI from spreading to the recently translocated autosomal compartment. X chromosome inactivation may be facilitated by booster elements (Gartler and Riggs 1983) proposed to be long interspersed elements, LINE1, (Lyon 1998). The occurrence of LINE-1 in the X chromosomes of a wide variety of eutherian lineages (Boyle *et al.* 1990, Bailey *et al.* 2000, Parish *et al.* 2002, Dobigny *et al.* 2004c, Waters *et al.* 2004), and more recently the presence of L1 around the human X inactivation centre with a drop off in distal Xp where more genes escape inactivation (Ross *et al.* 2005), gave support to the hypothesis that these elements play a regulatory role in controlling the spreading of the inactivation phenomenon (Gartler

and Riggs 1983). The data show, however, a ubiquitous distribution of LINE-1 on all chromosomes with some evidence of a banding pattern that is known to correspond to the G-positive regions in other species (Korenberg and Rykowsky 1988, Boyle *et al.* 1990). Those regions of the genome that are heterochromatic (including the IHB and the Y) were deficient in LINE-1. Importantly, and in marked contrast to the distribution shown in most mammals, the absence of enrichment on the X chromosome in this species reflects a similar pattern shown in some other rodent species (e.g. Casavant *et al.* 2000, Meles *et al.* 2007).

Autosomal additions on to the sex chromosomes, like those observed for *F. mechowi*, are considered as steps in the complex evolutionary processes that have led to the unique composition of the eutherian sex chromosomes. In brief their ontogeny reflects an autosomal origin (Ohno 1967) in which one element of the pair (the proto-Y chromosome) acquired a sex-determining locus across which recombination was suppressed leading to degradation and loss of functional genes (for reviews see Graves 1995, Charlesworth and Charlesworth 2000). This resulted in a small, generally heterochromatic and gene-poor Y, whereas the X remained relatively unchanged and is highly conserved in gene content in all placental mammals. In most placentals the Y and X chromosomes retained a terminal region of homology over which they recombine referred to as the pseudoautosomal region (PAR) (Burgoyne 1982) that plays a role for segregation of sex chromosomes during meiosis. Gene mapping and chromosome painting of the X chromosome between placentals, marsupials, monotremes (Graves 1995) and birds (Kohn *et al.* 2004) revealed that at least two subsequent additions of autosomal material (Graves and Watson 1991) occurred in the sex chromosomes of the eutherian lineage (Figure 15) each following

the same sequence of events as described in the addition-attrition hypothesis (Graves 1995).

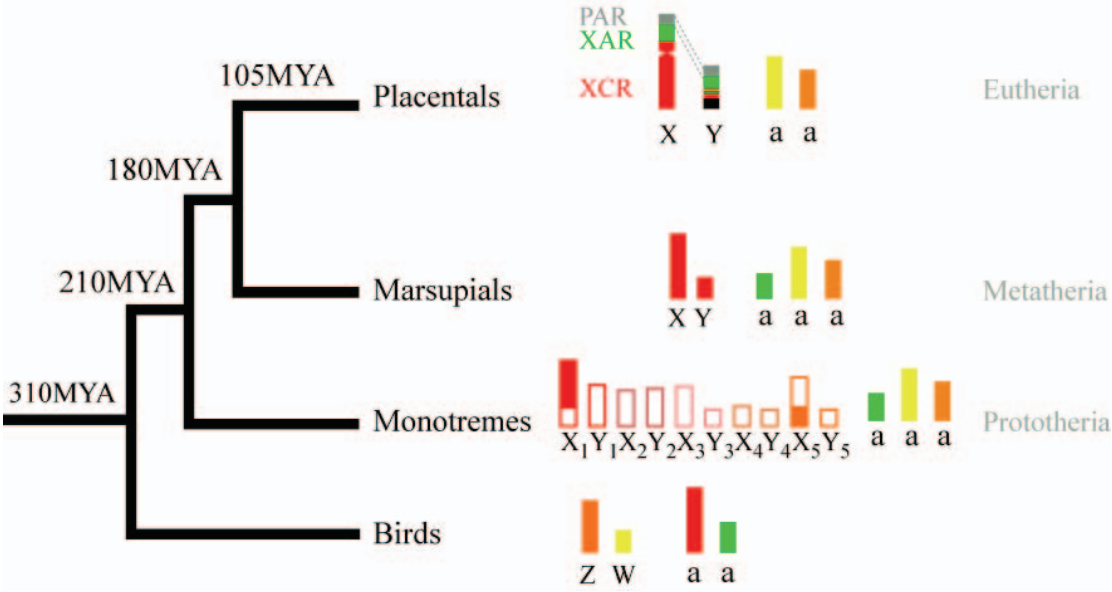

Figure 15: Schematic representation of the different sex chromosomes systems in placentals, marsupials, monotremes and birds and the relationships among them represented by a simplified phylogenetic tree with the estimated age of the clades on top of the branches. Birds show female heterogamety with a ZW female: ZZ male sex chromosome system. XCR= X Conserved Region, XAR= X recently Added Region, PAR= Pseudo Autosomal Region a= autosome.

The addition-attrition hypothesis assumes that a cycle of addition of material occurred to the sex chromosomes followed by gradual degradation (attrition) of the Y chromosome: an autosomal segment was added to the PAR of a differentiated sex chromosome, *i.e.* X chromosome, which was recombined to the PAR of the Y chromosome therefore extending the region of homology between X and Y. Once the X and Y containing the recently added regions became fixed in a population, the Y started to degrade and so genes on the Y recently added region (YAR) became inactive and were lost. The last addition (in green in Figure 15) must have occurred after marsupials diverged from eutherians 180 MYA since they correspond to

autosomes in non-eutherian mammals, but at sometime before the radiation of eutherians 105 MYA.

The first addition of an autosome onto the X would have led to a XY_1Y_2 situation, the Y_1 corresponding to the true Y and the Y_2 to the non-translocated copy of the autosomal segment. This system is known to occur in several mammalian species (Baker and Bickham 1980, Vassart *et al.* 1995) and may have been the first step in the evolution of the complex *F. mechowi* sex chromosomes. It seems likely that either the X chromosome or the autosomal segment must have possessed heterochromatin in a breakpoint region which, following the translocation, may have acted as an immediate barrier to the spread of X chromosome inactivation into the autosomal compartment. The newly translocated autosomal region would have subsequently recombined onto the Y (Graves and Foster 1994) and the free autosome homologue (Y_2) would have been selectively lost after becoming redundant.

If sex chromosome evolution in *F. mechowi* follows the addition-attrition model it is expected that pairing of the X and the Y during meiosis will involve a shorter and shorter autosomal fragment as rearrangements will accumulate on the Y and lead to suppression of recombination. That such a demunition of the Y-autosomal segments has occurred (or is currently occurring) cannot be detected due to the limitations of our methods. However, as predicted by the model, the loss of genes in the Y added region will, over evolutionary time, eventually result in an unequal gene content between females and males that can be balanced by the spread of the XCI to the translocated autosomal segment on one of the two Xs in the female which in turn will necessitate the loss of the IHB.

CHAPTER 3

DISSECTION OF A NON RECIPROCAL Y-AUTOSOME TRANSLOCATION IN *CRYPTOMYS HOTTENTOTUS*

3.1 INTRODUCTION

The recent recognition of *Fukomys* and *Cryptomys* as separate mole-rat genera (Kock *et al.* 2006) is underpinned by allozyme data (Honeycutt *et al.* 1987), nuclear and mitochondrial DNA markers (Allard and Honeycutt 1992, Ingram *et al.* 2004), as well as some chromosomal features (see Chapter 1). The diploid numbers of the *Fukomys* species vary considerably (Van Daele *et al.* 2004, 2007b) ranging from 2n=40 in *F. mechowi* (Macholan *et al.* 1993, Deuve *et al.* 2006) to 2n=78 in *F. damarensis* (Nevo *et al.* 1986). In sharp contrast, the monospecific *C. hottentotus* is reported to have an invariant 2n=54 (Nevo *et al.* 1986, Faulkes *et al.* 2004). This species, which occurs in the southern parts of Zimbabwe and ranges throughout South Africa, comprises four recognised subspecies (Bennett and Faulkes 2000): *C. h. hottentotus* (common mole-rat), *C. h. natalensis* (Natal mole-rat), *C. h. pretoriae* (highveld mole-rat) and *C. h. nimrodi* (Matabeleland mole-rat). Although previous work (Nevo *et al.* 1986) revealed subtle differences between the autosomal fundamental numbers of *C. h. natalensis* (aFN= 100) and *C. h. hottentotus* (aFN= 102), the conventionally stained karyotypes precluded detailed and meaningful comparisons among them. However, a preliminary survey of *C. hottentotus* conducted as part of a larger investigation into the chromosomal evolution of mole-rats revealed a female aFN of 100, 103 and 104 in *C. h. hottentotus*, *C. h. natalensis* and *C. h. pretoriae* respectively. More importantly, the results consistently showed that the males of the three subspecies were all characterised by 2n=53, while females had

invariant karyotypes with 2n=54, raising the possibility that a shared Y-autosome translocation could possibly underpin the recognition of the *C. hottentotus* clade.

Sex chromosome-autosome translocations are known to be deleterious (King 1993, Ashley 2002, Dobigny *et al.* 2004b) but are, nonetheless, not that uncommon in mammals (Veyrunes *et al.* 2004 and references therein). In fact, sex-autosome translocations involving both the X and the Y chromosomes have been documented in the African mole-rat species, *F. mechowi* (See Chapter 2 and Deuve *et al.* 2006). In contrast, however, the fixation of non-reciprocal Y-autosome translocation (not associated with an X-autosome translocation) is relatively rare, having been observed only in primates (*Alouatta*: Mudry *et al.* 2001; and *Aotus*: Pieczarka and Nagamachi 1988), mongooses (*Herpestes* and *Atilax*: Fredga 1972) and some bovids (Tragelaphini: Petit *et al.* 1994 and references therein). Moreover, in spite of the extensive suite of rearrangements shaping rodent genomes, Y-autosome translocations have only been noted in *Deltamys* (Sbalqueiro *et al.* 1984) and in a subspecies of *Mus minutoides* (Matthey 1964). In both human (i.e., Brisset *et al.* 2005) and cattle (Iannuzzi *et al.* 2001) the translocation manifests as clinical conditions that are often associated with azoospermia.

One would intuitively anticipate that the confirmation of a Y-autosome translocation would be a relatively trivial task using Y-chromosome painting probes. In the case of *C. hottentotus*, however, this is confounded by the heterochromatic nature of the Y and the consequent lack of hybridization of this chromosome when using available paints, even those from the relatively closely related *H. glaber* (~35 MY since common ancestry, Ingram *et al.* 2004, Deuve *et al.* 2006). Consequently given the high number of chromosomes and their generally small size, unequivocal evidence in support of the presumed Y-autosome translocation was problematic. To

overcome this an approach was implemented that relied on the visualization of synaptonemal proteins in male spermatocytes.

The structural axes of homologous chromosomes in mammals are closely conjoined along their lengths by a range of transverse proteinaceous filaments that form the synaptonemal complex (SC) during the first meiotic prophase (e.g. Moses 1956, 1969, Dobson *et al.* 1994, Schmekel *et al.* 1996). It is possible to differentially visualize both the lateral elements (composed of SCP3 and SCP2, Lammers *et al.* 1994) and the central region (composed by SCP1, among other proteins, Meuwissen *et al.* 1992) during synapsis. At pachytene, bivalents are fully synapsed along their homologous lengths so their detection by anti-SCP1 and anti-SCP3 immune staining will result in identical patterns. In most mammals, however, the X and Y chromosomes only share a small region of limited pairing termed the pseudoautosomal region (PAR, Burgoyne 1982), and therefore the central component, which is stained with anti-SCP1, is only present at the PAR. Consequently differences in SCP1 and SCP3 immunostaining provide a novel means of detecting the Y-autosome translocation in this African mole-rat species.

3.2 MATERIAL AND METHODS

The *C. h. natalensis*, *C. h. hottentotus* and *C. h. pretoriae* male and female specimens studied are listed in Table 3 (Chapter 2). The various localities from which specimens were sampled are shown in Figure 16 below.

Figure 16: Distribution of four *C. hottentotus* subspecies in South Africa (RSA) and Zimbabwe (ZIM). The sampling sites of *C. h. pretoriae* (P= Pretoria), *C. h. natalensis* (G= Glengarry, H= Howick) and *C. h. hottentotus* (St= Steinkopf, S= Sani-Pass and B= Bain's kloof) are shown.

3.2.1 Metaphase preparation and chromosome painting

Mitotic metaphases spreads were obtained from fibroblast cultures. Cell culture and the harvesting of cells followed standard procedures (See 2.2.1.1 in Chapter 2 for details). Chromosomes were sequentially G- and C-banded using trypsin (Seabright 1971) and barium hydroxide (Sumner 1972) respectively (see 2.2.1.2 and 2.2.1.3) Images were captured with a CCD camera coupled to an Olympus BX60 microscope.

We used the *H. glaber* (2n=60) chromosome-specific painting probes to confirm both the G-band homologies in the *C. hottentotus* karyotypes and the identification of the X chromosome in this species; the flow-sorting and characterization is described fully in Chapter 2. Hybridization of *H. glaber* painting probes to spermatocytes that had previously been subjected to immunostaining with SCP1 and SCP3 (see below) followed Scherthan and Cremer (1994). The denaturation step entailed treatment in 70% formamide 2xSSC, pH=7.2 at 70ºC for 5 min; slides were subsequently transferred to 3M sodium thiocyanate (NaSCN) for 3h at 65ºC and, following the hybridization step, washed in 0.05% SSC at 45ºC for 5 min. Biotinylated painting probes were detected with streptavidin conjugated to the fluorochrome Cy3 (Amersham Biosciences) and digoxigenin probes using an antibody coupled with FITC fluorochrome (Roche).

Preparations were counterstained with 4', 6' diamino-2-phenylindole (DAPI, Roche). The DAPI and Cy3 images were captured with a CCD camera coupled to an Olympus BX60 fluorescence microscope and analysed using Genus imaging System (Applied Imaging version 2.75).

3.2.2 Immunostaining of meiotic cells and visualization of the synaptonemal complex proteins

We followed Waters *et al.* (2007) for this aspect of the investigation. In brief, testis samples were dissected for immediate analysis or frozen in liquid nitrogen for later experimentation. Tissue was minced directly on a microscope slide in a drop of PBS at 4ºC. The spreading of the meiotic cells was facilitated by addition of 80µl of Lipsol (1% in water) at which point the suspension was left to stand for 35 min. The cells were fixed by the addition of 90µl of freshly prepared fixative (1% paraformaldehyde, 10% 50 mM sodium borohydride $NaBH_3$, 0.15% Triton X-100, pH 9.8) and the slides placed in humid chamber for 2h and subsequently air-dried. A final wash in 1% wetting agent (Ilfotol) was done prior to immunostaining.

Rabbit polyclonal serum was used against the SCP1 (Meuwissen *et al.* 1992) and SCP3 (Lammers *et al.* 1994) proteins. We sequentially immunostained meiotic preparations by SCP1 followed by SCP3 (Roig *et al.* 2004, with modifications). Anti-SCP1 was diluted at 1:400 in 4xSSC/0.05% Tween20 and incubated overnight at 4ºC in a humid chamber. The following day slides were washed with 4xSSC/0.05% Tween20. The proteins were detected using secondary antibody goat anti-rabbit FITC (Calbiochem, 1:100 diluted in 4xSSC/0.05% Tween 20) for 1h at 37ºC. The excess antibody was washed off with three changes of 4xSSC/0.05% Tween20 for 5 min each, and the preparations fixed with 1% paraformaldehyde. Cells were counterstained with DAPI (Roche) and mounted in anti-fade solution (Vectashield). DAPI and FITC images were

captured as above. After washing of the slides in water and then 4xSSC/0.05% Tween20, immunostaining with anti-SCP3 (1:500 in 4xSSC/0.05% Tween20) followed. Images were retrieved using the coordinates recorded above.

3.3 RESULTS AND DISCUSSION

The G-banded karyotypes of *C. h. natalensis, C. h. hottentotus* and *C. h. pretoriae* are presented in Figure 17 (a-c). Specimens of each of the subspecies were characterised by a 2n=54 (female)/ 2n=53 (male) karyotype; this is contrary to an earlier study (Nevo *et al.* 1986) which documents an invariant diploid number (2n=54) for both the sexes in *C. h. natalensis*. In addition to these data, Faulkes *et al.* (2004) report a 2n=54 diploid number in *C. h. pretoriae* but make no mention of any difference between sexes. For ease of presentation the 25 autosomal pairs have been grouped as is convention (1-25 in decreasing size). However, pair 26 is shown together with the two X chromosomes in the case of the female and to accommodate the Y-autosome translocation in males, the single autosome 26 (i.e., the X_2) together with the true X (X_1) and Y chromosome (Figure 17a-c).

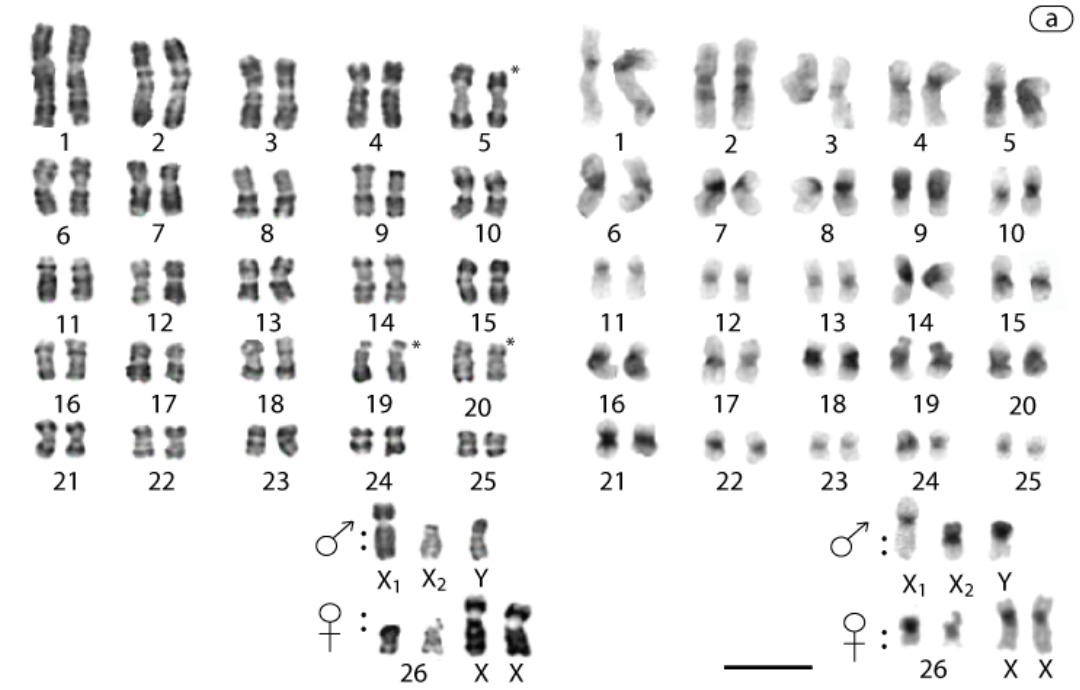
a
1 2 3 4 5*
6 7 8 9 10
11 12 13 14* 15*
16 17 18 19 20
21 22 23 24 25
♂: X1 X2 Y
♀: 26 X X
1 2 3 4 5
6 7 8 9 10
11 12 13 14 15
16 17 18 19 20
21 22 23 24 25
♂: X1 X2 Y
♀: 26 X X

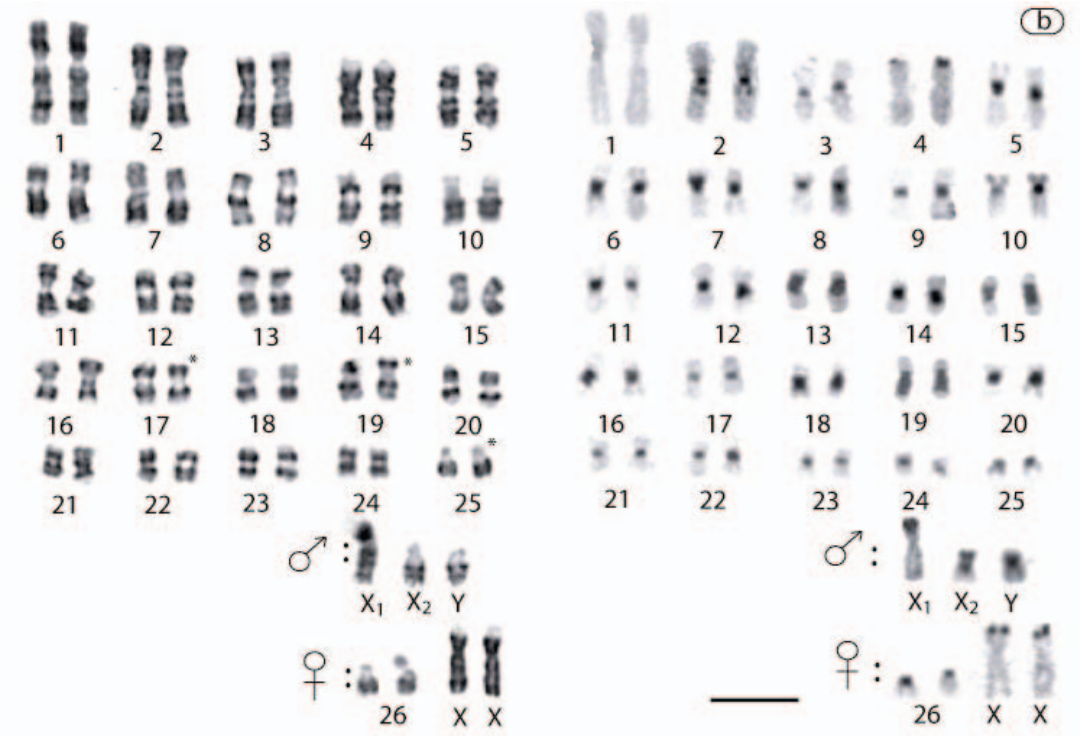
b
1 2 3 4 5
6 7 8 9 10
11 12 13 14 15
16 17* 18 19* 20
21 22 23 24 25*
♂: X1 X2 Y
♀: 26 X X
1 2 3 4 5
6 7 8 9 10
11 12 13 14 15
16 17 18 19 20
21 22 23 24 25
♂: X1 X2 Y
♀: 26 X X

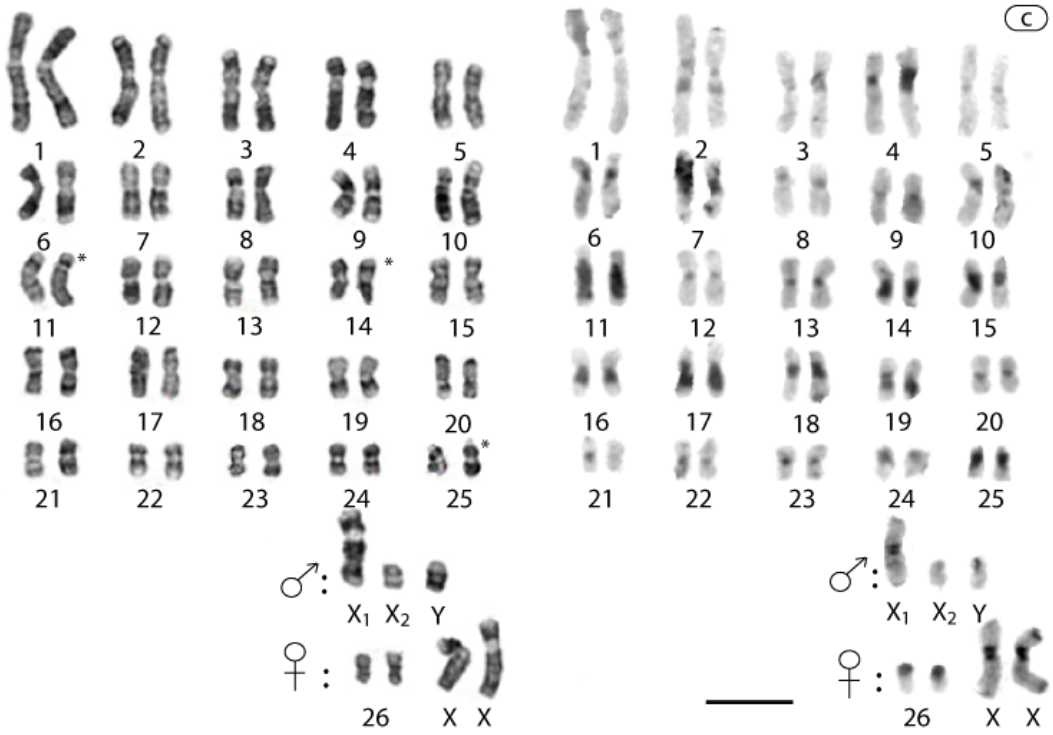

Figure 17 : G-banded and C-banded karyotypes of (**a**) *C. h. natalensis* (**b**) *C. h. hottentotus* and (**c**) *C. h. pretoriae*. The organization of the C-banded karyotypes was based on sequential staining. The sex chromosomes and the autosomes involved in the X_1X_2Y system are presented separately for the two sexes. Chromosomes are arranged according to morphology (biarmed and acrocentric) and ordered in decreasing size. Differences in heterochromatin resulted in positional changes of certain chromosomes (marked with an asterisk). The horizontal scale bars correspond to 100μm.

3.3.1 *Cryptomys hottentotus natalensis*

The standard stained karyotype presented by Nevo *et al.* (1986) (26 autosomal pairs of which 24 are biarmed giving females an aFN= 100) differs in subtle respects from that detected here (Figure 17a). The G-banded karyotype of *C. h. natalensis* comprises 25 bi-armed autosomal pairs (1-25); pair 26 was heteromorphic in the two females analysed comprising one metacentric and one acrocentric chromosome in each instance. These autosomes show a pericentromeric heterochromatic region that extends through to the terminus of the p arm but which is more prominent in the metacentric form. The X chromosome is a medium sized submetacentric chromosome (intermediate in size between pairs 4-5). One homologue of pair 26 is translocated to the Y (the Y portion of the Y-autosome translocation appears entirely heterochromatic

in C-banded preparations), with its unpaired homologue represented by X_2 (Figures 17a and 18). Other noteworthy features of the *C. h. natalensis* karyotype include (i) pair 5 that has a very large pericentromeric heterochromatic block encompassing the proximal two thirds of the q arm and extending distally to include the proximal third of 5p, and (ii) pair 19 which shows a secondary constriction in the proximal part of the heterochromatic p arm.

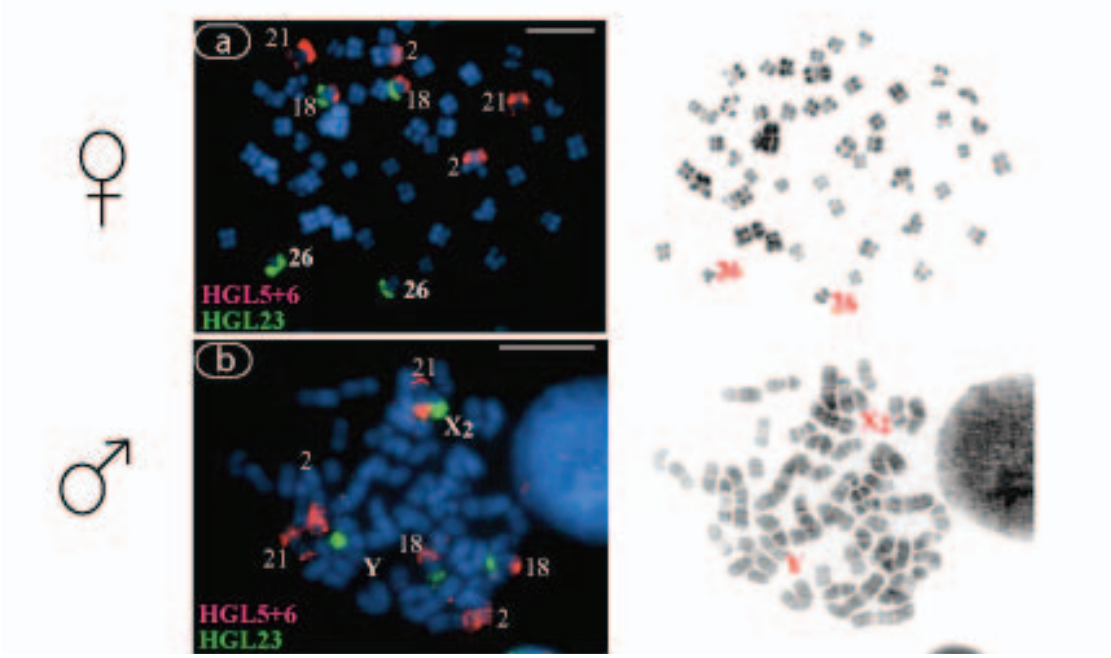

Figure 18: Double colour FISH on *C. h. natalensis* metaphase chromosomes using *H. glaber* chromosome paints HGL 5+6 detected with Cy3 (in pink) and HGL 23 detected with FITC (in green). The hybridized chromosomes' numbering corresponds to the *C. h. natalensis* karyotype presented in Figure 17a. (**a**) One of the two HGL 23 signals shows hybridization to pair 26, while in the male (**b**) the signal corresponds to the X_2 (i.e., chromosome 26) as well as the translocated partner which is fused to the Y. The inverted DAPI-stained images are included to facilitate the identification of the chromosomes. The horizontal scale bars correspond to 100µm.

3.3.2 *Cryptomys hottentotus hottentotus*

The standard stained karyotype presented by Nevo *et al.* (1986) shows females of this subspecies to have 26 autosomal pairs of which 25 are biarmed; pair 26 is depicted as acrocentric giving females an aFN= 102 (no males specimens were included in their study). In contrast the female karyotype presented in our Figure 17b

has 24 biarmed (1-24) and two acrocentric autosomal pairs (pairs 25 and 26) resulting in an aFN= 100. The X is identified as the fourth largest submetacentric by both studies. The pair 25 is acrocentric and, as in *C. h. natalensis* discussed above, the Y is translocated to chromosome 26 with its unfused acrocentric homologue represented as X_2 (Figure 17b). Both the X_2 and Y-autosome translocation have heterochromatic p arms. Based on G-band comparisons and FISH data, the acrocentric pair 25 in *C. h. hottentotus* corresponds to *C. h. natalensis* pair 19 (the positional difference is due to the larger size of this chromosome in *C. h. natalensis* resulting from heterochromatic addition). Other consistent differences observed between *C. h. natalensis* and *C. h. hottentotus*, and confirmed by the FISH data, are that *C. h. hottentotus* pair 17 shows reduced heterochromatin in comparison to its homologue (pair 5) in *C. h. natalensis*, and that the X and pair 4 in *C. h. hottentotus* show heterochromatin at the tips of the short arms which is in contrast to the centromeric C-bands observed in *C. h. natalensis*.

3.3.3 *Cryptomys hottentotus pretoriae*

This is the first karyotypic description of this subspecies. As with its subspecific relatives, *C. h. pretoriae* has a diploid number of 2n=53 (males), 2n=54 (females) and a female aFN= 104 (Figure 17c). The autosomal complement comprises 25 biarmed pairs (pairs 1-25) with pair 26 metacentric in females, as is the X_2 in males; in both chromosomes as well as the Y, the p arms are entirely heterochromatic. FISH experiments show that *C. h. pretoriae* pair 14 is homologous to *C. h. natalensis* pair 5 and to *C. h. hottentotus* pair 17, with the positional difference simply reflecting heterochromatic variation among subspecies. Other notable differences include *C. h. pretoriae* 11 which corresponds to chromosome 20 in *C. h. natalensis* and to 19 in *C. h. hottentotus* (excluding heterochromatin). As was the case with the previous

subspecies, C-bands of the *C. h. pretoriae* X chromosome appear taxon specific showing both a terminal heterochromatic p arm as well as a heterochromatic pericentromeric region.

In summary, the subtle karyotypic differences detected among *C. h. natalensis*, *C. h. hottentotus* and *C. h. pretoriae* (in respect of the C-banding patterns of several of the autosomes and the X chromosomes) all argue for an absence of gene flow among them, and therefore grounds for a possible revision of their taxonomic status. This hypothesis enjoys support from the analysis of mitochondrial RFLPs (Honeycutt *et al.* 1987) and the more recent sequencing results published by Faulkes *et al.* (2004). Both papers document substantial genetic differences among subspecies with Nei's D = 0.57 distinguishing *C. h. hottentotus* from *C. h. natalensis* (Honeycutt *et al.* 1987), and mtDNA cytochrome b sequence divergences of 11.6% between *C. h. pretoriae* and *C. h. natalensis*, 18% between *C. h. natalensis* and *C. h. hottentotus* and 16.4% recorded between *C. h. hottentotus* and *C. h. pretoriae* (Faulkes *et al.* 2004). When taken in their entirety, these data (the deep genetic divergence among taxa and their apparent karyotypic uniqueness) are clearly suggestive of the possible recognition of these mole-rats as distinct species.

3.3.4 Immunostaining of meiotic cells and visualization of the synaptonemal complex proteins

As detailed previously, the high diploid number, generally small sizes of the chromosomes comprising the karyotypes of the three southern mole-rat subspecies analysed herein (particularly the Y and pairs 24-26), and the heterochromatic nature of the Y chromosome made the identification and subsequent confirmation of the Y-autosome translocation problematic. To address this, meiotic prophase was studied by immunostaining the synaptonemal complex proteins.

Immunofluorescence of two of the proteins (SCP1 and SCP3) that constitute the synaptonemal complex (Figure 19a) revealed 26 discrete SC elements in the three subspecies representing 25 paired autosomes with the 26th SC, thought to involve three chromosomes, located within the sex body (Figure 19b). Sequential immunostaining differentially revealed: (i) the presence of the lateral elements (SCP3) anticipated in an autosomal bivalent as well in the X and Y chromosomes, and (ii) the absence of SCP1 signal on a single chromosome (the unpaired X) but, importantly, the presence of a central element is visible in the paired region of the Y-autosome translocation (Y) and its autosomal homologue (X_2) (arrowed, see Figure 19c, d and e). We extended this observation using the *H. glaber* X chromosome painting probe. Given the end-to-end association typical of the pairing between the X and Y chromosomes of this species, we anticipated that the probe would hybridize to the unpaired region revealed by the absence of SCP1 staining. This hypothesis was confirmed (Figure 19f) with the results summarised schematically in Figure 19g.

These data provide unequivocal evidence of an X_1X_2Y sex determining mechanism in these mole-rats. Given the deleterious nature of sex-autosome translocations in mammals (King 1993, Ashley 2002) it is improbable that the fusion identified in the three subspecies results from three independent events (i.e., results from convergence). The most parsimonious explanation for these results is that the translocation of the Y to an autosome occurred in their last common ancestor and, by extension, is likely to be present in the remaining subspecies, *C. h. nimrodi*, making this rare rearrangement a synapomorphy underpinning *Cryptomys* to the exclusion of all *Fukomys* species.

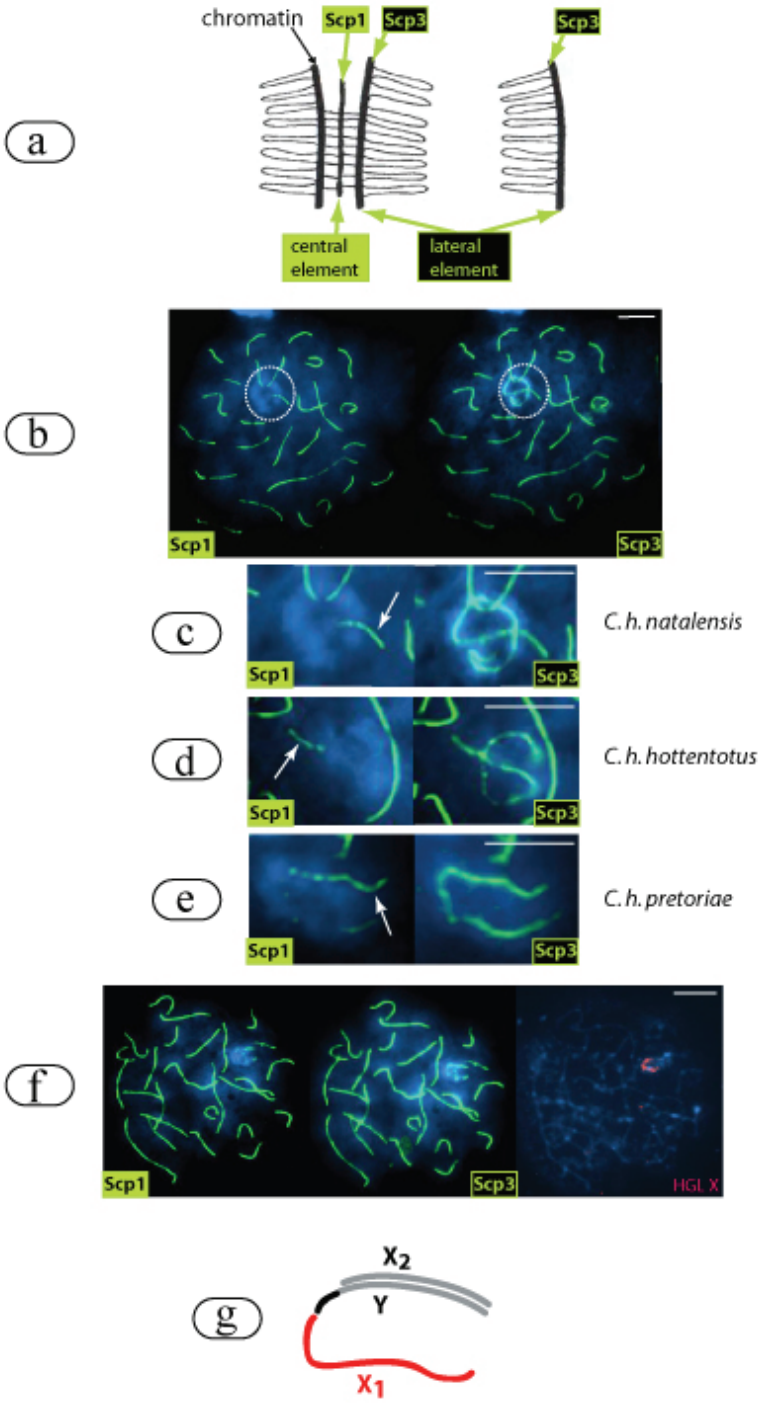

Figure 19: (**a**) Schematic representation of a synaptonemal complex (SC) showing its central and lateral elements and the corresponding proteins (SCP1 and SCP3) (redrawn from Dobson *et al.* 1994) which were detected by immunostaining in the present investigation. The diagram on the left shows the configuration for paired chromosomes and on the right, an unpaired chromosome that would be detected only by SCP3 immunofluorescence. (**b**) to (**e**): Spermatocytes of *C. hottentotus* subspecies sequentially immunostained with SCP1 and SCP3 with arrows indicating the region of synapsis between X_2 and Y. Bar = 10µm. (**f**) Sequential FISH with an *H. glaber* X chromosome painting probe (HGL X) on a *C. h. hottentotus* spermatocyte that was previously stained for the synaptonemal complex proteins SCP1 and SCP3. The position of the X chromosome in the sex body is evident from the FISH result. (**g**) Schematic representation of the trivalent X_1X_2Y detected in (b)-(f).

3.3.5 C-banding of spermatocytes

It was noted that in approximately 25% of the *C. h. natalensis* and *C. h. hottentotus* cells analysed (n=151), SCP3 immunostaining revealed two regions of asynapsis (neither of which were visible in the heterochromatically more depauperate *C. h. pretoriae*, see Figure 19e). One fell within the sex body, and the second protruded from the X_1X_2Y pairing configuration (arrowed in Figure 20a and schematically represented in Figure 20b). (In 75% of cases, SCP1 can be observed along the entire length of the X_2Y indicating pairing of the heterochromatic arms). In order to further examine this phenomenon, the orientation and C-banding patterns of the X_1X_2Y trivalent in *C. h. natalensis* were analysed during the first meiotic division. Figure 20c shows a spermatocyte in diakinesis. From three to five bivalents with one terminal or subterminal chiasma were observed, and between 19 and 21 bivalents with two terminal chiasmata were observed. There was always one bivalent with three chiasmata and one linearized trivalent characterised by two chiasmata. The longest element of the trivalent corresponds to X_1 and is characterised by a single site of pericentromeric heterochromatin (Figure 20d). The X_1, in turn, is in an end-to-end association with the Y chromosome through a terminal chiasma at Yp (presumably the PAR). This region of contact is C-band positive (and corresponds to the heterochromatic short arm of Yp – see Figure 17a-c) and is followed by the euchromatic portion of the translocated 26 that is in turn sassociated with its unfused homologue X_2 through a terminal chiasma. Interestingly, the C-positive block on the *C. h. natalensis* X_2 chromosome spans the centromere and the disjunction is clearly evident in Figure 20d.

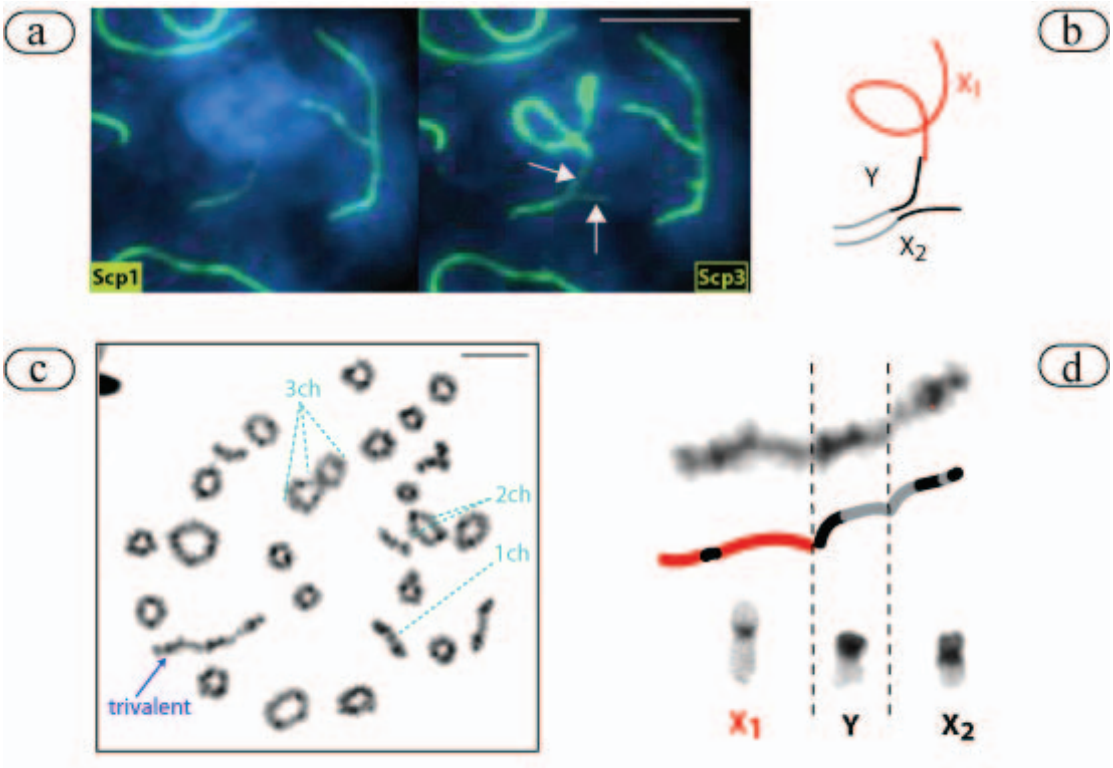

Figure 20: (**a**) Enlargement of a *C. h. natalensis* sex-trivalent sequentially immunostained for SCP1 and SCP3. The unpaired heterochromatic short arms of X_2 and the Y are indicated by arrows. Bar = 10µm. (**b**) Schematic interpretation of the trivalent observed in (a). (**c**) C-banding of a *C. h. natalensis* meiotic spread at diakinesis. Among the bivalents identified by C-banding, five have one terminal or subterminal chiasma (ch), 19 have two terminal chiasmata, and one has three chiasmata. The X_1X_2Y trivalent is indicated. Bar = 10µm. (**d**) Enlargement of the trivalent shown in (c) with explanatory schematic (red = X_1; black = heterochromatin; grey = euchromatin of X_2 and Y), and the corresponding C-banded metaphase chromosomes.

Asysnapsis between the original X (X_1) and the Y in all three subspecies is not surprising considering that these chromosomes are likely to be almost completely differentiated with the exception of a small PAR, as is observed in most placental mammals (including other rodents). However, these results also clearly show that asynapsis of X_2 and Y in *C. h. natalensis* and C. *h. hottentotus* occurs and that this involves their heterochromatic arms. As with previous observations in the mouse, where formation of a synaptonemal complex was observed across heterochromatic regions (although recombination nodules were less frequent than in euchromatin; Stack 1984, Anderson *et al.* 1999), we also observed synapsis of the autosomal

heterochromatic regions at pachytene in our species (Figure 19b) (which are heterochromatin rich; see Figure 17a-c). Hence, asynapsis within these mole-rat genomes was associated only with sex chromosomes.

The asynapsis observed between the Y and the X_2 p arms leads to the absence of chiasma formation in this region further emphasising that recombination is reduced between these chromosomes. Within this context it may be that in the mole-rats studied here, the involvement of heterochromatic arms is a prerequisite (or at least it can accelerate the process) for the suppression of recombination (necessary for Y/X_2 differentiation) since the sister taxon (*C. h. pretoriae*), which lacks these heterochromatic arms), displays complete synapsis of Y and X_2 in 100% of cells examined (n= 20). An early, critical event in sex chromosome evolution is the suppression of recombination, after which the sex specific chromosome begins to degrade and differentiation occurs (i.e. Y chromosomes in mammals; reviewed in Charlesworth 1991, Charlesworth and Charlesworth 2000; see also Chapter 2). This being the case, the reduced recombination observed here indicates that differentiation of the Y from X_2 might ultimately occur, resulting in X_2 becoming a true X (i.e., at least partly hemizygous in males), and that this may represent a critical early step in meiotic chain generation. Significantly any subsequent translocations of autosomes to unpaired parts of the sex chromosomes in this system, followed by suppression of recombination between the newly translocated regions, would lead to the development of the longer "meiotic multiples" (see Gruetzner et al. 2006) so elegantly shown for the platypus (Gruetzner *et al.* 2004, Rens *et al.* 2004 and Figure 15).

In conclusion, although Y-autosome translocations are often associated with male infertility in humans (Hsu 1994) due to the disruption of azoospermic factors (AZF) or defective pairing during meiosis (Brisset *et al.* 2005 and references therein),

any deleterious effects resulting from this rearrangement must have been circumvented in mole-rats. While its natural occurrence intuitively argues against any disruption of AZF, the final arbiter of correct segregation is the meiotic apparatus and the production of euploid gametes is likely to depend on a complex interaction between the specific morphology of the translocation chromosome and its ability to orient properly on the metaphase plate and segregate in alternative fashion. These and other selective constraints, including population characteristics that allow the fixation of the rearrangement, all contribute to the rarity of non-reciprocal Y-autosome translocations in mammals, and to this rearrangement's uniqueness in the *C. hottentotus* lineage.

CHAPTER 4

CHROMOSOMAL PHYLOGENY AND EVOLUTION OF THE AFRICAN MOLE-RATS (BATHYERGIDAE)

4.1 INTRODUCTION

Although the African mole-rats are strictly subterranean (see Chapter 1) they are extremely variable within their adaptive niche. They range in mass from ~30g up to 2kg, occur in a wide range of soil types (from sand to fine clay soils) and climates (mesic to xeric, Bennett and Faulkes 2000 and references therein), and their social organization extends from solitary through to eusocial (Jarvis and Bennett 1990). Perhaps not surprisingly, given their life histories and habitat preferences, chromosomal variation is pronounced and varies from a low of 2n=40 to a high of 2n=78 (Nevo *et al.* 1986, Macholan *et al.* 1993, Deuve *et al.* 2006). Of the species, the eusocial *H. glaber* (2n=60, George 1979, Capanna and Merani 1980) is considered to be the most basal, followed by the solitary *H. argenteocinereus* (2n=60, 62, George 1979, Scharff *et al.* 2001). Both monotypic genera occur in eastern and south-eastern Africa. Of the remaining taxa, the relationship between *Bathyergus, Georychus* and *Cryptomys sensu lato* is reflected in an unresolved trichotomy in most studies (Allard and Honeycutt 1992, Faulkes *et al.* 1997, Walton *et al.* 2000, Ingram *et al.* 2004), although one analysis (Faulkes *et al.* 2004) groups the solitary living *Bathyergus* and *Georychus* as sister genera. There is limited diploid number variation among them; early work by Matthey (1956) and Nevo *et al.* (1986) documents a 2n=54 in *B. janetta* and *G. capensis*, and a 2n=56 in *B. suillus*.

Cryptomys sensu lato is most recently considered to comprise two genera (Kock *et al.* 2006) which is supported by allozyme (Honeycutt *et al.* 1987), nuclear and mitochondrial DNA markers (Allard and Honeycutt 1992, Faulkes *et al.* 2004, Ingram *et al.* 2004). The first of these, *Fukomys*, shows marked chromosomal variation that extends from 2n=40 in *F. mechowi* (Macholan *et al.* 1993), which also carries an X and Y-autosome translocation (See Chapter 2 and Deuve *et al.* 2006), to either 2n=74 recorded for a female *F. damarensis* originating from northern Namibia, or 2n=78 reported for a male captured in the South African Kalahari (Nevo *et al.* 1986). The second genus, the monotypic *Cryptomys*, is thought to contain up to five (Ingram *et al.* 2004) or six (Faulkes *et al.* 2004) different subspecies, depending on the authority followed. Here, as elsewhere in the study, the taxonomy of Bennett and Faulkes (2000) is used and the following subspecies recognised: *C. hottentotus hottentotus* (common mole-rat), *C. h. natalensis* (Natal mole-rat), *C. h. pretoriae* (highveld mole-rat) and *C. h. nimrodi* (Matabeleland mole-rat). In contrast to *Fukomys*, and although both *Fukomys* and *Cryptomys* are regarded as social, all *Cryptomys* are characterised by a rather conserved karyotype (2n=54) with only heterochromatic differences among them (Nevo *et al.* 1986). They do, however, all share a Y-autosome translocation that underpins this phylogenetic group (Chapter 3).

Given this karyotypic variation and the premise that chromosome rearrangements have a low rate of convergence (Rokas and Holland 2000) and are therefore likely to be phylogenetically informative, we set out to identify chromosomal characters that could be used to reconstruct the evolutionary history of these endemic African rodents. Conventional banding methods and molecular cytogenetic approaches that relied on fluorescence *in situ* hybridization of mole-rat specific painting probes (Chapter 2, Deuve *et al.* 2006) were used to investigate the

unresolved intergeneric and interspecific relationships between *Bathyergus*, *Georychus* and *Cryptomys sensu lato*. Characters were polarised using an outgroup species, *T. swinderianus*. Additionally, we sought to validate the recognition of *Fukomys* as a lineage distinct from *Cryptomys sensu stricto* since this recognition is currently based only on molecules with no support from morphology (Kawalika and Burda 2007). Furthermore the use of a subterranean niche, which is synonymous with restricted mobility and spatial isolation, is known to have led to rapid chromosomal evolution in other families of subterranean rodents (i.e., Spalacidae) where the 2n is regarded to increase gradually towards arid regions that are associated with unpredictable climates (Nevo 1991, Nevo *et al.* 1994). These same parameters are thought to be responsible for the establishment of eusociality in both *H. glaber* and *F. damarensis* (Jarvis *et al.* 1994, Faulkes *et al.* 1997), and the confirmation of this in other bathergids would greatly enhance the generality of this hypothesis.

4.2 MATERIAL AND METHODS

4.2.1 Specimens studied

G- and C-banded karyotypes were prepared for representatives of *Bathyergus*, *Georychus*, *Heliophobius*, *Heterocephalus*, *Cryptomys* and *Fukomys*. We were limited in access to *Fukomys* and chose *F. mechowi* (2n=40, of which sex chromosomes have been studied in Chapter 2) and *F. damarensis* (2n=74, 78) as representative taxa since they reflect the two extremes in the diploid number of this genus. A third species, *F. darlingi,* was also included; it has 2n=54, a chromosome number that is shared with other African mole-rats (Aguilar 1993). See Table 3 in Chapter 2 for a summary of the species included in this investigation, their original localities, the number of specimens analysed, and their diploid numbers.

4.2.2 Metaphase preparation and chromosome painting

Mitotic metaphase spreads were obtained from fibroblast cultures and bone marrow cells. Cell culture and the harvesting of cells followed standard procedures (detailed in Chapter 2). Chromosomes were sequentially G- and C-banded using trypsin (Seabright 1971) and barium hydroxide (Sumner 1972) respectively. We used chromosome-specific painting probes derived from *H. glaber* (2n=60), previously described in 2.3.1 and in Deuve *et al.* (2006). *In situ* hybridization of *H. glaber* painting probes followed Yang *et al.* (1997a), reviewed in Rens *et al.* (2006), and was performed onto chromosomes of *H. argenteocinereus*, *B. janetta* and the *Fukomys* species, *F. mechowi*, *F. damarensis*, and *F. darlingi*. This was extended to include the outgroup species, *T. swinderianus*, which is the sister taxon to Bathyergidae (Huchon *et al.* 2002) and when the banding homologies were confounded by variation in heterochromatin, to specimens of the three *C. hottentotus* subspecies and *G. capensis*. See Chapter 2 for a detailed description of the fluorescence *in situ* hybridization method followed. Images were captured with a CCD camera coupled to an Olympus BX60 microscope and analysed using Genus imaging System (Applied Imaging version 2.75).

4.2.3 Phylogenetic analyses

Chromosomal segmental associations (adjacent syntenies) were used to establish a matrix of characters. Adjacent syntenies were coded from the cross-species painting data of eleven species/subspecies of African mole-rats and the outgroup, *T. swinderianus*. Three different coding strategies were implemented: (i) adjacent syntenies were scored as absent (0) or present (1), (ii) adjacent syntenies were scored as in (i) but we included the presence (1) or absence (0) of a centromere disrupting the adjacent synteny under consideration and (iii), using a multiple state approach, adjacent syntenies were coded as being absent (0), present on the same arm (1), present and disrupted by a centromere (2),

and present either on the same arm, or disrupted by a centromere (3). All characters were weighted = 1 except for the sex-autosome translocations (characters number 41, 42 and 55 in Table 5) which were given an arbitrary weight = 2 because of their known negative impact on the meiotic process (King 1993, Ashley 2002, Dobigny *et al.* 2004b). In addition, in some instances the only detectable difference between species' karyotypes was variation in heterochromatic distribution and amount; since these were consistent among taxa they were scored and included in our chromosomal matrix but given a weight of 0.5 due to their homoplasic nature. The most parsimonious phylogenetic tree was obtained using an exhaustive search in PAUP* v. 4.0b10 (Swofford 1999). The robustness of each node was assessed by bootstrap estimates of 1000 replications.

As a second approach at defining phylogenetic relationships among selected taxa based on shared chromosomal rearrangements, a computational method that has conventionally been used to trace the evolutionary process of genome reorganization based on DNA sequence or gene order data was used (Bourque and Pevzner 2002). The algorithm (Multiple Genome Rearrangement or MGR, http://www-cse.ucsd.edu/groups/bioinformatics/MGR) calculates the minimum number of rearrangements between synteny blocks (conserved homologous segments with a mostly conserved gene order) to explain the evolutionary changes between genomes. Briefly, when implemented with more than three genomes the algorithm searches for rearrangements that will reduce the overall genomic distance (i.e. the number of rearrangements in a most parsimonious scenario between multi-chromosomal genomes) until two genomes become identical (i.e. converge to the ancestor). One of them is subsequently removed and the search starts again with the remaining genomes until these are transformed into an identical genome. The algorithm is implemented to search for rearrangements that will not break a "conserved adjacency" (= a pair of markers that is

present in all genomes). The hybridization signals resulting from the *H. glaber* painting experiments (with no reference to centromere position or to intrachromosomal rearrangements since these cannot be identified using chromosome painting; see Robinson and Seiffert 2004) were analysed using GRIMM (Genome Rearrangements in Man and Mouse, http://www-cse.ucsd.edu/groups/bioinformatics/GRIMM). This algorithm optimizes the signs of the chromosomal regions that could not be determined unequivocally by G-band comparisons thus minimizing the genomic distances among species' genomes (Tesler 2002). Analysis of these signed data using MGR allowed the determination of the most parsimonious number of rearrangements between karyotypes, and the construction of a phylogeny. In so doing, the cross-species painting results from *F. damarensis*, *F. darlingi*, *F. mechowi* and the sister taxa *B. janetta* and *H. argenteocinereus* were used. *Heterocephalus glaber* was not included because we were unable to confidently assign chromosomal subregions in this highly rearranged karyotype. The rationale for using *B. janetta* was that it is representative of the 2n=54 karyotype (present in *B. suillus*, *G. capensis* and *C. hottentotus*). Since it was necessary to enforce part of the topology (i.e., the *Fukomys* ancestral karyotype - see discussion), two analyses were conducted. The first involved constraining the analysis to the three *Fukomys* species and *B. janetta,* and the second by constraining the analysis to the *Fukomys* species + *B. janetta*, and *H. argenteocinereus*.

4.3 RESULTS

4.3.1 *Heliophobius argenteocinereus*

We present a female karyotype (2n=62, aFN= 114) of a Tanzanian *H. argenteocinereus* specimen that comprises 27 biarmed autosomal pairs (HAR 1-27), three acrocentric (HAR 28-30) and an X chromosome of comparable size to the

largest autosome pair in the complement (Figure 21). Most of the chromosomes have large, lightly stained centromeric regions (see pairs 1, 3, 6, 7, 9, 10, 16, 19, 20, 22 and X) that are heterochromatic on C-banding (Figure 21b).

The regions of homology with *H. glaber* are indicated by vertical bars to the right of each chromosome pair. The *H. glaber* paints revealed 45 regions of homology. Those signals that were interrupted by unhybridized blocks of heterochromatin were considered conserved syntenies. Seven *H. glaber* chromosomes (HGL 8, 15, 16, 18, 19, 28 and 29) are retained *in toto* but fused with other autosomal segments (see HAR 2, 4, 6, 8, 10 and 17), and three (HGL 21, 25 and X) are retained as a single chromosome in *H. argenteocinereus* (HAR 19, 20, and X). Twelve *H. glaber* painting probes corresponding to HGL 1-3, 5, 6, 10-14, 17 and 23 produced two signals on *H. argenteocinereus* chromosomes (HAR 2-4, 5, 6, 9, 11, 13-18, 21-25, 27 and 29). *Heliophobius argenteocinereus* chromosome 5 is hybridized by HGL 6 but the synteny is disrupted by HGL 17. The *H. argenteocinereus* chromosomes HAR 1p, distal 3q and 12p are not hybridized by the HGL probes and are thought to reflect regions that would have been detected by paints for the two chromosomes for which we do not have painting probes, HGL 4 and 24.

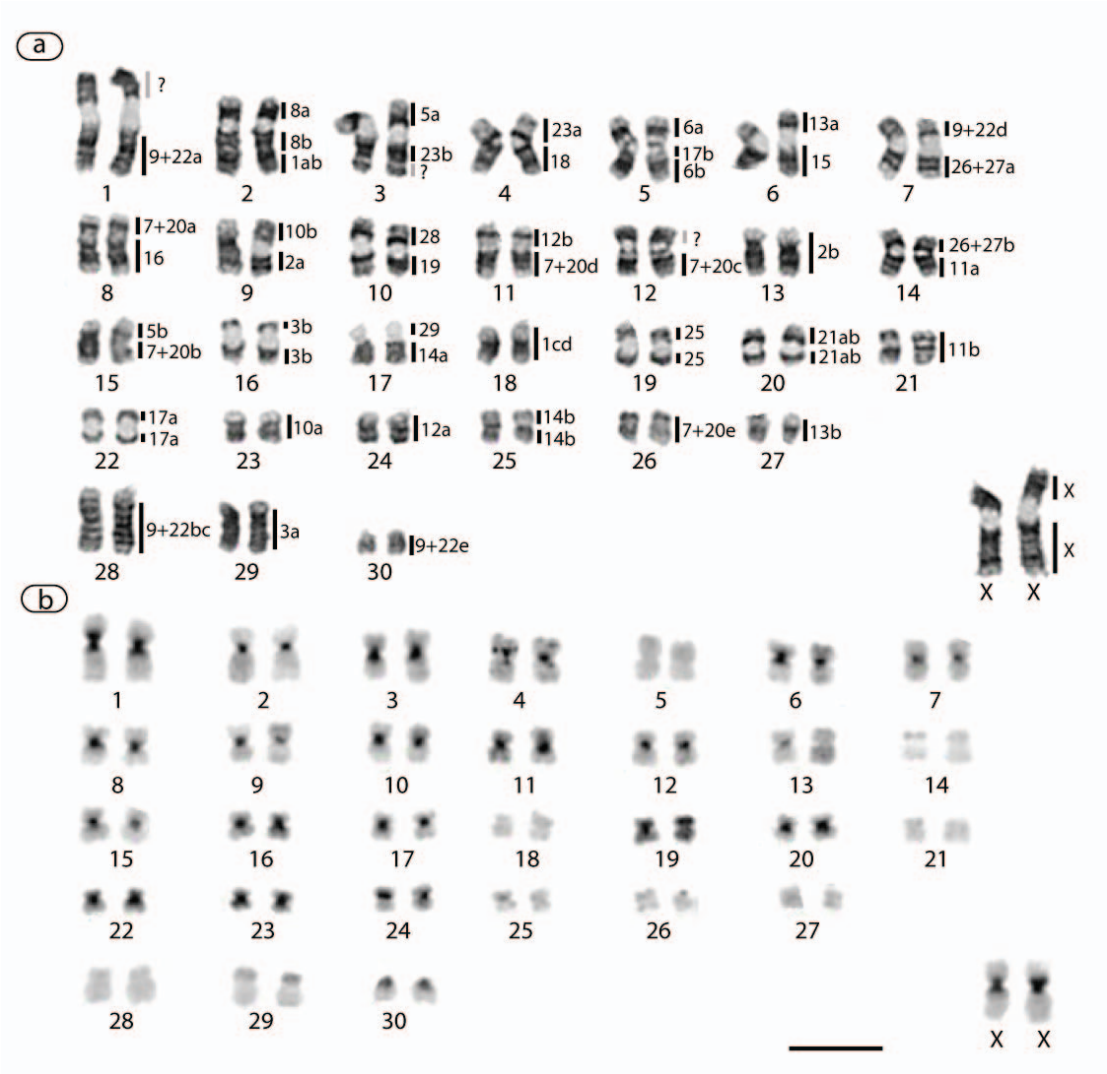

Figure 21: (**a**) G-banded and (**b**) C-banded karyotypes of *H. argenteocinereus* with (a) the approximate regions of homology to *H. glaber* as determined by cross-species painting shown to the right of each chromosomal pair. The letters a, b, c and d refer to homologies of subregions that were used to implement the MGR algorithm (see Table 6). The abbreviation ? = regions that have not been hybridized by any of the *H. glaber* paints. Bar = 100μm.

4.3.2 *Bathyergus* and *Georychus*

In agreement with previous work (Nevo *et al.* 1986), *B. janetta* has 2n=54 comprising 26 biarmed autosomal pairs (BJA 1-26, aFN= 104), a large metacentric X of similar size to BJA 2, and an acrocentric Y. Using sequential C-banding it was possible to show that heterochromatin was present in the X, BJA 11, BJA 16 and BJA 17 (Figure 22). In all instances the heterochromatic blocks were verified by C-

banding and by FISH. Although the sister species *B. suillus* has been described to have a karyotype of 2n=56 with three acrocentric autosomal pairs, the analyses consistently revealed a 2n=54 karyotype, identical to that of *B. janetta* (not shown).

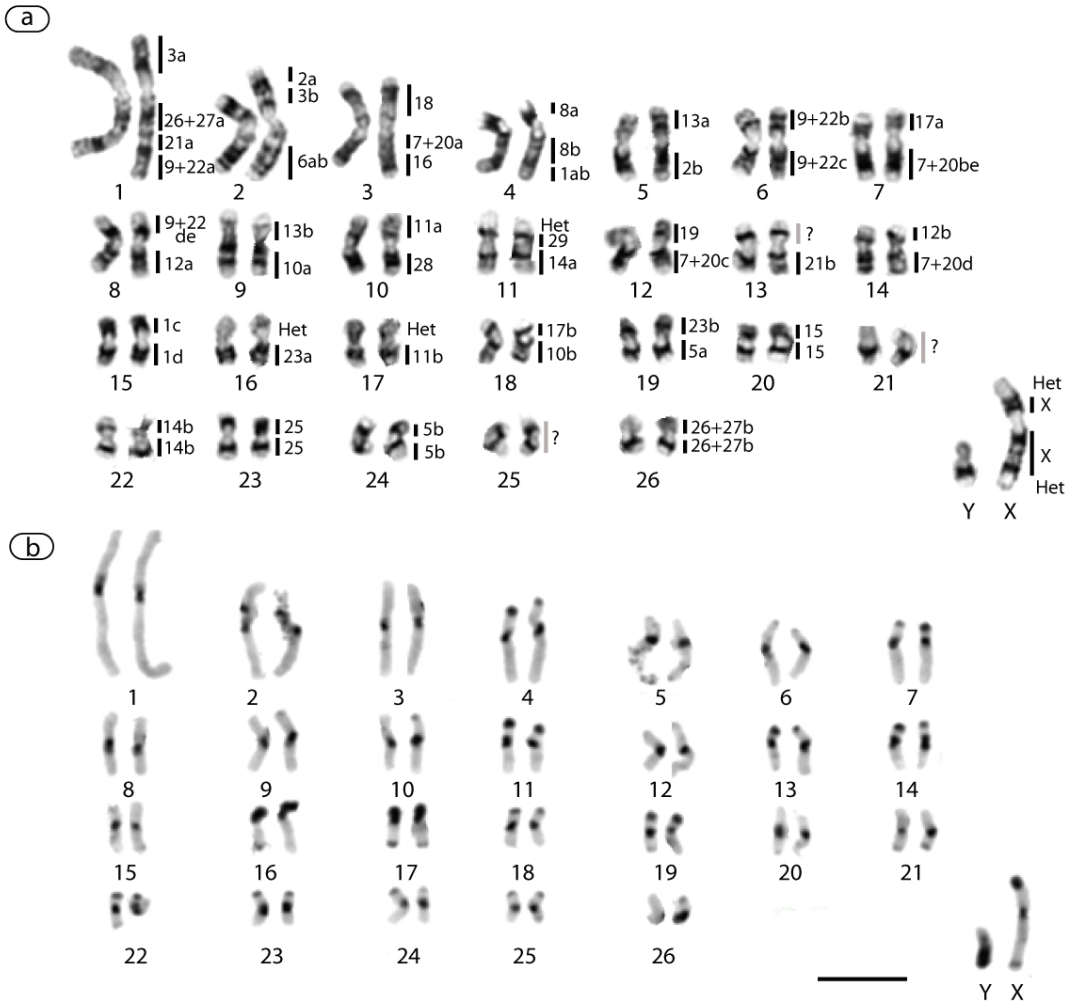

Figure 22: (**a**) G-banded and (**b**) C-banded karyotypes of *B. janetta* with (a) the approximate regions of homology to *H. glaber* as determined by cross-species painting shown to the right of each chromosomal pair. The letters a, b, c and d refer to homologies of subregions that were used to implement the MGR algorithm (see Table 6). The abbreviation Het = heterochromatin; ? = regions that have not been hybridized by any of the *H. glaber* paints. Bar = 100µm.

The first karyotypic description of *G. capensis* was presented by Matthey (1956), the findings of which were confirmed by Nevo *et al.* (1986). Both studies document a 2n=54 for the species with the two smallest autosomal pairs being

acrocentric in morphology (aFN= 100). Based on G-banding, C-banding and FISH comparisons, the *G. capensis* karyotype was found to be identical to that of both *B. janetta* and *B. suillus* (see the half-karyotype comparison in Figure23a), except that in *G. capensis* there was no evidence of heterochromatic variation (i.e., the entire chromosomes homologous to BJA 16 and BJA 17 were hybridized in *G. capensis*, see Figure23b).

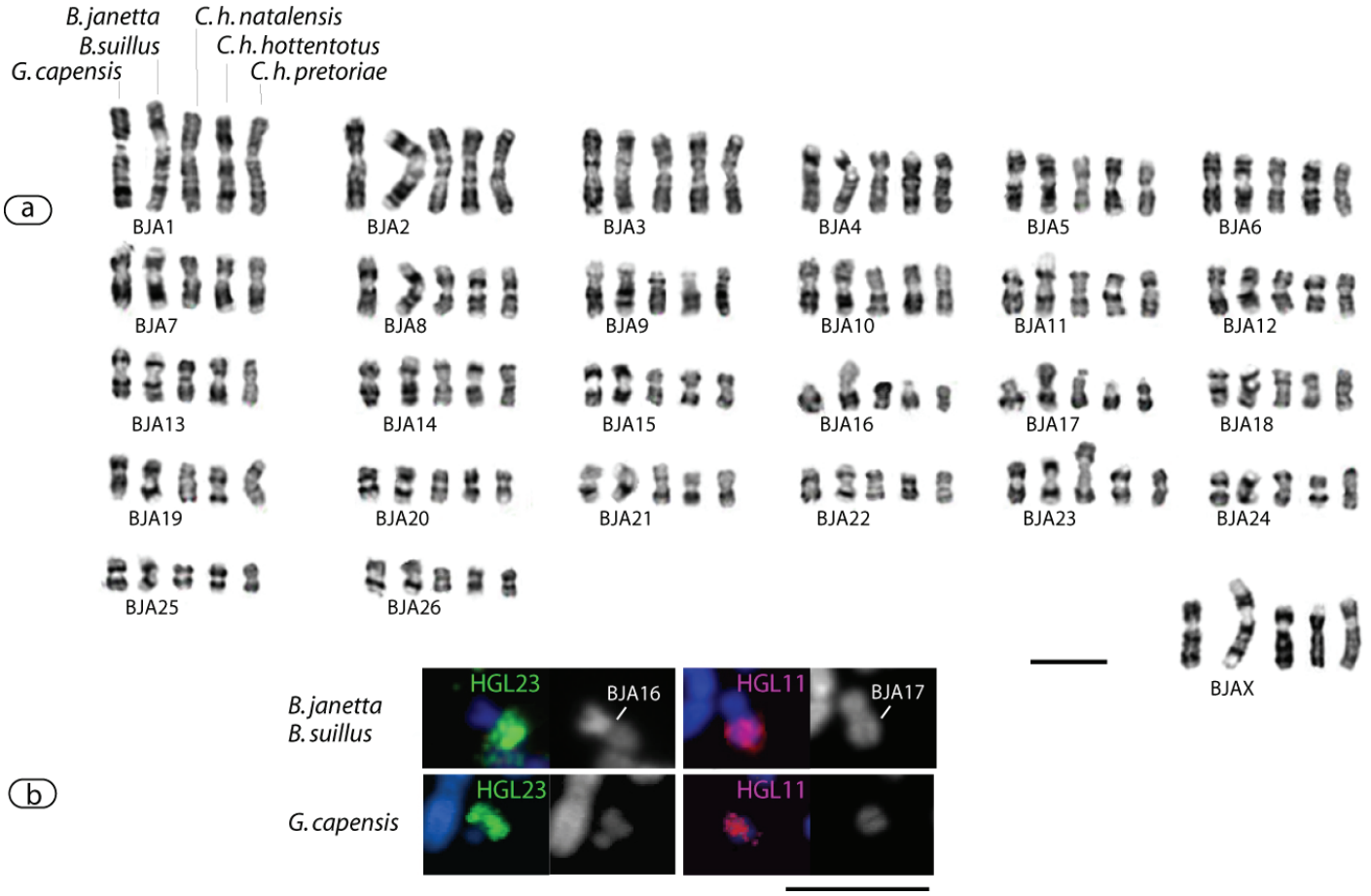

Figure 23: (**a**) Comparison of the G-banded half karyotypes of *G. capensis*, *B. janetta* (similar to *B. suillus*), *C. h. natalensis*, *C. h. hottentotus* and *C. h. pretoriae*. Chromosome numbering follows the *B. janetta* nomenclature (BJA). (**b**) Comparison of FISH results using HGL 23 (green) and HGL 11 (pink) in *Bathyergus* and *Georychus*. Bars = 100µm.

The HGL probes detected 43 conserved segments in *B. janetta*, *B. suillus* and *G. capensis*. Seven *H. glaber* chromosomes (6, 8, 16, 18, 19, 28 and 29) were found retained *in toto* in these species but fused to other autosomal segments (see BJA 2-4 and 10-12 in Figure 22). Three (HGL 15, 25 and X) are retained in their entirety as a single chromosome in all three species (corresponding to BJA 20, 23 and the X, Figure 22). Twelve *H. glaber* chromosomes paints (HGL 1-3, 5, 10-14, 17, 21 and 23) produce two signals on *B. janetta* chromosomes 1, 2, 4, 5, 7-11, 13-19, 22 and 24. Three chromosomes/regions in *B. janetta*, *B. suillus* and *G. capensis* were identified that were not hybridized by any of the HGL probes used in the study, these correspond to BJA 13p, 21 and 25 (Figure 22).

4.3.3 *Cryptomys hottentotus*

We established karyotypes for three of the four recognised *C. hottentotus* subspecies, *C. h. natalensis* (CHn), *C. h. hottentotus* (CHh) and *C. h. pretoriae* (CHp), all of which share a Y-autosome translocation that involves the chromosome homologous to BJA 16 (Chapter 3). Consequently, males of this species have 2n=53 whereas the females have 2n=54 and a karyotype that is identical to that of the other 2n=54 species (Figure 22, Figure23a).

4.3.4 *Fukomys*

The *F. darlingi* (FDAr – abbreviated in this manner to distinguish it from *F. damarensis* or FDAm) karyotype presented in Figure 24 has 14 biarmed and 12 acrocentric autosomal pairs (aFN= 80) and a diploid number of 2n=54, all in agreement with Aguilar's (1993) findings which were based on Giemsa staining and C-banding. Although the X was described by Aguilar as a medium size subtelocentric chromosome, it was identified by chromosome painting as the second largest biarmed chromosome of the karyotype, with a pronounced block of heterochromatin extending

from the middle of the p arm to its terminus. The Y is the smallest acrocentric chromosome in the complement. Cross-species hybridization with the HGL probes revealed 45 conserved chromosomal segments in the *F. darlingi* genome. Nine *H. glaber* chromosomes (HGL 6, 15, 16, 18, 19, 25, 28, 29 and X) were retained in their entirety of which four (HGL 6, 15, 19 and X) are present as single chromosomes (FDAr 6, 12, 26 and X), and five are fused to other autosomal segments on FDAr 2, 7, 8, 16 and 18. Twelve *H. glaber* probes (HGL 2, 3, 5, 8, 10-14, 17, 21 and 23) produced two signals each on *F. darlingi* chromosomes 1-4, 8, 10, 11, 13, 15-21, 24 and 25. The painting probe containing HGL 1 produced three signals on FDAr 3 and 22 respectively. Regions showing no hybridization (presumably corresponding to missing paints) are FDAr 4p, FDAr 4q proximal and FDAr 9.

Several *F. damarensis* (FDAm) specimens from South Africa and Namibia were examined all of which showed a constant diploid number of 2n=80 (Figure 25) which differs from the 2n=74 and 2n=78 documented by Nevo *et al.* (1986) for Namibian and South African specimens respectively, and an aFN= 84. The data show the karyotype of this species to comprise 36 acrocentric pairs (FDAm 1-36) and three biarmed autosomes (FDAm 37-39). The second largest acrocentric has a large heterochromatic block that varied in amount between the homologues (i.e., it was heteromorphic) in all specimens examined (n=17) and which comprised approximately half the length of this chromosome. The X chromosome also possesses a pronounced heterochromatic block, in this case on its p arm, which makes up approximately half the length of this chromosome. A similar expansion is evident on the Y (Figure 25).

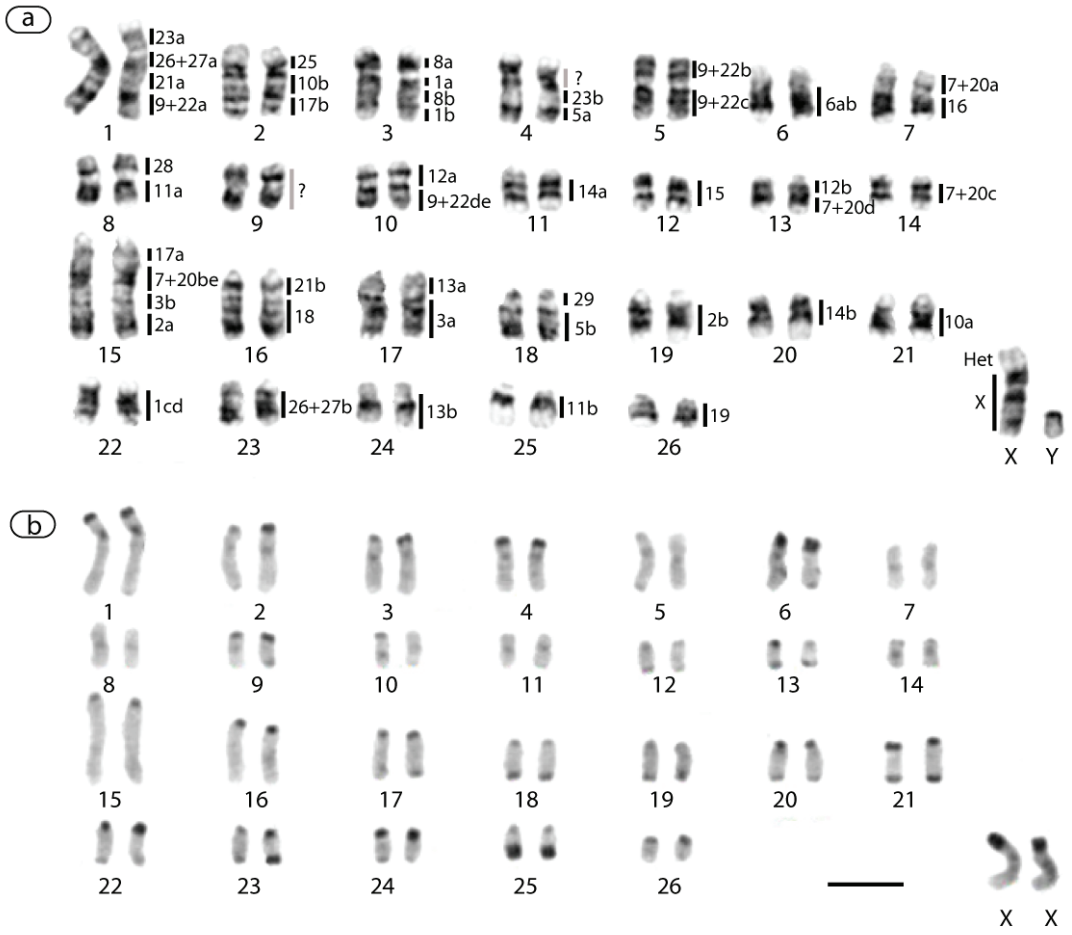

Figure 24: (**a**) G- and (**b**) C-banded karyotypes of *F. darlingi* showing in (a) the approximate regions of homology to *H. glaber* as determined by cross-species painting shown to the right of each chromosomal pair. The letters a, b, c and d refer to homologies of subregions that were used to implement the MGR algorithm (see Table 6) Bar = 100μm.

Hybridization of the *H. glaber* painting probes to *F. damarensis* revealed 47 conserved chromosomal segments. Six *H. glaber* chromosomes (HGL 6, 15, 18, 19, 25 and X) were retained as single chromosomes in the *F. damarensis* karyotype (corresponding respectively to FDAm 6, 8, 3, 18, 25 and X). In addition three other chromosome paints (HGL 16, 28 and 29) were conserved as a single chromosome but in this case fused to other autosomal segments (FDAm 2, 5 and 20). Twelve painting probes (HGL 2, 3, 5, 8, 10-14, 17, 21 and 23) produced two signals on FDAm 1, 4, 5, 7, 10, 11, 14-16, 21-23, 27-29, 32-36, 38 and 39; HGL 1 revealed four regions of hybridization on the pairs FDAm 4, 26 and 30 respectively. The regions FDAm 20q

distal, 30q distal and 37 were not hybridized by any of the available *H. glaber* painting probes.

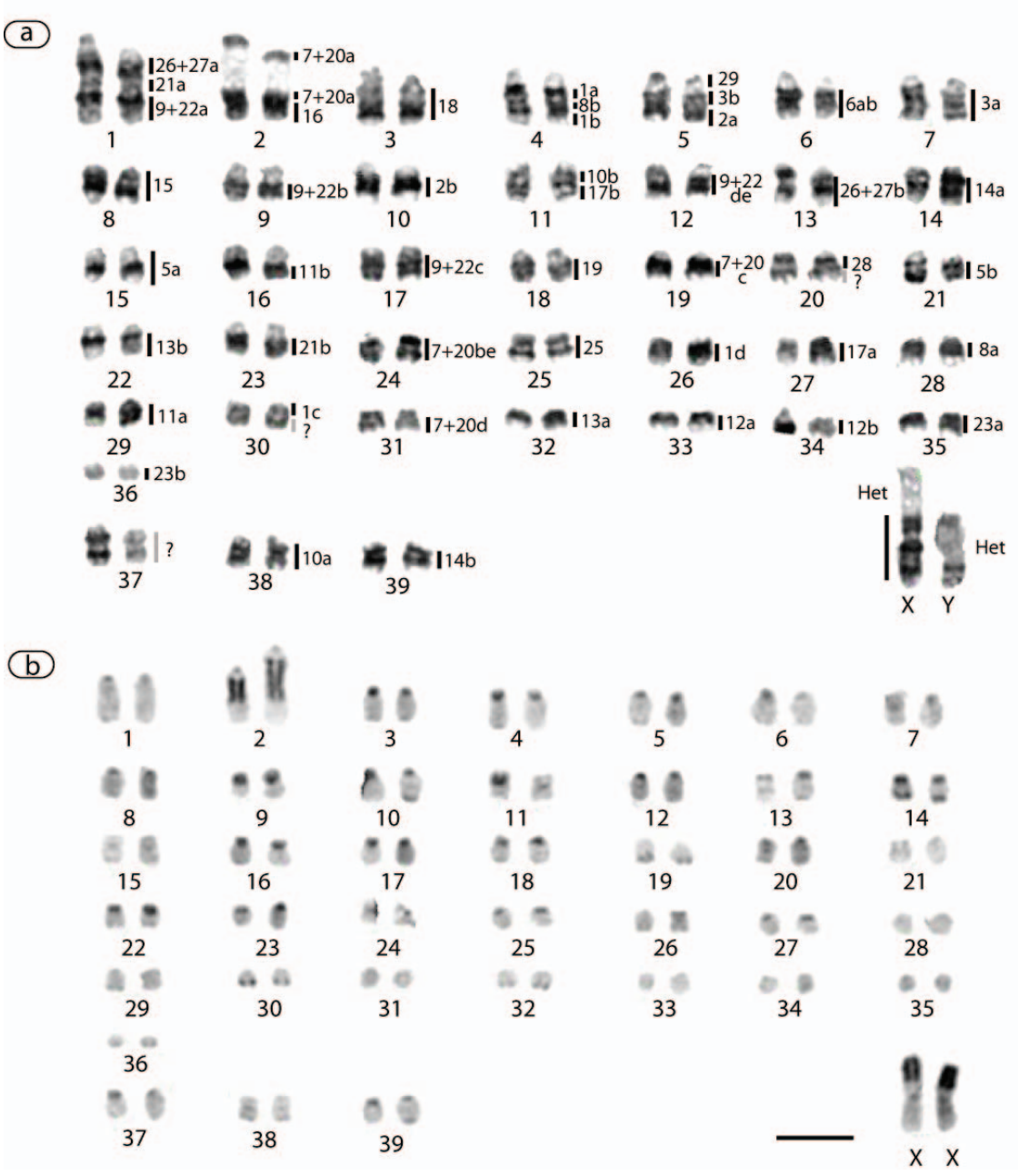

Figure 25: (**a**) G-banded and (**b**) C-banded karyotypes of *F. damarensis*. The approximate regions of homology to *H. glaber* as determined by cross-species painting are shown by vertical lines to the right of each chromosomal pair. The letters a, b, c and d refer to homologies of subregions that were used to implement the MGR algorithm (see Table 6). Het = heterochromatin. Bar = 100μm.

4.3.5 *Thryonomys swinderianus*

The cane rat, *T. swinderianus*, was used as outgroup in our investigation and its karyotype is presented Figure 26. The species has 2n=44 confirming an earlier report by Marczynska (1972) based on conventional Giemsa staining. It comprises 21 biarmed autosomal pairs (TSW 1-21, aFN= 84) and a biarmed X chromosome equivalent in size to autosomal pair 4. Cross-species painting with the *H. glaber* painting probes defined 33 segments of homology in the *T. swinderianus* genome. Seventeen of the paints (HGL 5, 6, 8, 11-13, 15-19, 21, 23, 25, 28, 29 and X) were retained as conserved syntenies in the *T. swinderianus* karyotype of which HGL 6, 11-13, 15 and X are present as single chromosomes (i.e., TSW 9, 16, 19-21 and X) and twelve are in association with other autosomal segments (TSW 1, 4, 5, 7, 11, 12, 14, 15 and 18). The painting probes HGL 1-3, 10 and 14 produced two signals on TSW 1-7, 10 and 18 respectively. The *T. swinderianus* chromosomal regions TSW 2q, 3p and 12p were not hybridized.

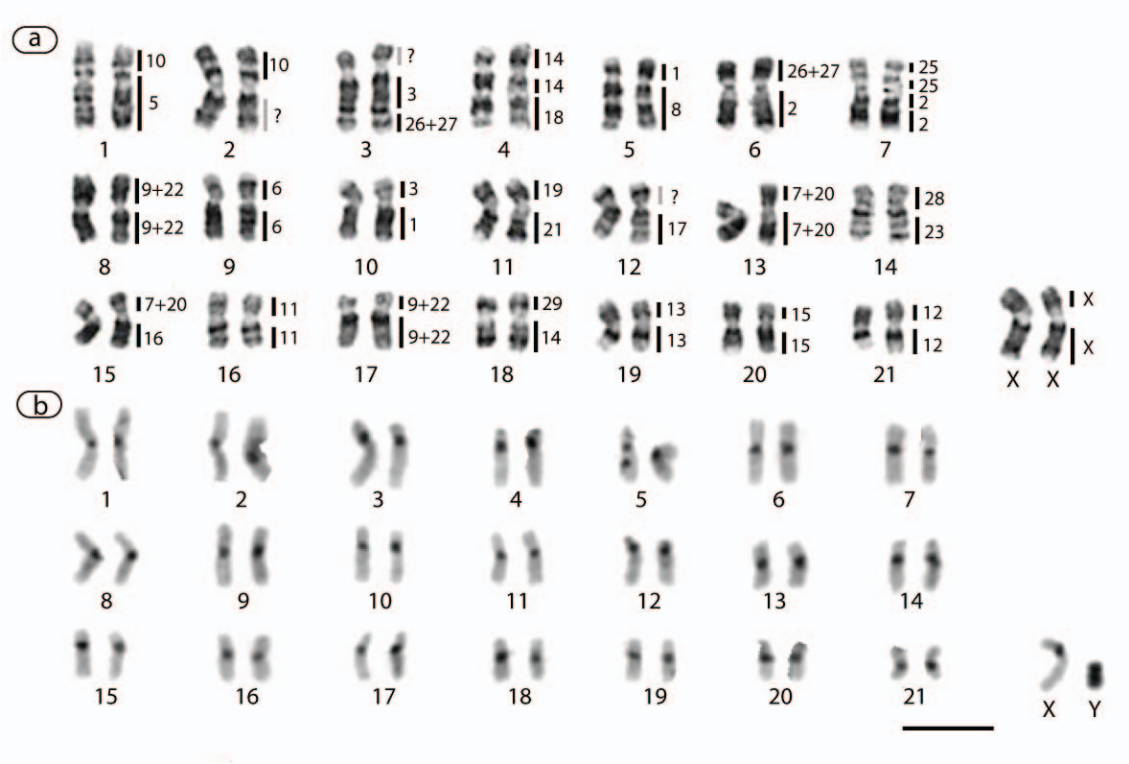

Figure 26: (**a**) G-banded and (**b**) C-banded karyotypes of *T. swinderianus* with (a) approximate regions of homology to *H. glaber* shown to the right of each chromosomal pair. Bar = 100µm.

Examples of chromosome painting among the different species using *H. glaber* painting probes are shown in Figure 27.

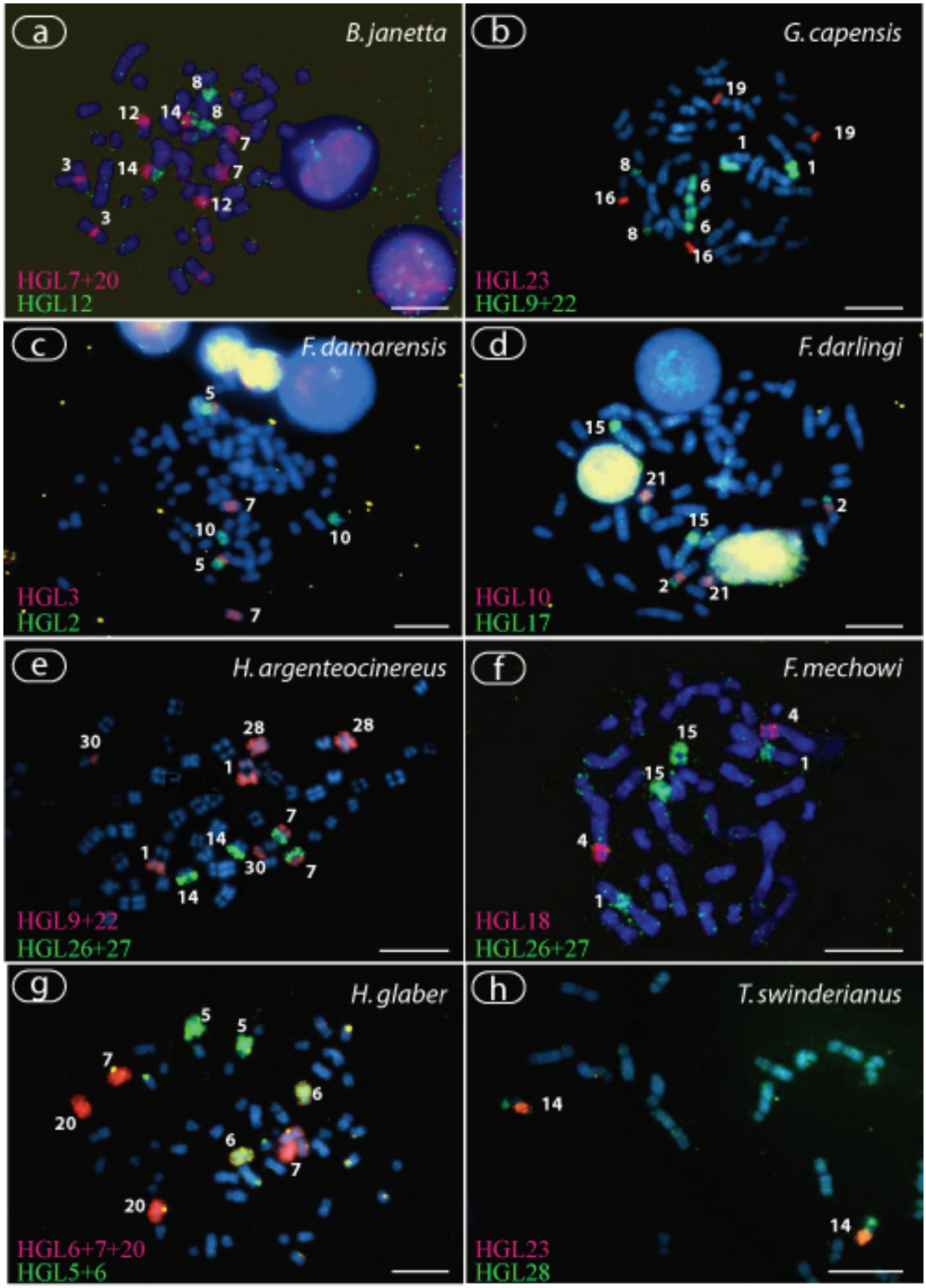

Figure 27: Examples of double colour FISH experiments using various *H. glaber* chromosomes paints labelled with biotin (pink signal) and digoxygenin (green signal). (**a**): HGL 7+20 and HGL 12 on *B. janetta*, (**b**): HGL 23 and HGL 9+22 on *G. capensis*, (**c**): HGL 3 and HGL 2 on *F. damarensis*, (**d**) HGL 10 and HGL 7 on *F. darlingi*, (**e**): HGL 9+22 and HGL 26+27 on *H. argenteocinereus*, (**f**): HGL 18 and HGL 26+27 on *F. mechowi*, (**g**): HGL 6+7+20 and HGL 5+6 on *H. glaber* and (**h**): HGL 23 and HGL 28 on *T. swinderianus*. Chromosome numbers of the target species refer to their respective karyotypes presented in Figures 10 and 21-26. Bars = 100µm.

4.3.6 Phylogenetic analysis based on adjacent syntenies

The cross-species chromosome painting experiments using a suite of *H. glaber* painting probes allowed us to delineate conserved segments and importantly, the adjacent syntenies or junctions between *H. glaber* and representatives of the six genera of the Bathyergidae (see Robinson and Seiffert 2004 for rationale underpinning the use of synteny junctions in phylogenetic analysis). The use of unidirectional painting has an influence on the precise identification of homologies among species. However, in the present study the highly conserved G-banding patterns in the different karyotypes could be used to confirm the homology of adjacent syntenies. For example, it is clear that adjacent syntenies detected in *B. janetta* are similarly conserved in the other two 2n=54 species (Figure 23a). In similar vein, the adjacent syntenies detected among *Fukomys* species that have different diploid numbers are convincingly supported by the correspondence in the G-banding patterns (see the half-karyotype comparisons in Figure 28).

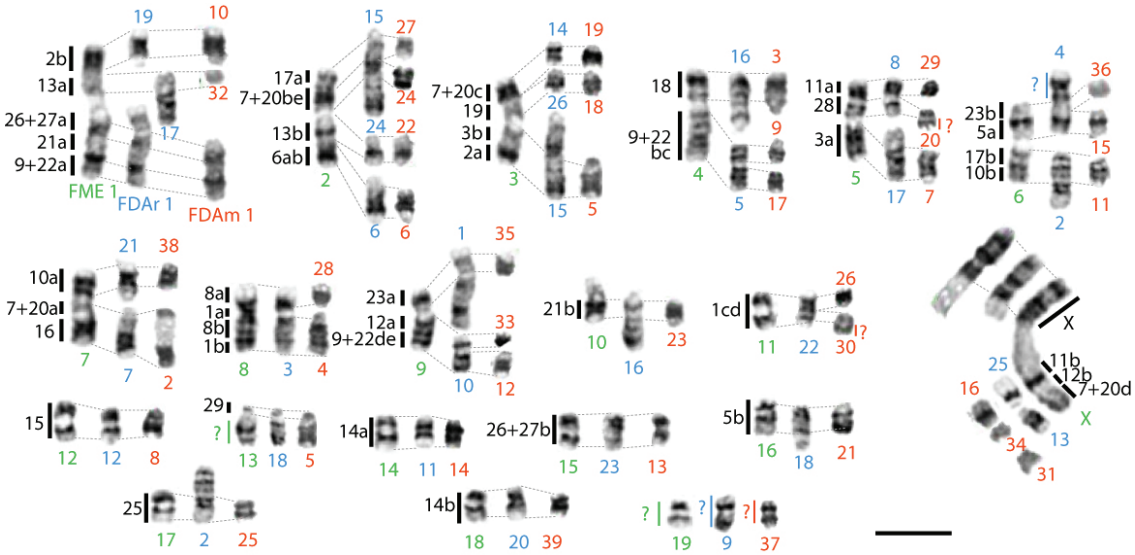

Figure 28: Comparative chromosome map of the three *Fukomys* species included in our study, *F. mechowi* (FME), *F. darlingi* (FDAr) and *F. damarensis* (FDAm) with *H. glaber* chromosomal homologies assigned to the left of *F. mechowi* chromosomes. Letters a, b, c, and d designate homologous subregions among the *Fukomys* karyotypes and those of *H. argenteocinereus* (Figure 21) and *B. janetta* (Figure 22). Bar = 100µm.

Likewise, it is probable that the conservation of a chromosome paint as a single signal in one species' genome reflects true conservation of the chromosome in this species, therefore these were also coded as conserved syntenies corresponding to *H. glaber* chromosome arms (see characters 58 to 70, Table 5). The coding of adjacent syntenies with no mention of centromeres (strategy (i) in 4.2.3), or the coding of adjacent syntenies and centromeres position in two different characters (strategy (ii) in 4.2.3) both resulted in a single tree that failed to retrieve *Fukomys* monophyly (not shown). This is in marked contrast to the strong support for this clade by DNA sequences (Faulkes *et al.* 2004, Ingram *et al.* 2004, Van Daele *et al.* 2007b). Moreover, we note that strategy (ii) tends to introduce over-weighting of characters since where a centromere position disrupts an adjacent synteny it is coded = 1 and the synteny is also coded =1 (i.e., the centromere cannot be present without the adjacent synteny being present as well). As a result, we adopted coding strategy (iii) for which the combination of chromosome painting and banding comparisons allowed us to establish 70 multi-state chromosomal characters (Table 5). By constraining the

Table 5: Chromosome presence/absence matrix subjected to PAUP*; absence of adjacent synteny (0), presence of adjacent synteny on the same arm (1), presence of adjacent synteny interrupted with a centromere (2), state 1 or 2 (3) and unknown state (?). Species names are abbreviated : *T. swinderianus* (TSW), *B. janetta* (BJA), *B. suillus* (BSU), *G. capensis* (GCA), *F. mechowi* (FME), *F. darlingi* (FDAr), *F. damarensis* (FDAm), *H. argenteocinereus* (HAR), *H. glaber* (HGL), *C. h. natalensis* (CHn), *C. h. hottentotus* (CHh) and *C. h. pretoriae* (CHp).

No.	Character	TSW	BJA	BSU	GCA	FME	FDAr	FDAm	HAR	HGL	CHn	CHh	CHp
1	1/3	2	0	0	0	0	0	0	0	0	0	0	0
2	1a/8b	2	1	1	1	1	1	1	1	0	1	1	1
3	8b/1b	0	0	0	0	1	1	1	0	0	0	0	0
4	2/25	2	0	0	0	0	0	0	0	0	0	0	0
5	2/3	0	1	1	1	1	1	1	0	0	1	1	1
6	2/10	0	0	0	0	0	0	0	2	0	0	0	0
7	2/13	0	1	1	1	1	0	0	0	0	1	1	1
8	2/26+27	2	0	0	0	0	0	0	0	0	0	0	0
9	3/26+27	1	2	2	2	0	0	0	0	0	2	2	2
10	3/6	0	2	2	2	0	0	0	0	0	2	2	2
11	3/13	0	0	0	0	0	1	0	0	0	0	0	0
12	3/19	0	0	0	0	2	0	0	0	0	0	0	0

13	3/28	0	0	0	0	2	0	0	0	0	0	0	0
14	3/29	0	0	0	0	0	0	1	0	0	0	0	0
15	5/10	2	0	0	0	0	0	0	0	0	0	0	0
16	5/23	0	2	2	2	1	1	0	2	0	2	2	2
17	5/7+20	0	0	0	0	0	0	0	2	0	0	0	0
18	5/17	0	0	0	0	2	0	0	0	0	0	0	0
19	5/29	0	0	0	0	0	1	0	0	0	0	0	0
20	6/17	0	0	0	0	0	0	0	2	0	0	0	0
21	6/13	0	0	0	0	1	0	0	0	0	0	0	0
22	7+20/3	0	0	0	0	0	1	0	0	0	0	0	0
23	7+20/10	0	0	0	0	2	0	0	0	0	0	0	0
24	7+20/12	0	2	2	2	1	2	0	2	0	2	2	2
25	7+20/13	0	0	0	0	2	0	0	0	0	0	0	0
26	7+20/16	2	1	1	1	1	2	1	2	0	1	1	1
27	7+20/18	0	2	2	2	0	0	0	0	0	2	2	2
28	7+20/19	0	2	2	2	1	0	0	0	0	2	2	2
29	7+20/17	0	2	2	2	1	1	0	0	0	2	2	2
30	9+22/12	0	2	2	2	1	1	0	0	0	2	2	2
31	9+22/18	0	0	0	0	2	0	0	0	0	0	0	0
32	9+22/21	0	1	1	1	1	1	1	0	0	1	1	1
33	9+22/26+27	0	0	0	0	0	0	0	2	0	0	0	0
34	10/13	0	2	2	2	0	0	0	0	0	2	2	2
35	10/17	0	2	2	2	1	1	1	0	0	2	2	2
36	10/25	0	0	0	0	0	2	0	0	0	0	0	0
37	11/12	0	0	0	0	1	0	0	0	0	0	0	0
38	11/26+27	0	0	0	0	0	0	0	2	0	0	0	0
39	11/28	0	2	2	2	1	2	0	0	0	2	2	2
40	11/Het	0	2	2	0	0	0	0	0	0	?	0	?
41	11/X	0	0	0	0	1	0	0	0	0	0	0	0
42	11/Y	0	0	0	0	1	0	0	0	0	0	0	0
43	12/23	0	0	0	0	2	0	0	0	0	0	0	0
44	13/15	0	0	0	0	0	0	0	2	0	0	0	0
45	13/26+27	0	0	0	0	2	0	0	0	0	0	0	0
46	14/18	1	0	0	0	0	0	0	0	0	0	0	0
47	14/29	2	2	2	2	0	0	0	2	0	2	2	2
48	18/21	0	0	0	0	0	1	0	0	0	0	0	0
49	18/23	0	0	0	0	0	0	0	2	0	0	0	0
50	19/21	2	0	0	0	0	0	0	0	0	0	0	0
51	19/28	0	0	0	0	0	0	0	2	0	0	0	0
52	21/26+27	0	1	1	1	1	1	1	0	0	1	1	1
53	23/28	2	0	0	0	0	0	0	0	0	0	0	0
54	23/Het	0	2	2	0	0	0	0	0	0	0	0	0
55	23/Y	0	0	0	0	0	0	0	0	0	1	1	1
56	23/26+27	0	0	0	0	0	2	0	0	0	0	0	0
57	29/Het	0	1	1	0	0	0	0	0	0	0	0	0
58	2p/2q	0	0	0	0	0	0	0	0	2	0	0	0
59	3p/3q	0	0	0	0	0	0	0	0	2	0	0	0
60	5p/5q	1	0	0	0	0	0	0	0	2	0	0	0
61	6p/6q	3	1	1	1	1	1	1	0	2	1	1	1
62	8p/8q	1	3	3	3	0	0	0	3	2	3	3	3
63	10p/10q	0	0	0	0	0	0	0	0	2	0	0	0
64	11p/11q	3	0	0	0	0	0	0	0	2	0	0	0
65	12p/12q	3	0	0	0	0	0	0	0	2	0	0	0
66	13p/13q	3	0	0	0	0	0	0	0	2	0	0	0
67	14p/14q	0	0	0	0	0	0	0	0	2	0	0	0

68	17p/17q	1	0	0	0	0	0	0	0	2	0	0	0
69	21p/21q	1	0	0	0	0	0	0	0	2	0	0	0
70	23p/23q	1	0	0	0	0	0	0	0	2	0	0	0

in-group taxa to be monophyletic, and using the exhaustive search option in PAUP*, the maximum parsimony analysis resulted in a single most parsimonious tree of 93.5 steps with a consistency index = 0.9358, a retention index = 0.9149, and a homoplasy index = 0.0642 (Figure 29a).

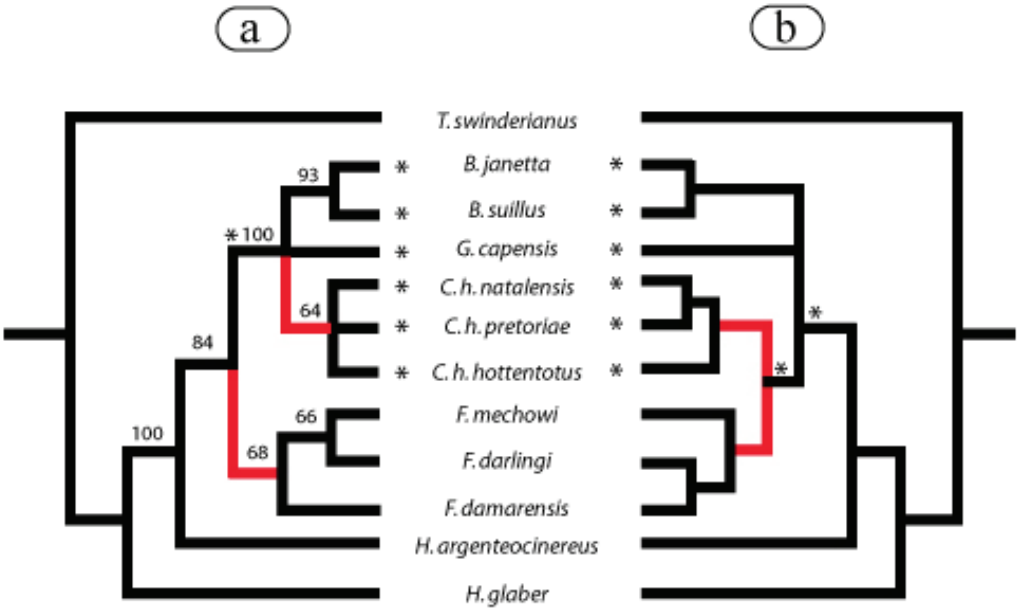

Figure 29: Comparison of phylogenetic trees obtained using (**a**) chromosomal characters and (**b**) nucleotide substitutions (redrawn from Ingram *et al.* 2004 and Van Daele *et al.* 2007b). Bootstrap values (above branches) obtained after 1000 replications in PAUP*. Conflict at generic level between the trees is indicated by red branches. The presence of the 2n=54 karyotype is marked with asterisks at the end of the branches for extant species and on top of ancestral branches when indicating the ancestral state.

4.3.7 Phylogenetic analysis based on chromosome rearrangements

A subset of the species used in PAUP* (see above) were analysed using the Bourque and Pevzner (2002) MGR algorithm to retrieve phylogenetic relationships among *F. damarensis*, *F. darlingi*, *F. mechowi* and two other mole-rat species, *B. janetta* and *H. argenteocinereus* (Table 6).

Table 6: List of the MGR characters used with the corresponding HGL segment per chromosome and per species. A total of 50 hybridization signals (characters) were scored for each species analysed (BJA, FME, FDAr, FDAm and HAR, see Figures 21, 22, 24, 25 and 28 for the source of these data). Each character was allocated a number from 1-50 that was maintained across the various species (e.g., 3a corresponds to MGR 7 in BJA, FME and all other taxa). The orientation of the regions for use in the MGR analysis were optimized by G-band comparison and the additional use of the GRIMM algorithm. This allowed the assignment of a (+) or (-) sign to each region (see the MGR character column). The MGR character numbers (1-50) were imported into the MGR programme allowing for the identification of the most parsimonious suite of rearrangements among karyotypes (see text for details). BJA = *B. janetta*, FME = *F. mechowi*, FDAr = *F. darlingi*, FDAm = *F. damarensis* and HAR = *H. argenteocinereus*, chr = chromosome.

Coding of the genomes to be implemented in MGR															
BJA			FME			FDAr			FDAm			HAR			
chr	synteny	MGR	chr	synteny	MGR	chr	synteny	MGR	chr	synteny	MGR	chr	synteny	MGR	
1	3a	**+7**	1	2b	**+6**	1	23a	**+43**	1	26+27a	**+46**	1	9+22a	**+20**	
	26+27a	**+46**		13a	**+31**		26+27a	**+46**		21a	**+41**	2	8a	**+18**	
	21a	**+41**		26+27a	**+46**		21a	**+41**		9+22a	**+20**		8b	**+19**	
	9+22a	**+20**		21a	**+41**		9+22a	**+20**	2	7+20a	**+13**		1a	**+1**	
2	2a	**+5**		9+22a	**+20**	2	25	**-45**		16	**+36**		1b	**+2**	
	3b	**+8**	2	17a	**+37**		10b	**+26**	3	18	**+39**	3	23b	**+44**	
	6a	**+11**		7+20b	**+14**		17b	**+38**	4	1a	**-1**		5a	**+9**	
	6b	**+12**		7+20e	**+17**	3	8a	**+18**		8b	**-19**	4	23a	**+43**	
3	18	**-39**		13b	**-32**		1a	**-1**		1b	**+2**		18	**+39**	
	7+20a	**+13**		6a	**+11**		8b	**-19**	5	29	**-49**	5	6a	**-11**	
	16	**+36**		6b	**+12**		1b	**+2**		3b	**+8**		17b	**-38**	
4	8a	**+18**	3	7+20c	**+15**	4	23b	**+44**		2a	**+5**		6b	**+12**	
	8b	**+19**		19	**+40**		5a	**+9**	6	6a	**+11**	6	13a	**-31**	
	1a	**+1**		3b	**+8**	5	9+22b	**+21**		6b	**+12**		15	**+35**	
	1b	**+2**		2a	**+5**		9+22c	**+22**	7	3a	**+7**	7	9+22d	**-23**	
5	13a	**+31**	4	18	**+39**	6	6a	**+11**	8	15	**+35**		26+27a	**+46**	
	2b	**+6**		9+22b	**+21**		6b	**+12**	9	9+22b	**+21**	8	7+20a	**+13**	
6	9+22b	**+21**		9+22c	**+22**	7	7+20a	**+13**	10	2b	**+6**		16	**+36**	
	9+22c	**+22**	5	11a	**+27**		16	**+36**	11	10b	**+26**	9	10b	**+26**	
7	17a	**+37**		28	**+48**	8	28	**+48**		17b	**+38**		2a	**-5**	
	7+20b	**+14**		3a	**-7**		11a	**+27**	12	9+22d	**+23**	10	28	**+48**	
	7+20e	**+17**	6	23b	**+44**	10	9+22d	**+23**		9+22e	**+24**		19	**+40**	
8	9+22d	**+23**		5a	**+9**		9+22e	**+24**	13	26+27b	**+47**	11	7+20d	**+16**	
	9+22e	**+24**		17b	**+38**		12a	**+29**	14	14a	**+33**		12b	**+30**	
	12a	**+29**		10b	**+26**	11	14a	**+33**	15	5a	**+9**	12	7+20c	**+15**	
9	13b	**+32**	7	10a	**+25**	12	15	**+35**	16	11b	**+28**	13	2b	**+6**	
	10a	**+25**		7+20a	**+13**	13	12b	**+30**	17	9+22c	**+22**	14	26+27b	**+47**	
10	11a	**+27**		16	**+36**		7+20d	**+16**	18	19	**+40**		11a	**-27**	
	28	**+48**	8	8a	**+18**	14	7+20c	**+15**	19	7+20c	**+15**	15	5b	**+10**	
11	29	**+49**		1a	**-1**	15	17a	**+37**	20	28	**+48**		7+20b	**+14**	
	14a	**+33**		8b	**-19**		7+20b	**+14**	21	5b	**+10**	16	3b	**+8**	
12	19	**+40**		1b	**+2**		7+20e	**+17**	22	13b	**+32**	17	29	**+49**	
	7+20c	**+15**	9	9+22d	**+23**		3b	**+8**	23	21b	**+42**		14a	**+33**	
13	21b	**+42**		9+22e	**+24**		2a	**+5**	24	7+20b	**+14**	18	1c	**+3**	
14	12b	**+30**		12a	**+29**	16	21b	**+42**		7+20e	**+17**		1d	**+4**	
	7+20d	**+16**		23a	**+43**		18	**+39**	25	25	**+45**	19	25	**+45**	
15	1c	**+3**	10	21b	**+42**	17	13a	**+31**	26	1d	**+4**	20	21a	**+41**	
	1d	**+4**	11	1c	**+3**		3a	**+7**	27	17a	**+37**		21b	**+42**	

Table 6 continued

16	23a	**+43**		1d	**+4**	18	29	**+49**	28	8a	**+18**	21	11b	**+28**
17	11b	**+28**	12	15	**+35**		5b	**+10**	29	11a	**+27**	22	17a	**+37**
18	17b	**+38**	13	29	**+49**	19	2b	**+6**	30	1c	**+3**	23	10a	**+25**
	10b	**+26**	14	14a	**+33**	20	14b	**+34**	31	7+20d	**+16**	24	12a	**+29**
19	23b	**+44**	15	26+27b	**+47**	21	10a	**+25**	32	13a	**+31**	25	14b	**+34**
	5a	**+9**	16	5b	**+10**	22	1c	**+3**	33	12a	**+29**	26	7+20e	**+17**
20	15	**+35**	17	25	**+45**		1d	**+4**	34	12b	**+30**	27	13b	**+32**
22	14b	**+34**	18	14b	**+34**	23	26+27b	**+47**	35	23a	**+43**	28	9+22b	**+21**
23	25	**+45**	20	X	**-50**	24	13b	**+32**	36	23b	**+44**		9+22c	**+22**
24	5b	**+10**		11b	**-28**	25	11b	**+28**	38	10a	**+25**	29	3a	**+7**
26	26+27b	**+47**		12b	**+30**	26	19	**+40**	39	14b	**+34**	30	9+22e	**+24**
27	X	**+50**		7+20d	**+16**	27	X	**+50**	40	X	**+50**	31	X	**+50**

The findings from this analysis (Figure 30) are in agreement with the molecular data (Van Daele *et al.* 2007b), that is that *F. damarensis* and *F. darlingi* form a monophyletic clade to the exclusion of *F. mechowi*, relationships that are supported by a high number of chromosomal rearrangements. MGR retrieved four rearrangements between the 2n=54 ancestor of the *Cryptomys sensu lato* lineages, and to the lineage leading to *Fukomys*. There are five rearrangements that support a sister species relationship between *F. damarensis* and *F. darlingi*, while ten autapomorphies were retrieved for *F. damarensis*, six for *F. darlingi* and ten for *F. mechowi*. Sixteen rearrangements underpin the monophyly of *H. argenteocinereus* whose position in the phylogram is ambiguous due to the absence of *H. glaber* in our dataset. The rearrangements are detailed in Appendix 2.

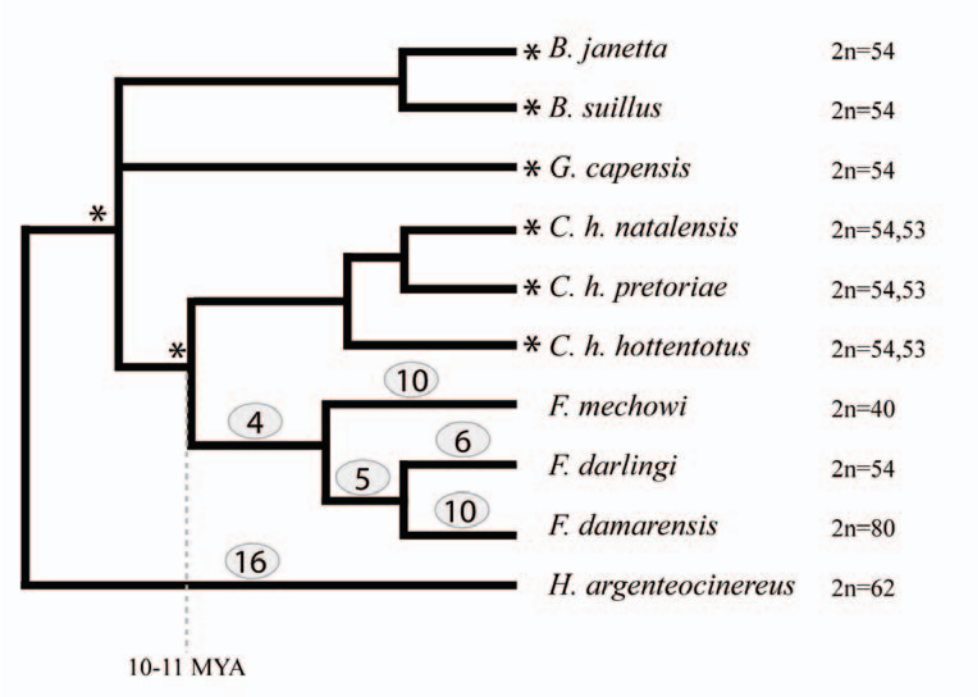

Figure 30: Phylogenetic tree derived from the MGR algorithm showing the numbers of chromosomal rearrangements that underpin evolutionary relationships among species. The numbers of rearrangements estimated by MGR are given above each branch. The presence of the 2n=54 karyotype is marked by asterisks and species diploid numbers are given to the extreme right. *Cryptomys* and *Fukomys* are thought to have diverged 10-11 MYA (Ingram *et al.* 2004).

4.4 DISCUSSION

4.4.1 Karyotypic discrepancies among published reports

George (1979) reported an identical 2n=60 karyotype for *H. glaber* and a Kenyan specimen of *H. argenteocinereus*. Scharff *et al.* (2001) subsequently found *H. argenteocinereus* from Zambia to possess a different diploid number (2n=62) from that of George's (1979) Kenyan specimen, but the authors did not include karyotypes in support of this. Interestingly, the genetic distance between *H. argenteocinereus* populations are high (Ingram *et al.* 2004), with a 12S rRNA corrected pairwise difference of 7.3% between populations on either side of the Rift Valley suggesting that a detailed analysis of specimens from these regions would be beneficial in determining the status of *H. argenteocinereus* and its current recognition as a single species. The data confirm that *H. argenteocinereus* specimens from the West side of

the African Rift have a diploid number of 2n=62 and, also, that this species' karyotype is markedly different in its organization from that of *H. glaber*.

Previous work by Matthey (1956) and Nevo *et al.* (1986) reported *B. janetta* (2n=54) and *B. suillus* (2n=56) to differ not only with respect to diploid number, but also with respect to the presence of three autosomal acrocentric chromosome pairs in *B. suillus*, whereas the *B. janetta* karyotype has only metacentric autosomes. These finding are not consistent with our data either in terms of diploid number or chromosome morphology. Interestingly, the two species are thought to have a hybrid zone at the border of their distribution area (Faulkes *et al.* 2004) and, at least at the level of resolution permitted here, karyotype differences in the two taxa are probably not likely to present a barrier to the existence of such a phenomenon.

Finally, a consistent 2n=80 is reported for *F. damarensis* (for ten specimens from South Africa and seven from Namibia); this is higher than the 2n=74, 78 described by Nevo *et al.* (1986) for this species. It should be noted that these three different reports may reflect intraspecific variation within this species, although this will only be verified through more comprehensive karyotypic surveys.

4.4.2 Conflict in the topology of trees retrieved from analyses of chromosomes and DNA sequences

The chromosomal tree retrieved by PAUP* (Figure 29a) supports the monophyly of each genus and the first divergence of *Heterocephalus* followed by *Heliophobius*, findings that are consistent with the sequence data (Faulkes *et al.* 2004, Ingram *et al.* 2004). However, some of the chromosomal evolutionary relationships are in conflict with the molecular tree. Indeed, whereas sequences strongly support the monophyly of a clade containing *Cryptomys* and *Fukomys* (in red on Figure 29) as sister groups (Allard and Honeycutt 1992, Faulkes *et al.* 1997, Walton *et al.* 2000,

Faulkes *et al.* 2004, Ingram *et al.* 2004), which until very recently were part of the same genus (Kock *et al.* 2006), the chromosomal tree shows this clade to be paraphyletic. This is reflected by grouping *Bathyergus*, *Georychus* and *Cryptomys* in a strongly supported monophyletic clade (bootstrap support= 100). These three genera have a 2n=54 karyotype and, with the exception of a Y-autosome translocation that is specific to *Cryptomys*, the differences between the three genera concern only minor heterochromatic variation (Figure 23a). In other words, the karyotypes are almost identical and their association is supported by six synapomorphic characters (numbered 9, 10, 27, 30, 34 and 35, Table 5) which, if excluded from the matrix, result in a consensus tree with an unresolved polytomy containing *Bathyergus*, *Georychus*, *Cryptomys* and *Fukomys*. Moreover, no synapomorphy could be identified uniting *Fukomys* and *Cryptomys* suggesting that the chromosomal data are simply not informative at the level of resolution permitted by cross-species FISH.

Although they are morphologically very different from the other genera, neither *Cryptomys* nor *Fukomys* are clearly distinguishable from each other using traditional morphometric criteria (Van Daele *et al.* 2007a) possibly suggesting some support for the monophyly of *Cryptomys sensu lato* as is suggested by the sequence based tree (Figure 29b). Mapping the 2n=54 karyotype (*Bathyergus*, *Georychus* and *Cryptomys*) on this tree (asterisks in Figure 29b) shows that the probable ancestor to *Fukomys* was also likely to have had a 2n=54 karyotype. This inconsistency between trees is the reason for the second contradiction – the association between *F. mechowi* and *F. darlingi* underpinned by chromosomes (Figure 29a) in contrast to the sister species relationship for *F. darlingi* + *F. damarensis* suggested by sequences (Figure 29b). The chromosomal character states 16, 29 and 30 (Table 5) support the *F. mechowi* + *F. darlingi* association, all of which are absent in *F. damarensis*. According to the chromosomal tree these three characters had a state = 0 in the

Fukomys ancestor and therefore the most parsimonious topology places *F. mechowi* with *F. darlingi*. Interestingly, had the ancestral character state been = 2 (as is the case for the 2n=54 karyotype, the probable ancestor to *Fukomys*), it would have been equally parsimonious to find support for *F. mechowi* + *F. darlingi* or *F. darlingi* + *F. damarensis* (2 steps), and the relationships would have remained unresolved using these characters. To further scrutinize this conflict in topology, we ran a parsimony analysis that included only the three *Fukomys* species and the 2n=54 karyotype as the outgroup. The results (one tree of 44 steps, consistency index = 1, retention index = 1, homoplasy index = 0; tree not shown) show that the characters 16, 29 and 30 no longer unite *F. mechowi* and *F. darlingi*, and that only one synapomorphy is shared by any two *Fukomys* species (character 7), in this case *F. darlingi* + *F. damarensis*, an outcome that is consistent with the molecular tree.

4.4.3 Chromosomal differentiation within *Fukomys*

Although the presence or absence of the adjacent syntenies (junctions between conserved segments) used in the phylogenetic analysis above result from chromosomal rearrangement, they are themselves not the rearrangements. An alternative approach (Dobigny *et al.* 2004a) in the use of chromosomal characters in phylogeny reconstruction is to use the actual rearrangement as the character and its presence or absence the character state. The similarity in the 2n=54 karyotypes of *Bathyergus, Georychus* and *Cryptomys* provide grounds for this karyotype's recognition as being that of their last common ancestor (discussed above), and also of *Fukomys* (see Figure 29b). However, due to the highly rearranged nature of the *Fukomys* species' karyotypes (with respect to their 2n=54 ancestor), the manual identification of rearrangements among them using parsimony proved problematic and we opted to follow a computational approach. The MGR algorithm (Bourque and

Pevzner 2002) computationally retrieves the most parsimonious suite of rearrangements among multiple genomes, and from these data it infers phylogenetic relationships. Although limited in the number of species that could be used with this approach (*B. janetta*, *B. suillus*, *G. capensis* and *C. hottentotus* have all retained the ancestral karyotype, and *H. glaber* was not included, see Material and Methods), the algorithm allowed for the transformation of a 2n=54-like ancestor into the karyotypes of the three *Fukomys* species, *F. damarensis*, *F. darlingi* and *F. mechowi*. The resultant topology ((*F. damarensis* + *F. darlingi*), *F. mechowi*) was well supported and consistent with relationships suggested by nucleotide sequences (Van Daele *et al.* 2007b). Among the four synapomorphies identified by MGR as uniting the three *Fukomys* species (Figure 30), one, an inversion, can be observed in all the three karyotypes (Figure 28, i.e., the inversion of HGL 8+HGL 1 seen in FME 8, FDAr 3 and FDAm 4). Because it is retained in *F. mechowi* which is basal in the *Fukomys* phylogeny (Van Daele *et al.* 2007b), this most probably represents a synapomorphy for the genus. The analysis retrieved five synapomorphies that underpin the sister relationship of *F. darlingi* + *F. damarensis*, six autapomorphies characterise the *F. darlingi* lineage, ten the *F. damarensis* lineage, and ten autapomorphies distinguish *F. mechowi* from its nearest relatives (Figure 30). Some of these computationally derived rearrangements are visible in the banded karyotypes of the extant species (e.g., the fission of HGL 19 from HGL 7+20c that unites *F. darlingi* + *F. damarensis* as sister species). Finally, among the sixteen rearrangements that support *H. argenteocinereus* monophyly, one inversion (identifiable on *H. argenteocinereus* chromosome 5) is visible in the G-banded karyotype (Figure 21).

4.4.4 Contrasting tempo of chromosomal change

This study of chromosomal evolution in *Bathyergidae* provides evidence of a marked dichotomy in chromosomal evolution between *Cryptomys* and *Fukomys*, with a single rearrangement punctuating the *Cryptomys* evolutionary history in the last 10-11 MY (a sex-autosome translocation that is shared by the three *C. hottentotus* subspecies, see Chapter 2), whereas 35 rearrangements have been fixed during the same period in the *Fukomys* species analysed herein (divergences according to Ingram *et al.* 2004, indicated in Figure 30). These contrasting patterns question the cause of these differences leading to Van Daele *et al.* (2004) proposing that karyotypic differentiation in *Fukomys* is strongly correlated with existing river networks in the Zambezi Valley which probably resulted in vicariance and allopatric speciation (Burda 2001, Cotterill 2003, Van Daele *et al.* 2007b). In sharp contrast, *Cryptomys sensu stricto* is found in a significantly less fractured and certainly more arid environment with possibly greater gene flow between local demes.

In this regard it is interesting that Nevo and colleagues noted that the diploid numbers of Israeli (*Spalax ehrenbergi*) and Turkish (*S. leucodon*) mole-rats increase (as do the levels of heterozygosity) on a clinal gradient of increased aridity (Nevo 1991, Nevo *et al.* 1994). These authors therefore argued for an adaptive role resulting from karyotype fragmentation. In a striking parallel, *F. damarensis*, which also has the most fissioned karyotype among the species analysed, is similarly found to inhabit areas of low and unpredictable rainfall compared to its congenerics (Bennett and Faulkes 2000). Although intriguing, the hypothesis is simply conjecture at this stage given that we have no comparable data for *H. glaber*, a lineage that also inhabits arid and unpredictable environments. Moreover, harsh environments have been used to explain the development of eusociality in both *H. glaber* and *F. damarensis* (Jarvis *et al.* 1994, Faulkes *et al.* 1997), and it is equally feasible that the fixation of fissions in

these species is facilitated by reproductive traits that are peculiar to eusocial systems, rather than to fitness associated with adaptation to arid environments.

In conclusion, it is shown that the African mole-rats of the genera *Bathyergus*, *Georychus* and *Cryptomys* are karyotypically highly conservative in comparison to *Heterocephalus*, *Heliophobius* and *Fukomys*. A cladistic analysis of the adjacent syntenies detected using cross-species FISH suggests evolutionary relationships for several taxa that differ from those retrieved from nucleotide substitution data (e.g., Faulkes *et al.* 2004, Ingram *et al.* 2004, Van Daele *et al.* 2007b). When constraining the 2n=54 karyotype of the *Fukomys* ancestor, the relationships ((*F. darlingi* + *F. damarensis*), *F. mechowi*) are consistent with sequence based studies, but with very little support from the adjacent syntenies detected herein. In contrast, reanalysis using a computational approach (Bourque and Pevzner 2002) that relied on chromosomal rearrangements suggest that these affiliations are actually substantiated by a large number of chromosomal rearrangements, many of which are no longer visible among the extant species. The fixation of these chromosomal mutations has probably been favoured by environmental factors and/or a particular social structure, both hypotheses that should be addressed through more comprehensive investigations that include ecological, physiological and behavioural processes.

CHAPTER 5

SUMMARY

The pioneer cytogenetic studies conducted by Matthey, George, Nevo and others (Matthey 1956, George 1979, Nevo *et al.* 1986), clearly illustrated that African mole-rats were characterised by high karyotypic diversity (Appendix 1). These early findings prompted a comprehensive cytogenetic study of the Bathyergidae, the substance of which forms the basis of this dissertation. The many chromosomal rearrangements differentiating the extant karyotypes were studied in a phylogenetic framework and the resulting relationships compared to those based on morphological criteria (De Graaff 1981), allozyme data (Nevo *et al.* 1987) and DNA sequences (Honeycutt *et al.* 1987, Allard and Honeycutt 1992, Faulkes *et al.* 1997, Walton *et al.* 2000, Faulkes *et al.* 2004, Ingram *et al.* 2004, Van Daele *et al.* 2007b).

Flow-sorted painting probes isolated from *H. glaber* (2n=60) were used in cross-species chromosome painting experiments to determine homologous chromosomal regions between two species of mole-rats, the naked mole-rat, *H. glaber* (2n=60) and the giant mole-rat, *F. mechowi* (2n=40). The most striking difference in the karyotypes of the two taxa concerns their sex chromosomes. The *H. glaber* painting probes identified a complex series of translocations that involved the fractionation of four autosomes and the subsequent translocation of segments to the sex chromosomes and to autosomal partners in the *F. mechowi* genome. As observed for other sex chromosome-autosome translocations (reviewed in Dobigny *et al.* 2004b) an IHB was detected in *F. mechowi* sex chromosomes at the boundary with the translocated autosomal segment. It was argued that the IHB facilitated the establishment of this rearrangement preventing XCI from spreading to the recently

translocated autosomal compartment. The likely sequence of evolutionary events that has led to the contemporary composition of the *F. mechowi* sex chromosomes were interpreted in the light of prevailing views on the genesis of sex chromosomes in mammals (Graves 1995).

Although *Fukomys* is characterised by considerable karyotypic diversity (Van Daele *et al.* 2004), its sister clade *Cryptomys* was described as having a conserved 2n=54 (Nevo *et al.* 1986, Faulkes *et al.* 2004) but with variation in the FN among subspecies. A comprehensive cytogenetic survey of the common-mole-rat, *C. hottentotus*, was conducted using G- and C-banding, FISH, and the analysis of meiotic chromosomes based on the immunostaining of proteins involved in the formation of synaptonemal complex (SCP1 and SCP3). We identified the presence of a Y-autosome translocation that is responsible for a fixed diploid number difference between males (2n=53) and females (2n=54), a character that likely defines the *C. hottentotus* lineage. Immunostaining, combined with C-banding of spermatocytes, revealed a linearized sex trivalent with X_1 at one end, and X_2 at the other, with evidence of reduced recombination between Y and X_2 that seems to be heterochromatin dependant in the *C. hottentotus* lineage. We suggest that this could depict the likely initial step in the differentiation of a true neo-X, and that this may mimic an early stage in the mammalian meiotic chain formation, an evolutionary process that has been taken to an extreme in a monotreme mammal, the platypus (Gruetzner *et al.* 2006).

Finally, given the usefulness of chromosomal characters investigating evolutionary relationships (e.g. Neusser *et al.* 2001, Veyrunes *et al.* 2006) we extended cross-species chromosome painting to representatives of the six genera and an outgroup species, *T. swinderianus*. A chromosomal phylogeny based on the

cladistic analysis of adjacent syntenies detected by cross-species chromosome painting was not consistent with that obtained using DNA sequences (Faulkes *et al.* 2004, Ingram *et al.* 2004, Van Daele *et al.* 2007b) due, in large part, to the conserved nature of the *Bathyergus, Georychus* and *Cryptomys* karyotypes. In marked contrast, the *Fukomys* and *Heliophobius* species showed extensive chromosome reshuffling permitting their analysis by a computational approach that has conventionally been employed in comparative genomic studies for retrieving phylogenetic information based on DNA sequence or gene order data. Using the multiple genome rearrangements (MGR) algorithm (Bourque and Pevzner 2002) and chromosomal rearrangement data detected among *F. damarensis*, *F. darlingi*, *F. mechowi* and the sister taxa *B. janetta* and *H. argenteocinereus*, cytogenetic support for the monophyly of *Fukomys* and a sister association for *F. darlingi* + *F. damarensis* was retrieved. This mirrored the published sequence based topology (Van Daele *et al.* 2007b). We show that *F. damarensis*, a lineage adapted to arid and climatically unpredictable environments in Southern Africa (Bennett and Faulkes 2000), is characterised by a large number of fissions, the fixation of which has probably been favoured by environmental factors and/or its particular eusocial structure.

REFERENCES

Aguilar GH (1993) The karyotype and taxonomic status of *Cryptomys hottentotus darlingi* (Rodentia, Bathyergidae). *S Afr J Zool* **28**: 201-204.

Allard MW and Honeycutt RL (1992) Nucleotide sequence variation in the mitochondrial 12s rRNA gene and the phylogeny of African mole-rats. *Mol Biol Evol* **9**: 27-40.

Anderson LK, Reeves A, Webb LM and Ashley T (1999) Distribution of crossing over on mouse synaptonemal complexes using immunofluorescent localization of MLH1 protein. *Genetics* **151**: 1569-1579.

Ashley T (2002) X-Autosome translocations, meiotic synapsis, chromosome evolution and speciation. *Cytogenet Genome Res* **96**: 33-39.

Bailey J, Carrel L, Chakravarti A and Eichler E (2000) Molecular evidence for a relationship between LINE-1 elements and X chromosome inactivation : The Lyon repeat hypothesis. *Proc Natl Acad Sci USA* **97**: 6634-6639.

Baker BH, Williams LA, Miller JA and Fitch FJ (1971) Sequence and geochronology of the Kenya rift volcanics. *Tectonophysics* **11**: 191-215.

Baker RJ and Bickham JW (1980) Karyotypic evolution in bats: evidence of extensive and conservative chromosomal evolution in closely related taxa. *Syst Zool* **29**: 239-253.

Bennett NC (1988) The trend toward sociality in three species of southern African mole-rats (Bathyergidae): causes and consequences. PhD thesis, University of Cape Town, South Africa.

Bennett NC and Faulkes CG (2000) African Mole-Rats: Ecology and Eusociality. Cambridge: Cambridge University Press.

Bennett NC and Jarvis JUM (2004) *Cryptomys damarensis*. *Mammalian Species* **756**: 1-5.

Bishop WW, Miller JA and Fitch FJ (1969) New potassium-argon age determinations relevant to the Miocene fossil mammals sequence in East Africa. *American Journal of Science* **267**: 669-699.

Bourque G and Pevzner PA (2002) Genome-Scale Evolution: Reconstructing gene order in the ancestral species. *Genome Res* **12**: 26-36.

Bourque G, Zdobnov EM, Bork P, Pevzner PA and Tesler G (2005) Comparative architectures of mammalian and chicken genomes reveal highly variable rates of genomic rearrangements across different lineages. *Genome Res* **15**: 98-110.

Bourque G (2006) Analysing Genome Rearrangements. In: Lengauer T (ed) Bioinformatics: From Genomes to Therapies. Wiley-VCH.

Bourque G, Tesler G and Pevzner PA (2006) The convergence of cytogenetics and rearrangement-based models for ancestral genome reconstruction. *Genome Res* **16**: 311-313.

Boyle AL, Ballard SG and Ward DC (1990) Differential distribution of long and short interspersed element sequences in the mouse genome: Chromosome karyotyping by fluorescence *in situ* hybridization. *Proc Natl Acad Sci USA* **87**: 7757-7761.

Brett RA (1991) The population structure of naked mole-rat colonies. In: Sherman PW, Jarvis JUM, Alexander RD (eds) The biology of the Naked Mole-Rat. Princeton University Press, Princeton, NJ, pp 99-136.

Brisset S, Izard V, Misrahi M, Aboura A, Madoux S, Ferlicot S, Schoevaert D, Soufir JC, Frydman R and Tachdjian G (2005) Cytogenetic, molecular and testicular tissue studies in an infertile 45,X male carrying an unbalanced (Y;22) translocation: Case report. *Hum Reprod* **20**: 2168-2172.

Burda H, Zima J, Scharff A, Macholan M and Kawalika M (1999) The karyotypes of *Cryptomys anselli* sp. nova and *Cryptomys kafuensis* sp. nova of the common mole-rat from Zambia (Rodentia, Bathyergidae). *Z Saugetierkunde* **64**: 36-50.

Burda H (2001) Determinants of the distribution and radiation of African mole-rats (Bathyergidae, Rodentia). Ecology or geography? Proceedings of the 8th International Symposium on African Small Mammals. IRD Editions, Paris.

Burda H, Sumbera R, Chitaukali WN and Dryden GL (2005) Taxonomic status and remarks on ecology of the Malawian mole-rat *Cryptomys whytei* (Rodentia, Bathyergidae). *Acta Theriologica* **50**: 529-536.

Burgoyne PS (1982) Genetic homology and crossing over in the X and Y chromosomes of mammals. *Hum Genet* **61**.

Capanna E and Merani MS (1980) Karyotypes of somalian rodent populations. *Ital J Zool* **3**: 45-51.

Carleton MD and Musser GG (2005) Order Rodentia. In: Wilson DE, Reeder DM (eds) Mammal species of the world: a taxonomic and geographic reference 3rd edition. The John Hopkins University Press.

Casavant NC, Scott L, Cantrell MA, Wiggins LE, Baker RJ and Wichman HA (2000) The End of the LINE?: Lack of Recent L1 Activity in a Group of South American Rodents. *Genetics* **154**: 1809-1817.

Charlesworth B (1991) The evolution of sex chromosomes. *Science* **251**: 1030-1033.

Charlesworth B and Charlesworth D (2000) The degeneration of Y chromosomes. *Phil Trans Biol Sci* **355**: 1563-1572.

Cotterill FPD (2003) Geomorphological influences on vicariant evolution in some African mammals in the Zambezi Basin: some lessons for conservation. In: Plowman AB (ed) Proceedings of the Ecology and Conservation of Mini-antelope: An International Symposium on Duiker and Dwarf Antelope in Africa. Filander Verlag, Furth, pp 11-58.

De Graaff G (1981) Hystricomorpha *incerta sedis* Bathyergidae: Mole-rats. In: Butterworth (ed) The rodents fo Southern Africa. Johannesburg, pp 63-82.

De Oliveira EHC, Neusser M, Pieczarka JC, Nagamachi C, Sbalqueiro IJ and Muller S (2005) Phylogenetic inferences of Atelinae (Platyrrhini) based on multi-directional chromosome painting in *Brachyteles arachnoides*, *Ateles paniscus* and *Ateles b. marginatus*. *Cytogenet Genome Res* **108**: 183-190.

Deuve JL, Bennett NC, O'Brien PCM, Ferguson-Smith MA, Faulkes CG, Britton-Davidian J and Robinson TJ (2006) Complex evolution of X and Y autosomal translocations in the giant mole-rat, *Cryptomys mechowi* (Bathyergidae). *Chromosome Res* **14**: 681-691.

Dobigny G, Aniskin V and Volobouev V (2002) Explosive chromosome evolution and speciation in the gerbil genus *Taterillus* (Rodentia, Gerbillinae): a case of two new cryptic species. *Cytogenet Genome Res* **96**: 117-124.

Dobigny G, Ducroz JF, Robinson TJ and Volobouev V (2004a) Cytogenetics and cladistics. *Syst Biol* **53**: 470-484.

Dobigny G, Ozouf-Costaz C and Bonillo C (2004b) Viability of X-autosome translocations in mammals: an epigenomic hypothesis from a rodent case-study. *Chromosoma* **113**: 34-41.

Dobigny G, Ozouf-Costaz C, Waters PD, Bonillo C, Coutanceau JP and Volobouev V (2004c) LINE-1 amplification accompanies explosive genome repatterning in rodents. *Chromosome Res* **12**: 787-793.

Dobigny G, Aniskin V, Granjon L, Cornette R and Volobouev V (2005) Recent radiation in West African *Taterillus* (Rodentia, Gerbillinae): the concerted role of chromosome and climatic changes. *Heredity* **95**: 358-368.

Dobson MJ, Pearlman RE, Karaiskakis A, Spyropoulos B and Moens PB (1994) Synaptonemal complex proteins: occurence, epitope mapping and chromosome disjunction. *J Cell Sci* **107**: 2749-2760.

Elbinger CJ (1989) Tectonic development of the western branch of the East African rift system. *Geological Society of American Bulletin* **1**: 885-903.

Eloff G (1958) The structural and functionnal degeneration of the eye of South African rodent moles *Cryptomys bigalkei* and *Bathyergus maritimus*. *S Afr J Sci* **54**: 293-302.

Faulkes CG, Bennett NC, Bruford MW, O'Brien HP, Aguilar GH and Jarvis JUM (1997) Ecological constraints drive social evolution in the African mole-rats. *Proc R Soc Lond B Biol Sci* **264**: 1619-1627.

Faulkes CG, Verheyen E, Verheyen W, Jarvis JUM and Bennett NC (2004) Phylogeographical patterns of genetic divergence and speciation in African mole-rats (Family: Bathyergidae). *Mol Ecol* **13**: 613-629.

Ferguson-Smith MA, Yang F and O'Brien PCM (1998) Comparative mapping using chromosome sorting and painting. *ILAR J* **39**: 68-76.

Fredga K (1972) Comparative chromosome studies in mongooses (Carnivora, Viverridae). I. Idiograms of 12 species and karyotype evolution in Herpestinae. *Hereditas* **1**: 1-74.

Froenicke L, Garcia Caldes M, Graphodatsky AS, Muller S, Lyons LA, Robinson TJ, Volleth M, Yang F and Wienberg J (2006) Are molecular cytogenetics and bioinformatics suggesting diverging models of ancestral mammalian genomes? *Genome Res* **16**: 306-310.

Gartler SM and Riggs AD (1983) Mammalian X-chromosome inactivation. *Annu Rev Genet* **17**: 155-190.

George W (1979) Conservatism in the karyotypes of two African mole-rats (Rodentia, Bathyergidae). *Z Saugetierkunde* **44**: 278-285.

Graves JAM and Watson JM (1991) Mammalian sex chromosomes: Evolution of organization and function. *Chromosoma* **101**: 63-68.

Graves JAM and Foster JW (1994) Evolution of mammalian sex chromosomes and sex-determining genes. *Internat Rev Cytol* **154**.

Graves JAM (1995) The origin and function of the mammalian Y chromosome and Y-borne genes an evolving understanding. *Bioessays* **17**: 311-320.

Gruetzner F, Rens W, Tsend-Ayush E, El-Mogharbel N, O'Brien PCM, Jones RC, Ferguson-Smith MA and Graves JAM (2004) In the platypus a meiotic chain of ten sex chromosomes shares genes with the bird Z and mammal X chromosomes. *Nature* **432**: 913-917.

Gruetzner F, Ashley T, Rowell DM and Graves JAM (2006) How did the platypus get its sex chromosome chain? A comparison of meiotic multiples and sex chromosomes in plants and animals. *Chromosoma* **115**: 75-88.

Hamilton WD (1964) The genetical evolution of social behaviour. *J Theor Biol* **7**: 1-52.

Hannenhalli S and Pevzner PA (1995) Transforming men into mice: polynomial algorithm for genomic distance problem. Proceedings of the Thirty-sixth IEEE

Symposium of Foundations of Computer Science. IEEE Press, Los Alamtos, California, pp 581-592.

Honeycutt RL, Edwards SV, Nelson K and Nevo E (1987) Mitochondrial DNA variation and the phylogeny of African mole-rats. *Syst Zool* **36**: 280-292.

Honeycutt RL, Allard MW and Edwards SV (1991) Systematics and evolution of the family Bathyergidae. In: Sherman PW, Jarvis JUM, Alexander RD (eds) The Biology of the Naked Mole-Rat. Princeton University Press, New-York., pp 45-65.

Hsu LYF (1994) Phenotype/Karyotype correlations of Y chromosome aneuploidy with emphasis on structural aberrations in postnatally diagnosed cases. *Am J Med Genet* **53**: 108-140.

Huchon D and Douzery EJP (2001) From the old world to the new world: a molecular chronicle of the phylogeny and biogeography of hystricognath rodents. *Mol Phylogenet Evol* **20**: 238-251.

Huchon D, Madsen O, Sibbald MJJB, Ament K, Stanhope MJ, Catzeflis F, de Jong WW and Douzery EJP (2002) Rodent phylogeny and a timescale for the evolution of Glires: evidence from an extensive taxon sampling using three nuclear genes. *Mol Biol Evol* **19**: 1053-1065.

Huchon D, Chevret P, Jordan U, Kilpatrick CW, Ranwez V, Jenkins PD, Brosius J and Schmitz J (2007) Multiple molecular evidence for a living mammalian fossil. *Proc Natl Acad Sci USA* **104**: 7495-7499.

Iannuzzi L, Molteni L, Di Meo GP, De Giovanni A, Perucatti A, Succi G, Incarnato D, Eggen A and Cribiu EP (2001) A case of azoospermia in a bull carrying a Y-autosome reciprocal translocation. *Cytogenet Cell Genet* **95**: 225-227.

Ingram CM, Burda H and Honeycutt RL (2004) Molecular phylogenetics and taxonomy of the African mole-rats, genus *Cryptomys* and the new genus *Coetomys* Gray, 1864. *Mol Phylogenet Evol* **31**: 997-1014.

Janecek LL, Honeycutt RL, Rautenbach IL, Erasmus BH, Reig S and Schlitter DA (1992) Allozyme variation and systematics of African mole-rats (Rodentia, Bathyergidae). *Biochem Syst Ecol* **20**: 401-416.

Jarvis JUM (1978) Energetics of survival in *Heterocephalus glaber*, the naked mole-rat (Rodentia: Bathyergidae). *Bull Carnegie Mus Nat Hist* **6**: 81-87.

Jarvis JUM (1981) Eu-sociality in a mammal-cooperative breeding in naked mole-rat *Heterocephalus glaber* colonies. *Science* **212**: 571-573.

Jarvis JUM and Bennett NC (1990) The evolutionary history, population biology and social structure of African mole-rats: Family Bathyergidae In: Nevo E, Reig OA (eds) Evolution of Subterranean Mammals at the Organismal and Molecular Levels. Wiley Liss, New-York, pp 97-128.

Jarvis JUM and Bennett NC (1991) Ecology and behaviour of the family Bathyergidae. In: Sherman PW, Jarvis JUM, Alexander RD (eds) The biology of the Naked Mole-Rat. pp 66-96.

Jarvis JUM and Bennett NC (1993) Eusociality has evolved independently in two genera of bathyergids mole-rat but occurs in no other subterranean mammal. *Behav Ecol Sociobiol* **33**: 353-360.

Jarvis JUM, O'Riain MJ, Bennett NC and Sherman PW (1994) Mammalian eusociality: a family affair. *Trends Ecol Evol* **9**: 47-51.

Kawalika M, Burda H and Bruggert D (2001) Was Zambia a cradle of the genus *Cryptomys* (Bathyergidae, Rodentia)? *African Small mammals IRD Editions*: 253-261.

Kawalika M and Burda H (2007) Giant Mole-rats, *Fukomys mechowii*, 13 Years on the Stage. In: Begall S, Burda H, Schleich CE (eds) Subterranean Rodents: News from Underground. Springer-Verlag, Berlin Heidelberg.

King M (1993) Species evolution: the role of chromosomal change. Cambridge University, Cambridge.

Kock D, Ingram CM, Frabotta LJ, Honeycutt RL and Burda H (2006) On the nomenclature of Bathyergidae and *Fukomys* n.gen. (Mammalia: Rodentia). *Zootaxa* **1142**: 51-55.

Kohn M, Kehrer-Sawatzki H, Vogel W, Graves JAM and Hameister H (2004) Wide genome comparisons reveal the origins of the human X chromosome. *Trends Genet* **20**: 598-603.

Korenberg JR and Rykowsky MC (1988) Human genome organization: Alu, Lines, and the molecular structure of metaphase chromosome bands. *Cell* **53**: 391-400.

Lammers JHM, Offenberg HH, van Aalderen M, Vink ACG, Dietrich AJJ and Heyting C (1994) The gene encoding a major component of the lateral element of the synaptonemal complex of the rat is related to X-linked lymphocyte-regulating genes. *Mol Cell Biol* **14**: 1137-1146.

Lavocat R (1973) Les rongeurs du Miocene d'Afrique Orientale. I Miocene inferieur. Institut de Montpellier 1. p 284.

Lavocat R (1978) Rodentia and Lagomorpha. In: Maglio VJ, Cooke HBS (eds) Evolution of the African Mammals. Harvard Univ. Pr., Cambridge.

Li T, O'Brien PCM, Biltueva L, Fu B, Wang J, Nie W, Ferguson-Smith MA, Graphodatsky AS and Yang F (2004) Evolution of genome organizations of squirrels (Sciuridae) revealed by cross-species chromosome painting. *Chromosome Res* **12**: 317-335.

Lovegrove BG and Wissel C (1988) Sociality in mole-rats: metabolic scaling and the role of risk sensitivity. *Oecologia* **74**: 600-606.

Lovegrove BG (1991) The evolution of eusociality in mole-rats (Bathyergidae): a question of risks, numbers and costs. *Behav Ecol Sociobiol* **28**: 37-45.

Lyon MF (1961) Gene action in the X-chromosome of the mouse (*Mus musculus* L). *Nature* **190**: 372-373.

Lyon MF (1998) X-chromosome inactivation: a repeat hypothesis. *Cytogenet Cell Genet* **80**: 133-137.

Macholan M, Burda H, Zima J, Misek I and Kawalika M (1993) Karyotype of the Giant Mole-Rat, *Cryptomys mechowi* (Rodentia, Bathyergidae). *Cytogenet Cell Genet* **64**: 261-263.

Macholan M, Scharff A, Burda H, Zima J and Grutjen O (1998) The karyotype and taxonomic status of *Cryptomys amatus* (Wroughton, 1907) from Zambia (Rodentia, Bathyergidae). *Z Saugetierkunde* **63**: 186-190.

Marczynska B (1972) Karyological analysis of African Cane rat *Thryonomys swinderianus* (Temm.). *Cytologia* **37**: 513-517.

Matsubara K, Nishida-Umehara C, Tsuchiya K, Nukaya D and Matsuda Y (2004) Karyotypic evolution of *Apodemus* (Muridae, Rodentia) inferred from comparative FISH analyses. *Chromosome Res* **12**: 383-395.

Matthey R (1956) Nouveaux apports a la cytologie comparee des rongeurs. *Chromosoma* **7**: 670-692.

Matthey R (1964) Un type nouveau de chromosomes sexuels multiples chez une souris Africaine du groupe *Mus* (Leggada) *minutoides* (Mammalia-Rodentia). *Chromosoma* **16**: 351-364.

Meles S, Adega F, Guedes-Pinto H and Chaves R (2007) The karyotype and sex chromosomes of *Praomys tullbergi* (Muridae, Rodentia): A detailed chraracterization. *Micron* (In Press).

Meuwissen TLJ, Offenberg HH, Dietrich AJJ, Riesewijk A, van Iersel M and Heyting C (1992) A coiled-coil related protein specific for synapsed regions of meiotic prophase chromosomes. *EMBO* **11**: 5091-5100.

Moses MJ (1956) Chromosomal structures in crayfish spermatocytes. *J Biophy Biochem Cytol* **2**: 215-218.

Moses MJ (1969) Structure and function of the synaptonemal complex. *Genetics* **61**: Suppl:41-45.

Mudry MD, Rahn IM and Solari AJ (2001) Meiosis and chromosome painting of sex chromosome systems in Ceboidea. *Am J Primatol* **54**: 65-78.

Muller S, Hollatz M and Wienberg J (2003) Chromosomal phylogeny and evolution of gibbons (Hylobatidae). *Hum Genet* **113**: 493-501.

Murphy WJ, Larkin DM, Everts-van der Wind A, Bourque G, Tesler G, Auvil L, Beever JE, Chowdhary BP, Galibert F, Gatzke L, Hitte C, Meyers SN, Milan D, Ostrander EA, Pape G, Parker HG, Raudsepp T, Rogatcheva MB, Schook LB, Skow LC, Welge M, Womack JE, O'Brien SJ, Pevzner PA and Lewin HA (2005) Dynamics of mammalian chromosome evolution inferred from multispecies comparative maps. *Science* **309**: 613-617.

Neusser M, Stanyon R, Bigoni F, Wienberg J and Muller S (2001) Molecular cytotaxonomy of New World monkeys (Platyrrhini)-comparative analysis of five species by multi-color chromosome painting gives evidence for a classification of *Callimico goeldii* within the family of Callitrichidae. *Cytogenet Cell Genet* **94**: 206-216.

Nevo E, Capanna E, Corti M, Jarvis JUM and Hickman GC (1986) Karyotype differentiation in the endemic subterranean Mole-rats of South Africa (Rodentia, Bathyergidae). *Z Saugetierkunde* **51**: 36-49.

Nevo E, Ben-Shlomo R, Beiles A, Jarvis JUM and Hickman GC (1987) Allozyme differentiation and systematics of the endemic subterranean mole-rats of South Africa. *Biochem Syst Ecol* **15**: 489-502.

Nevo E (1991) Evolutionary theory and processes of active speciation and adaptive radiation in subterranean mole rats, *Spalax ehrenbergi* superspecies in Israel. *Evol Biol* **25**: 1-125.

Nevo E, Filippucci MG, Redi C, Korol A and Beiles A (1994) Chromosomal speciation and adaptive radiation of mole rats in Asia Minor correlated with increased ecological stress. *Proc Natl Acad Sci USA* **91**: 8160-8164.

Nie W, Wang J, O'Brien PCM, Fu B, Ying T, Ferguson-Smith MA and Yang F (2002) The genome phylogeny of domestic cat, red panda and five mustelid species revealed by comparative chromosome painting and G-banding. *Chromosome Res* **10**: 209-222.

Nowak RM (1999) Walker's Mammals of the World. Sixth edition. The Johns Hopkins University Press, Baltimore and London.

O'Brien SJ and Stanyon R (1999) Phylogenomics: Ancestral primate viewed. *Nature* **402**: 365-366.

O'Riain MJ, Jarvis JUM and Faulkes CG (1996) A dispersive morph in the naked mole-rat. *Nature* **380**: 619-621.

Ohno S, Kaplan WD and Kinosita R (1959) Formation of the sex chromatin by a single X-chromosome in liver cells of *Rattus norvegicus*. *Exp Cell Res* **18**: 415-418.

Ohno S (1967) Sex Chromosomes and Sex Linked Genes. Springer, New York 1967.

Pack SD, Borodin PM, Serov OL and Searle JB (1993) The X-autosome translocation in the common shrew (*Sorex araneus* L.): late replication in female somatic cells and pairing in male meiosis. *Chromosoma* **102**: 355-360.

Parish DA, Vise P, Wichman HA, Bull JJ and Baker RJ (2002) Distribution of LINEs and other repetitive elements in the karyotype of the bat *Carollia*: implications for X-chromosome inactivation. *Cytogenet Genome Res* **96**: 191-197.

Perelman PL, Graphodatsky AS, Serdukova NA, Nie W, Alkalaeva EZ, Fu B, Robinson TJ and Yang F (2005) Karyotypic conservatism in the suborder Feliformia (Order Carnivora). *Cytogenet Genome Res* **108**: 348-354.

Petit P, Vermeesch JR, Marynen P and de Meurichy W (1994) Comparative cytogenetic study in the subfamily Tragelaphinae. 11th Europ Coll Cytogenet Domest Anim. pp 109-113.

Pieczarka JC and Nagamachi CY (1988) Cytogenetic studies of *Aotus* from eastern Amazonia: Y/autosome rearrangement. *Am J Primatol* **14**: 255-263.

Priest JH, Heady JE and Priest RE (1967) Delayed onset of replication of human X chromosomes. *J Cell Biol* **35**: 483-487.

Ratomponirina C, Viegas-Pequignot E, Dutrillaux B, Petter F and Rumpler Y (1986) Synaptonemal complexes in Gerbillidae: probable role of intercalated heterochromatin in gonosome-autosome translocations. *Cytogenet Cell Genet* **43**: 161-167.

Rens W, Grutzner F, O'Brien PCM, Fairclough H, Graves JAM and Ferguson-Smith MA (2004) Resolution and evolution of the duck-billed platypus karyotype with an $X_1Y_1X_2Y_2X_3Y_3X_4Y_4X_5Y_5$ male sex chromosome constitution. *Proc Natl Acad Sci USA* **101**: 16257-16261.

Rens W, Fu B, O'Brien PCM and Ferguson-Smith MA (2006) Cross-species chromosomes painting. *Nature Protocols* **1**: 783-790.

Robinson TJ and Seiffert ER (2004) Afrotherian origins and interrelationships: New views and future prospects. *Curr Top Dev Biol* **63**: 37-60.

Robinson TJ, Ruiz-Herrera A and Froenicke L (2006) Dissecting the mammalian genome - new insights into chromosomal evolution. *Trends Genet* **22**: 297-301.

Roig I, Liebe B, Egozcue J, Cabero L, Garcia M and Scherthan H (2004) Female-specific features of recombinational double-stranded DNA repair in relation to synapsis and telomere dynamics in human oocytes. *Chromosoma* **113**: 22-33.

Rokas A and Holland PWH (2000) Rare genomic changes as a tool for phylogenetics. *Trends Ecol Evol* **15**: 454-459.

Ross MT, Grafham DV, Coffey AJ and 279 other co-authors (2005) The DNA sequence of the human X chromosome. *Nature* **434**: 325-337.

Russell LB and Bangham JW (1961) Variegated-type position effects in the mouse. *Genetics* **46**: 509-525.

Sanderson MJ (2003) r8s: inferring absolute rates of molecular evolution and divergence times in the absence of a molecular clock. *Bioinformatics* **19**: 301-302.

Sbalqueiro IJ, Mattevi MS and Oliveira LF (1984) An X1X1X2X2/X1X2Y mechanism of sex determination in a South American rodent, *Deltamys kempi* (Rodentia, Cricetidae). *Cytogenet Cell Genet* **38**: 50-55.

Scharff A, Macholan M, Zima J and Burda H (2001) A new karyotype of *Heliophobius argenteocinereus* (Bathyergidae, Rodentia) from Zambia with field notes on the species. *Mamm biol* **66**: 376-378.

Scherthan H and Cremer T (1994) Nonisotopic *in situ* hybridization in paraffin-embedded tissue sections. In: Adolph KW (ed) Methods in Molecular Genetics, Vol5, Gene and Chromosome Analysis Part C. Academic Press, San Diego, pp 223-238.

Scherthan H, Cremer T, Arnason U, Weier H-U, Lima-de-Faria A and Froenicke L (1994) Comparative chromosome painting discloses homologous segments in distantly related mammals. *Nature Genetics* **6**: 342-347.

Schmekel K, Meuwissen TLJ, Dietrich AJJ, Vink ACG, van Marle J, van Veen H and Heyting C (1996) Organization of SCP1 protein molecules within synaptonemal complexes of rat. *Exp Cell Res* **226**: 20-30.

Seabright M (1971) A rapid banding technique for human chromosomes. *Lancet* **2**: 971-972.

Skinner JD and Chimimba CT (2005) The Mammals of the Southern African Subregion. Cambridge University Press.

Stack SM (1984) Heterochromatin, the synaptonemal complex and crossing over. *J Cell Sci* **71**: 159-176.

Sumner AT (1972) A simple method for demonstrating centromeric heterochromatin. *Exp Cell Res* **75**: 304-309.

Swofford DL (1999) PAUP*. *Phylogenetic Analysis Using Parsimony (* and other Methods)*. Massachussetts, MA: Sinauer Associates.

Takagi N (1974) Differentiation of the X chromosome in early female mouse embryos. *Exp Cell Res* **86**: 127-135.

Telenius H, Pelmear AH, Tunnacliffe A, Carter NP, Behmel A, Ferguson-Smith MA, Nordenskjold M, Pfragner R and Ponder BAJ (1992) Cytogenetic analysis by

chromosome painting using DOP-PCR amplified flow sorted chromosomes. *Genes Chromosomes Cancer* **4**: 257-263.

Tesler G (2002) Efficient Algorithms for Multichromosomal Genome Rearrangements. *J Comput Syst Sci* **65**: 587-609.

Thomas DSG and Shaw PA (1988) Late Cainozoic drainage evolution in the Zambezi basin: geomorphological evidence from the Kalahari rim. *J African Earth Sci* **7**: 611-618.

Tucker PK (1986) Sex chromosome-autosome translocations in the leaf-nosed bats, family Phyllostomidae.I. Mitotic analyses of the subfamilies Stenodermatinae and Phyllostominae. *Cytogenet Cell Genet* **43**: 19-27.

Van Couvering JAH and Van Couvering JA (1976) Early Miocene mammal fossils from East Africa: aspects of geology, faunistics and paleoecology. In: Isaac GL, McCown ER (eds) Human Origins: Louis Leakey and the East African Evidence. Benjamin, W.A., Menlo Park, CA.

Van Daele PAAG, Dammann P, Meier JL, Kawalika M, Van De Woestijne C and Burda H (2004) Chromosomal diversity in mole-rats of the genus *Cryptomys* (Rodentia: Bathyergidae) from the Zambezian region: with descriptions of new karyotypes. *J Zool Lond* **264**: 317-326.

Van Daele PAAG, Faulkes CG, Verheyen E and Adriaens D (2007a) African Mole-rats (Bathyergidae): A Complex Radiation in Tropical Soils. In: Begall S, Burda H, Schleich CE (eds) Subterranean Rodents: News from Underground. Springer-Verlag, Berlin Heidelberg.

Van Daele PAAG, Verheyen E, Brunain M and Adriaens D (2007b) Cytochrome b sequence analysis reveals differential molecular evolution in African mole-rats of the chromosomally hyperdiverse genus *Fukomys* (Bathyergidae, Rodentia) from the Zambezian region. *Mol Phylogenet Evol* **45**: 142-157.

Vassart M, Seguela A and Hayes H (1995) Chromosomal evolution in Gazelles. *J Hered* **86**: 158-167.

Veyrunes F, Catalan J, Sicard B, Robinson TJ, Duplantier J-M, Granjon L, Dobigny G and Britton-Davidian J (2004) Autosome and sex chromosome diversity among the African pygmy mice, subgenus *Nannomys* (Murinae; *Mus)*. *Chromosome Res* **12**: 369-382.

Veyrunes F, Dobigny G, Yang F, O'Brien PCM, Catalan J, Robinson TJ and Britton-Davidian J (2006) Phylogenomics of the genus *Mus* (Rodentia; Muridae): extensive genome repatterning is not restricted to the house mouse. *Proc R Soc B*: ??

Veyrunes F, Watson J, Robinson TJ and Britton-Davidian J (2007) Accumulation of rare sex chromosomes rearrangements in the African pygmy mouse, *Mus* (*Nannomys*) *minutoides*: a whole-arm reciprocal translocation (WART) involving an X-autosome fusion. *Chromosome Res* **15**: 223-230.

Viegas-Pequignot E, Benazzou T, Dutrillaux B and Petter F (1982) Complex evolution of sex chromosomes in Gerbillidae (Rodentia). *Cytogenet Cell Genet* **34**: 158-167.

Volobouev V, Aniskin VM, Lecompte E and Ducroz JF (2002) Patterns of karyotype evolution in complexes of sibling species within three genera of African murid rodents inferred from the comparison of cytogenetic and molecular data. *Cytogenet Genome Res* **96**: 261-275.

Walton AH, Nedbal MA and Honeycutt RL (2000) Evidence from intron 1 of the nuclear transthyretin (Prealbumin) gene for the phylogeny of African mole-rats (Bathyergidae). *Mol Phylogenet Evol* **16**: 467-474.

Waters PD, Dobigny G, Pardini AT and Robinson TJ (2004) LINE-1 distribution in Afrotheria and Xenarthra: implications for understanding the evolution of LINE-1 in eutherian genomes. *Chromosoma* **113**: 137-144.

Waters PD, Ruiz-Herrera A, Dobigny G, Garcia Caldes M and Robinson TJ (2007) Sex chromosomes of basal placental mammals. *Chromosoma* **116**: 511-518.

Williams SL, Schlitter DA and Robbins LW (1983) Morphological variation in a natural population of *Cryptomys* (Rodentia: Bathyergidae) from Cameroon. *Ann Mus R Afr Centr Sc Zool* **237**.

Wilson EO (1971) The Insect Societies. Harvard University Press, Cambridge Mass.

Yang F, Carter NP, Shi L and Ferguson-Smith MA (1995) A comparative study of karyotypes of muntjacs by chromosome painting. *Chromosoma* **103**: 642-652.

Yang F, Muller S, Just R and Ferguson-Smith MA (1997a) Comparative chromosome painting in Mammals: Human and the Indian Muntjac (*Muntiacus muntjak vaginalis*). *Genomics* **39**: 396-401.

Yang F, O'Brien PCM, Wienberg J and Ferguson-Smith MA (1997b) A reappraisal of the tandem fusion theory of karyotype evolution in the Indian muntjac using chromosome painting. *Chromosome Res* **5**: 109-117.

APPENDICES

Appendix 1: Summary of published cytogenetic data for the Bathyergidae. 2n= diploid number, FN= Fundamental Number (number of chromosome arms), aFN= autosomal FN, FN(XX)= FN for autosome plus the two X chromosomes, Acro= Acrocentric, GB= G-banding, CB= C-banding, NOR= Nucleolus Organizer Region

Species	2n	FN		Autosome morphology		Sex chromosome morphology		Chromosome staining				References
		aFN	FN (XX)	Bi-armed	Acro.	X	Y	GB	CB	NOR	DAPI	
Heterocephalus glaber	60			19	10	SM	dot	√			√	George 1979, Capanna and Merani 1980
Heliophobius argenteocinereus	60	114	118	28	1	M	dot	√				George 1979
	62	114		27	3		dot					Scharff *et al.* 2001
Bathyergus janetta	54	104		26	0	M	A			√	√	Nevo *et al.* 1986
B. suillus	56	96		24	3	M				√	√	Nevo *et al.* 1986
Georychus capensis	54	100		24	2		ST		√	√	√	Matthey 1956, Nevo *et al.* 1986
Cryptomys hottentotus hottentotus	54	102		25	1	SM	?		√	√	√	Nevo *et al.* 1986
C. h. natalensis	54	100		24	2	SM	A		√	√	√	Nevo *et al.* 1986
Fukomys bocagei	58											Burda 2001
F. mechowi	40	76		19	0	SM	SM	√	√	√	√	Macholan *et al.* 1998
Undescribed species from Salujinga, Zambia	44		76	16	6						√	Van Daele *et al.* 2004
F. whytei	46	76		15	8							Kawalika *et al.* 2001, Burda *et al.* 2005
F. amatus	50	92	96	22	2	M	A	√	√	√		Macholan *et al.* 1998
Undescribed species from Kasama, Zambia	64	86		11	21						√	Kawalika *et al.* 2001
F. micklemi	58,60	82	86	10,13	19,15	M	dot				√	Van Daele *et al.* 2004
F. kafuensis	58		82	11	17	M	dot	√	√		√	Burda *et al.* 1999
F. anselli	68	75-78		5	28	M	dot	√	√	√	√	Burda *et al.* 1999
Undescribed species from Chinyingi,	52	72	76	9	18	M	dot				√	Van Daele *et al.* 2004

Zambia												
Undescribed species from Lochinvar, Zambia	45		78	16+1 w/o homolog	6						√	Van Daele *et al.* 2004
Undescribed species from Monze, Zambia	54		78	12	15						√	Van Daele *et al.* 2004
Undescribed species from Dongo, Zambia	42	74	78	17	3	M	dot				√	Van Daele *et al.* 2004
Undescribed species from Kalomo, Zambia	50	72	76	12	12	M	dot					Faulkes *et al.* 1997
Undescribed species from Watopa, Zambia	56	72	76	9	18	M	dot				√	Van Daele *et al.* 2004
Undescribed species from Livingstone, Zambia	56	76	80	11	16	M	dot				√	Van Daele *et al.* 2004
F. damarensis	74,78			?/8	?/30	M	SM			√	√	Nevo *et al.* 1986
F. darlingi	54	80		14	12	ST	M		√	√	√	Aguilar 1993
F. foxi	66,70		130,138	29	3	SM	M					Williams *et al.* 1983

Appendix 2: Schematic outcome of the MGR analysis of the chromosomal rearrangements distinguishing three species of *Fukomys* and *H. argenteocinereus*. The ancestral karyotypes are presented in the squares, and a likely suite of rearrangements characterising each lineage are presented above each branch. Tr = Translocation, Inv = Inversion, Fu = Fusion, Fi = Fission.